

**UNIVERSITA' DEGLI STUDI DI NAPOLI**  
**FEDERICO II**

**SCUOLA POLITECNICA E DELLE SCIENZE DI BASE**  
**Area Didattica di Scienze Matematiche, Fisiche e Naturali**



**DOTTORATO DI RICERCA IN BIOLOGIA**  
**AVANZATA**  
**XXVIII CICLO**

**Heterologous expression and biochemical characterization of  
innovative bacterial carbonic anhydrases involved in the carbon  
cycle and microbial virulence.**

**Coordinatore:**  
**Ch.mo Prof.**  
**Luciano Gaudio**

**Tutor**  
**Ch.ma Prof.ssa**  
**Rosaria Scudiero**  
**Co-Tutor**  
**Dott. Clemente Capasso**

**PhD. Student**  
**Viviana De Luca**

**ANNO ACCADEMICO 2013 - 2016**

## Summary

|                      |     |
|----------------------|-----|
| Abbreviations .....  | i   |
| List of Figures..... | iii |
| List of Tables ..... | v   |
| Riassunto.....       | vi  |
| Abstract.....        | vii |

|   |           |
|---|-----------|
| <b>Chapter 1. Introduction.....</b>                               | <b>1</b>  |
| <b>1.1 Carbonic anhydrases. ....</b>                              | <b>1</b>  |
| <b>1.2 Physiological role of CAs .....</b>                        | <b>1</b>  |
| <b>1.3 CA classes.....</b>  | <b>2</b>  |
| <b>1.4 Catalytic mechanism.....</b>                               | <b>4</b>  |
| <b>1.5 Characteristics of the CA-classes.....</b>                 | <b>7</b>  |
| <i>1.5.1 <math>\alpha</math>-CAs .....</i>                        | <i>7</i>  |
| <i>1.5.2 <math>\beta</math>-CA.....</i>                           | <i>9</i>  |
| <i>1.5.3 <math>\gamma</math>-CA .....</i>                         | <i>10</i> |
| <i>1.5.4 <math>\delta</math>- e <math>\zeta</math>-CA .....</i>   | <i>12</i> |
| <i>1.5.5 <math>\eta</math>-CA, the last discovered class.....</i> | <i>13</i> |
| <b>1.6 Inhibitors .....</b>                                       | <b>14</b> |
| <b>1.7 Activators.....</b>  | <b>16</b> |

|   |           |
|---|-----------|
| <b>Chapter 2. Biotechnological and Biomedical application of CAs.....</b> | <b>17</b> |
|---|-----------|

|   |           |
|---|-----------|
| 2.1 Carbon capture and storage (CCS) .....                                      | 17        |
| 2.2 Carbonic anhydrases from pathogens as druggable enzymes .....               | 21        |
| 2.2.1 Pathogens .....   | 21        |
| 2.2.2 Bacterial CAs.....  | 22        |
| 2.2.3 Protozoan CAs .....   | 24        |
| <br>  |           |
| <b>Chapter 3. Materials and Method .....</b>                                    | <b>25</b> |
| 3.1 Identification of the CA genes in thermophilic and pathogenic bacteria..... | 25        |
| 3.2 Bacterial Strains used for heterologous protein expression .....            | 25        |
| 3.2.1 <i>E. coli</i> BL21(DE3).....   | 25        |
| 3.2.2 <i>E. coli</i> ArcticExpress (DE3).....                                   | 26        |
| 3.2.3 <i>E. coli</i> DH5a.....  | 26        |
| 3.3 Culture medium: LB (Luria-Bertani) .....                                    | 27        |
| 3.4 Expression vector: pET15b (Novagen).....                                    | 27        |
| 3.5 Cloning procedure.....  | 28        |
| 3.5.1 Construct preparation .....   | 28        |
| 3.5.2 Plasmid DNA amplification into <i>E. coli</i> DH5a cells .....            | 28        |
| 3.5.3 Vector digestion .....  | 29        |
| 3.5.4 Ligation Reaction .....   | 30        |
| 3.5.5 Clone identification .....  | 31        |
| 3.5.6 Construct amplification .....   | 31        |
| 3.6 Expression of heterologous proteins in <i>E. coli</i> cells.....            | 31        |
| 3.6.1 Small scale optimization .....  | 31        |

|   |           |
|---|-----------|
| 3.6.2 <i>Large scale expression</i> .....                                 | 31        |
| 3.7 Purification of recombinant CA .....                                  | 32        |
| 3.7.1 <i>Affinity chromatography</i> .....                                | 32        |
| 3.7.2 <i>SDS-PAGE analysis of protein fractions</i> .....                 | 33        |
| 3.7.3 <i>Determination of protein concentration</i> .....                 | 33        |
| 3.8 Biochemical characterization.....                                     | 34        |
| 3.8.1 <i>Determination of CA hydratase activity in solution</i> .....     | 34        |
| 3.8.2 <i><math>\alpha</math>CA esterase activity assay</i> .....          | 35        |
| 3.8.3 <i>Protonography</i> .....  | 35        |
| 3.8.4 <i>Thermoactivity</i> .....   | 36        |
| 3.8.5 <i>Thermostability</i> .....  | 36        |
| 3.8.6 <i>Determination of the kinetics and inhibition constants</i> ..... | 36        |
| 3.9 Immobilization .....  | 37        |
| 3.9.1 <i>Enzyme immobilization on polyurethane foam</i> .....             | 37        |
| 3.9.2 <i>Bioreactor</i> .....   | 38        |
| 3.9.3 <i>Preparation of Magnetic Particles</i> .....                      | 38        |
| 3.9.4 <i>Immobilization of CA on MP</i> .....                             | 39        |
| 3.9.5 <i>Activity measurement of immobilized CA on MP</i> .....           | 39        |
| <br>  |           |
| <b>Chapter 4. Biotechnological application results</b> .....              | <b>40</b> |
| 4.1 Biomimetic capture of CO <sub>2</sub> .....                           | 40        |
| 4.2 Protein identification .....  | 40        |
| 4.3 Primary structure analysis .....                                      | 41        |

|  |           |
|--|-----------|
| 4.4 Cloning sequencing and production of expression vector .....               | 42        |
| 4.5 Optimal expression conditions and production of the recombinant proteins . | 42        |
| 4.6 Purification of the recombinant proteins .....                             | 42        |
| 4.7 Characterization.....  | 43        |
| 4.7.1 Activity .....   | 43        |
| 4.7.2 Kinetic Constans.....  | 44        |
| 4.7.3 Thermoactivity and Thermostability.....                                  | 44        |
| 4.8 X-ray structure.....   | 46        |
| 4.8.1 SspCA .....  | 46        |
| 4.8.2 SazCA .....  | 47        |
| 4.9 Immobilization .....   | 49        |
| 4.9.1 Polyurethane .....   | 49        |
| 4.9.2 Paramagnetic parcticles .....  | 52        |
| 4.10 Inhibition studies.....   | 53        |
| <br>   |           |
| <b>Chapter 5. Biomedical application results.....</b>                          | <b>55</b> |
| 5.1 <i>Vibrio Cholerae</i> .....   | 55        |
| 5.1.1 <i>VchCA</i> .....   | 55        |
| 5.1.2 <i>VchCA<math>\beta</math></i> .....                                     | 57        |
| 5.1.3 <i>VchCA<math>\gamma</math></i> .....                                    | 57        |
| 5.2 Cloning sequencing and production of expression vector .....               | 58        |
| 5.3 Optimal growing condition and recombinant protein production .....         | 58        |
| 5.4 Purification .....   | 58        |

|  |           |
|--|-----------|
| <b>5.5 Biochemical characterization.....</b>               | <b>59</b> |
| <i>5.5.1 Activity .....</i>                                | <i>59</i> |
| <i>5.5.2 Kinetic constants .....</i>                       | <i>60</i> |
| <i>5.5.3 Thermoactivity and Thermostability.....</i>       | <i>62</i> |
| <i>5.5.4 Protonography .....</i>                           | <i>63</i> |
| <b>5.6 Inhibition.....</b>                                 | <b>65</b> |
| <i>5.6.1 Sulfonamides and the bioisosteres.....</i>        | <i>65</i> |
| <i>5.6.2 Anions .....</i>                                  | <i>69</i> |
| <b>5.7 Plasmodium falciparum .....</b>                     | <b>71</b> |
| <i>5.7.1 <math>\eta</math>-CA inhibition studies .....</i> | <i>74</i> |
| <br>   |           |
| <b>Chapter 6. Evolutionary aspects.....</b>                | <b>76</b> |
| <br>   |           |
| <b>Chapter 7. Discussion .....</b>                         | <b>82</b> |
| <b>7.1 Biotechnological application .....</b>              | <b>82</b> |
| <b>7.2 Biomedical application .....</b>                    | <b>83</b> |
| <b>7.3 Phylogenetic analysis .....</b>                     | <b>85</b> |
| <b>7.4 Conclusions.....</b>                                | <b>86</b> |
| <br>   |           |
| <b>Bibliography .....</b>                                  | <b>87</b> |

## **Abbreviations**

|          |   |
|----------|---|
| AAZ      | Acetazolamide                                   |
| ATP      | Adenosine triphosphate                          |
| AZM      | acetazolamide                                   |
| bCA      | bovine carbonic anhydrase                       |
| BRZ      | Brinzolamide                                    |
| BSA      | Bovine serum albumin                            |
| BTB      | Bromothymol blue                                |
| BZA      | Benzolamide                                     |
| CA       | Carbonic anhydrase                              |
| CAA      | Carbonic anhydrase activator                    |
| CAI      | Carbonic anhydrase inhibitor                    |
| cAMP-CRP | Cyclic adenosine monophosphate receptor protein |
| CARP     | Carbonic anhydrase related protein              |
| CLX      | Cyclothiazide                                   |
| DCP      | Diclofenamide                                   |
| DTT      | Dithiothreitol                                  |
| DZA      | Dorzolamide                                     |
| EDTA     | Ethylenediaminetetraacetic acid                 |
| EZA      | Ethoxzolamide                                   |
| FPLC     | Fast protein liquid chromatography              |

|       |   |
|-------|---|
| hCA   | human carbonic anhydrase                                |
| HCT   | Hydrochlorothiazide                                     |
| IND   | Indapamide  |
| IPTG  | Isopropyl- $\beta$ -D-1-thiogalactopyranoside           |
| LB    | Luria Bertani   |
| MCS   | Multiple cloning site                                   |
| MP    | Magnetic particles                                      |
| MZA   | Metazolamide  |
| PfCA1 | <i>Plasmodium falciparum</i> carbonic anhydrase         |
| p-NpA | Paranitrophenil acetate                                 |
| PU    | polyurethane  |
| SAC   | Saccharin   |
| SazCA | <i>Sulfurihydrogenibium azorense</i> carbonic anhydrase |
| SDS   | Sodium dodecyl sulfate                                  |
| SLP   | Sulpiride   |
| SLT   | Sulthiame   |
| SspCA | <i>Sulfurihydrogenibium sp.</i> Carbonic anhydrase      |
| TPM   | Topiramate  |
| VchCA | <i>Vibrio cholerae</i> carbonic anhydrase               |
| WAU   | Wilbur Andreson Units                                   |
| ZNS   | Zonisamide  |

## List of figures

|                |    |
|----------------|----|
| Figure 1.....  | 3  |
| Figure 2.....  | 5  |
| Figure 3.....  | 6  |
| Figure 4.....  | 7  |
| Figure 5.....  | 9  |
| Figure 6.....  | 10 |
| Figure 7.....  | 11 |
| Figure 8.....  | 12 |
| Figure 9.....  | 13 |
| Figure 10..... | 15 |
| Figure 11..... | 15 |
| Figure 12..... | 18 |
| Figure 13..... | 19 |
| Figure 14..... | 28 |
| Figure 15..... | 32 |
| Figure 16..... | 39 |
| Figure 17..... | 41 |
| Figure 18..... | 43 |
| Figure 19..... | 46 |
| Figure 20..... | 47 |

|                |    |
|----------------|----|
| Figure 21..... | 48 |
| Figure 22..... | 49 |
| Figure 23..... | 50 |
| Figure 24..... | 50 |
| Figure 25..... | 51 |
| Figure 26..... | 52 |
| Figure 27..... | 56 |
| Figure 28..... | 56 |
| Figure 29..... | 57 |
| Figure 30..... | 59 |
| Figure 31..... | 62 |
| Figure 32..... | 63 |
| Figure 33..... | 64 |
| Figure 34..... | 66 |
| Figure 35..... | 72 |
| Figure 36..... | 73 |
| Figure 37..... | 76 |
| Figure 38..... | 77 |
| Figure 39..... | 79 |
| Figure 40..... | 80 |

## List of tables

|                 |    |
|-----------------|----|
| Table I.....    | 20 |
| Table II.....   | 20 |
| Table III.....  | 23 |
| Table IV.....   | 27 |
| Table V.....    | 44 |
| Table VI.....   | 44 |
| Table VII.....  | 51 |
| Table VIII..... | 54 |
| Table IX.....   | 60 |
| Table X.....    | 60 |
| Table XI.....   | 61 |
| Table XII.....  | 67 |
| Table XIII..... | 70 |
| Table XIV.....  | 74 |

## Riassunto

La conversione dell'anidride carbonica (CO<sub>2</sub>) in bicarbonato (HCO<sub>3</sub><sup>-</sup>) e protoni (H<sup>+</sup>) è una reazione fisiologicamente rilevante in tutti gli organismi viventi. La reazione  $\text{CO}_2 + \text{H}_2\text{O} \rightleftharpoons \text{HCO}_3^- + \text{H}^+$  non catalizzata è lenta a pH fisiologici e quindi, nei sistemi biologici, è accelerata da catalizzatori enzimatici, noti con il nome di anidrasi carboniche (CA, EC 4.2.1.1). Le CA sono state trovate in quasi tutti i tessuti di mammiferi e tipi cellulari, e sono coinvolte nel trasporto della CO<sub>2</sub> e in altri importanti processi fisiologici.

Nella presente tesi è riportata la caratterizzazione biochimica di CA termostabili e termoattive identificate nel genoma di estremofili appartenenti al genere *Sulfurihydrogenibium*. Inoltre, è stato eseguito un ampio studio sul profilo di inibizione delle CA identificate nel genoma di organismi patogeni per l'uomo, quali *Vibrio cholerae* e *Plasmodium falciparum*.

Le CA identificate nel genoma di *S. yellowstonense* e *S. azorense* sono risultate essere cataliticamente attive ad alte temperature e dopo immobilizzazione su supporti polimerici o paramagnetici. E' stato dimostrato che tali CA sono ottimi candidati da impiegare nel processo di cattura della CO<sub>2</sub>.

Le CA identificate nei patogeni suddetti sono state caratterizzate biochimicamente ed è stato condotto un ampio studio del loro profilo d'inibizione utilizzando gli inibitori classici delle CA, come sulfamidici e anioni. Tali studi sono fondamentali per ricerca di potenziali antibiotici con un nuovo meccanismo d'azione. Inoltre, la presente tesi ha contribuito alla scoperta di una nuova famiglia genica di CA, indicata con la lettera greca η; all'introduzione di una nuova tecnica, denominata protonografia, utile per l'identificazione dell'attività delle CA su gel di poliacrilamide; e all'analisi filogenetica delle CA di classe α, β e γ identificate nel genoma dei batteri Gram-positivi e Gram-negativi.

## Abstract

The conversion of carbon dioxide (CO<sub>2</sub>) to bicarbonate (HCO<sub>3</sub><sup>-</sup>) and protons (H<sup>+</sup>) is a physiologically relevant reaction in all life kingdoms. The uncatalyzed hydration-dehydration reaction  $\text{CO}_2 + \text{H}_2\text{O} \rightleftharpoons \text{HCO}_3^- + \text{H}^+$  is slow at physiological pH and thus, in biological systems, the reaction is accelerated by enzymatic catalysts, called carbonic anhydrases (CAs, EC 4.2.1.1). CA isozymes have been found in virtually all mammalian tissues and cell types, where they function in CO<sub>2</sub> transport and other physiological processes.

Here, are described the biochemical characterization of thermostable and thermoactive CAs from extremophiles belonging to the genus *Sulfurihydrogenibium*. Moreover, it has been carried out a wide study concerning the inhibition profiles of CAs identified in the genome of pathogens causing disease in humans, such as *Vibrio cholerae* and *Plasmodium falciparum*.

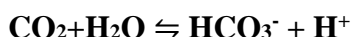
CAs identified in the genome of *S. yellowstonense* and *S. azorense* were found to be active at high temperatures and preserved its activity after immobilization on paramagnetic or polymeric supports. It has been demonstrated that these CAs are good candidates in the CO<sub>2</sub> capture process.

CAs from the pathogens aforementioned were biochemically characterized and an extensive inhibition profile was carried out using the classical CAs inhibitors such as sulfonamides and anions. These studies have contributed to the search of antibiotics with a novel mechanism of action. Additionally, the present thesis has contributed to the discovery of the  $\eta$ -CA, a new genetic families of CAs; to the introduction of a new technique, named protonography, useful for the identification of CA activity on a polyacrylamide gel; and to the phylogenetic analysis of the  $\alpha$ -,  $\beta$ - and  $\gamma$ -CAs identified in the genome of the Gram-positive and Gram-negative bacteria.

# Chapter 1. Introduction

## 1.1 Carbonic anhydrases

Carbonic anhydrases (CAs, EC 4.2.1.1) are ubiquitous metalloenzymes present in all life kingdoms: Archaea, Bacteria and Eucarya. Formed by the convergent evolution of at least six families of genes ( $\alpha$ ,  $\beta$ ,  $\gamma$ ,  $\delta$ ,  $\zeta$  and  $\eta$ ). CAs have been identified for the first time in red blood cells of bovine (Meldrum N.U. & Roughton F.J. 1933). Later, they have been found in all mammalian tissues, but also in plants, algae and bacteria. CAs owe their ubiquity to the ability to catalyze a simple but physiologically relevant reaction for living being (Capasso C. & Supuran C.T. 2015), i.e. the reversible hydration of carbon dioxide with the formation of bicarbonate and protons according to the following formula:



The reaction of hydration of  $\text{CO}_2$  consists of four reactions:

- 1)  $\text{CO}_{2(\text{g})} \rightleftharpoons \text{CO}_{2(\text{aq})}$  reaction of dissolution in aqueous phase
- 2)  $\text{CO}_{2(\text{aq})} + \text{H}_2\text{O} \rightleftharpoons \text{H}_2\text{CO}_3$  hydration reaction (carbonic acid production)
- 3)  $\text{H}_2\text{CO}_3 \rightleftharpoons \text{HCO}_3^- + \text{H}^+$  ionization reaction (bicarbonate production)
- 4)  $\text{HCO}_3^- \rightleftharpoons \text{CO}_3^{2-} + \text{H}^+$  dissociation reaction (carbonate formation)

In physiological conditions and in the absence of the catalyst, the reaction 2 is the limiting step of the entire process and, the  $k_{\text{cat}}$  assumes a value of  $1.5 \times 10^{-1} \text{ s}^{-1}$  (Edsall J.T. 1968). The carbonic anhydrase, able to convert a million molecules of  $\text{CO}_2$  per second, increases the value of the  $k_{\text{cat}}$  from  $10^{-1} \text{ s}^{-1}$  to  $10^5 \text{ s}^{-1}$ . CAs are among the fastest enzymes known.

## 1.2 Physiological role of CAs

CAs in mammals are involved in breathing and transport of carbon dioxide and bicarbonate in tissues and lungs, in the homeostasis of pH and  $\text{CO}_2$  in biosynthetic reactions such as gluconeogenesis, lipogenesis, ureagenesis, where the bicarbonate acts as a substrate for the reaction of carboxylation, bone resorption, calcification and tumorigenicity (Supuran C.T., *et al.* 2015). However, in microorganisms, in addition to the transport of carbon dioxide

bicarbonate and its supply of for biosynthetic reactions, carbonic anhydrases are involved in: a) carbon fixation for the photosynthetic process; b) metabolism of xenobiotics (degradation of the cyanate in *E. coli*); c) pH regulation; d) survival of the pathogen within the host organism; d) synthesis of purine and pyrimidine as in the protozoan *Plasmodium falciparum* (Supuran C.T. & Capasso C. 2014).

In mammals, at the level of the peripheral tissue, due to the pressure gradient, the carbon dioxide, produced by the aerobic metabolism, leave the cells and enter the blood, dissolving in the plasma (reaction 1). From here, about 90% of the carbon dioxide enters the red blood cells and, thanks to the action of carbonic anhydrase reacts with water, forming carbonic acid (reaction 2) which in turn dissociates into bicarbonate ion and hydrogen ion (reaction 3). Bicarbonate leaves the red blood cell by a protein antiporter. This transport process, defined exchange of chlorides, exchanges one  $\text{HCO}_3^-$  ion with a  $\text{Cl}^-$  ion. The exchange takes place in the ratio of 1: 1 by maintaining electrical neutrality and, consequently, the membrane potential of the cell is not changed. The ion  $\text{HCO}_3^-$  is converted to carbonate and protons  $\text{H}^+$  (reaction 4), which are linked by hemoglobin, which acts as a buffer (Boron W.F. 2010). At the alveolar level, however, the  $\text{CO}_2$  concentration is lower than that in the peripheral tissues, while there is a higher concentration of bicarbonate that is pumped inside the red cell. Here, by the action of the reverse reaction catalyzed by the CAs, the bicarbonate is converted into carbonic acid, which will give water and carbon dioxide. The  $\text{CO}_2$  thus produced, is released into the blood and, passing by diffusion through the walls of the alveolus, is exhaled. The direction of the reaction, therefore, depends on the concentration of  $\text{CO}_2$ : if this is low (as in the lungs), the acid is dissociated, with release of carbon dioxide; If this is high, dioxide binds water to form carbonates that are transported by the blood to the lungs (Boron W.F. 2010).

### 1.3 CA classes

Until now were identified 6 distinct gene families of CAs (Supuran C.T. & Capasso C. 2014):

- $\alpha$ -CA: invertebrates, fungi, protozoa, corals, algae, cytoplasm of green plants and some bacteria



In mammals, there are only  $\alpha$ -CA, of which 16 isoforms were identified, marked with Roman numbers (Supuran C.T. *et al.*, 2008; Supuran C.T., *et al.* 2004; Scozzafava A., *et al.* 2000; Winum J.Y. *et al.* 2006; Saczewski F., *et al.* 2006; De Simone G., *et al.* 2006). These isoenzymes can be distinguished according to the different tissue distribution, subcellular localization and catalytic activity (Supuran C.T. 2008). In particular, we divide the mammalian  $\alpha$ -CA in:

- cytosolic (isoenzymes I, II, III, IV, VIII)
- mitochondrial (isoenzymes VA, VB)
- membrane-bound (isoenzymes IV, IX, XII, XIV, XV)
- secreted in saliva (isoenzyme VI)

#### **1.4 Catalytic mechanism**

In Figure 1 is reported the alignment of the  $\alpha$ -CA amino acid sequences: four human isoforms (hCA I, hCA II, hCAVA and hCA VI) and two bacterial CAs represented by SspCA, identified in the genome of the thermophilic bacterium *Sulfurihydrogenibium yellowstonense* and, VchCA present in the genome of the mesophilic bacterium *Vibrio cholerae*. In the alignment are highlighted the amino acid residues involved in the catalytic mechanism of the  $\alpha$ -CAs, which consists of four steps. In the first step zinc ion, present in the catalytic site of the enzyme, is bound to the hydroxyl ion (Figure 2, Panel A). This configuration corresponds to the active form of the enzyme. The substrate CO<sub>2</sub> is bound in a hydrophobic pocket near the Zn(II) ion, defined among others by residues Val121, Val143 and Leu198 (in the human isoform hCA II). Orientated in a favorable position for the nucleophilic attack of the enzyme, CO<sub>2</sub> is transformed into bicarbonate. (Figure 2, Panel B). The bicarbonate ion is then displaced by a water molecule and released in solution (Figure 2, Panel C). In this way, the water molecule coordinated to the zinc, generates the acidic form of the enzyme, which is catalytically inactive (Figure 2, Panel D). The catalytically active form of the enzyme is regenerated through the reaction of transfer of a proton from the active site of the enzyme to the environment (Figure 2, Panel A). The speed of this transfer is highly dependent on the

residue His64 known as "proton shuttle residue" (Supuran C.T. 2008)(see Figure 2).

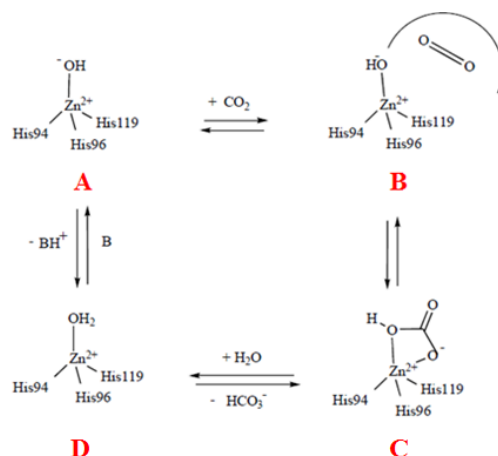


**Figure 2.** Schematic representation of the catalytic mechanism of a  $\alpha$ -CAs.

In the catalytically very active isoenzymes, such as hCA II hCA IV, VII and hCA hCA IX, the transfer process of the proton from the enzyme to the environment is assisted by His64 positioned at the entrance of the active site and, by a cluster of histidine (His4, His3, His17, His15 and His10), which protrude from the edge of the active site of the enzyme on the surface, ensuring efficient removal of the proton by the enzyme (Figure 3). This explains why they are the most active known CAs ( $k_{cat}/K_M$  about  $1.5 \times 10^8 \text{ M}^{-1} \text{ s}^{-1}$ ) (Supuran C.T. 2008). In other CA, such as the hCA III, the catalytic efficiency is lower because the residue His64 was absent and in position 198, a phenylalanine replaces the residue of leucine causing a steric hindrance near the catalytic site (Chegwidden W.R., Carter N.D., Edwards Y.H. 2000).  $\alpha$ -CAs are also able to catalyze the hydrolysis of esters/thioesters, (for example 4-nitrophenyl acetate (4-NpA) hydrolysis, as well as other hydrolytic reactions); while no esterase activity was detected so far for enzymes belonging to the other five CA genetic families. (Del Prete S, *et al.* 2014; Guzel O., *et al.* 2010).

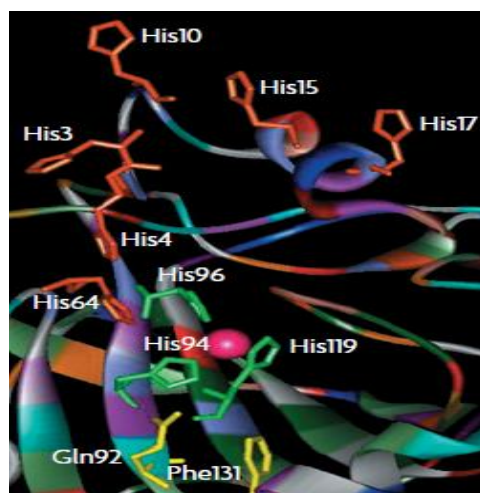


**Figure 3.** Structure of the active site of hCAII.

Are also known catalytically inactive isoforms of  $\alpha$ -CAs, indicated as CARPs (Carbonic Anhydrase Related Proteins). The CARPs occur independently or as domains of other proteins in animals (both vertebrates and invertebrates) and viruses. Although these proteins show a high degree of homology with the other known CA isoforms (hCA I–VII, IX, and XII–XIV), they distinguish themselves from the catalytically active CAs by a salient feature: they lack one, two or all three zinc ligands from the enzyme active site, that is, His94, 96 and 119 (the hCA I numbering system). The phylogenetic analysis shows that these proteins are highly conserved across the species. The three CARPs in vertebrates are known as CARP VIII, X and XI. Most of these CARPs are predominantly expressed in central nervous system. Among the three vertebrate CA isoforms, CARP VIII is functionally associated with motor coordination in human, mouse and zebrafish and certain types of cancers in humans. Vertebrate expression studies show that CARP X is exclusively expressed in the brain. CARP XI is only found in tetrapods and is highly expressed in the central nervous system (CNS) of humans and mice and is also associated with several cancers. CARP VIII has been shown to coordinate the function of other proteins by protein-protein interaction, and viral CARPs participate in attachment to host cells, but the precise biological function of CARP X and XI is still unknown. (Aspatwar A., *et al.* 2014).

## 1.5 Characteristics of the CA classes

### 1.5.1 $\alpha$ -CAs

The most studied class of carbonic anhydrase, as well as that of which there are the largest number of three-dimensional structures, is the  $\alpha$ -class. They contain the zinc ion ( $Zn^{2+}$ ) in their active site coordinated by three histidine residues (His94, His96 and His119) and a water molecule/hydroxide ion (see Figure 4). Available  $\alpha$ -CA structures, including most isoforms of human CA (hCA), reveal that the zinc ion is located in the pocket of the active site deep 15 Å (Figure 4).

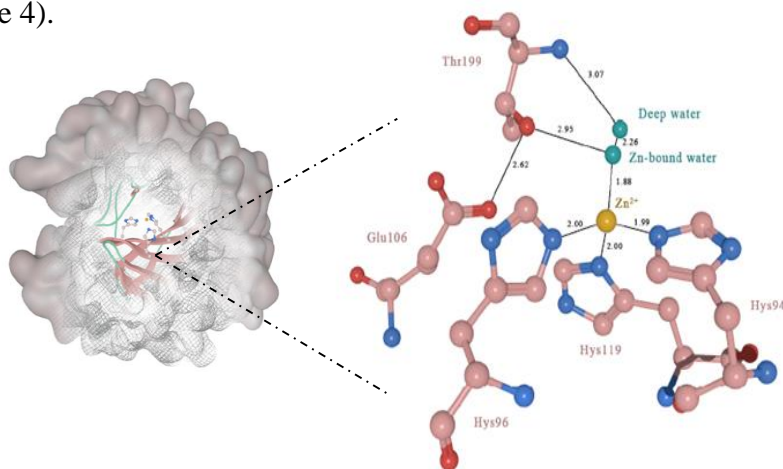
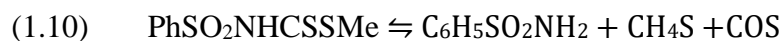
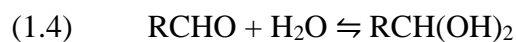
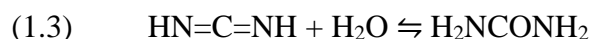
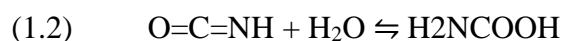


**Figure 4.** 3D structure and a particular of the active site of the human isoform II (hCAII). Legend: Orange sphere is the zinc ion; His 94, His 96, His119 are the amino acid residues of the catalytic triad; Thr199 and Glu106 are gate-keeping residues.

The water molecule bound to the zinc forms a hydrogen bond with the hydroxyl of Thr199, in turn linked to the carboxyl group of Glu106 (Supuran C.T., 2008). These interactions increase the nucleophilicity of the water molecule bound to the Zn(II) and orient the substrate ( $CO_2$ ) in a favorable position for nucleophilic attack. It is interesting to note that the above-mentioned residues, are conserved in all human CAs with catalytic activity (Figure 1), with the exception of the human isoform hCAVA where the proton shuttle residues is missing. Up to date are available the crystallographic structures of  $\alpha$  class CAs, such as hCA I, hCA II, hCA III, hCA IV, hCA V, hCA IX, hCA XII and hCA XIV (Alterio V., *et al.* 2012). Interesting, two human isoforms hCA IX and XII are associated with cancer and are involved in the pH regulation and progression of the tumor. The  $\alpha$ -CA are normally found in monomeric form with a molecular weight of approximately 29 kDa, with the

exception of hCA VI, hCA IX and XII which occur as dimers (Boztas B., *et al.* 2015; Dudutiene V., *et al.* 2014). The bacterial  $\alpha$ -CAs, such as those identified in the genome of *Sulfurihydrogenibium yellowstonense*, *S. azorensis* and *Neisseria gonorrhoeae*, are dimers formed by two identical active monomers. Among the various classes of CAs, the  $\alpha$ -class are the most active. The reactions catalyzed by  $\alpha$ -CA, as well as the physiological reaction of hydration of CO<sub>2</sub> (Supuran C.T. 2008) are: hydration of cyanide to carbonic acid (1.1), or of cyanamide to urea (1.2 – 1.3), hydration of aldehydes to geminal diol (1.4), hydrolysis of carboxylic or sulphonic esters (1.5 – 1.6) in addition to other minor hydrolytic processes (1.7 – 1.9). Recently, it has been demonstrated that  $\alpha$ -CA possess also the thioesterase activity (1.10) (Tanc M., *et al.* 2015) (see list below).

List of reactions catalyzed by  $\alpha$ -CAs:



(Ar = 2,4-dinitrophenyl)

(R = Me; Ph)



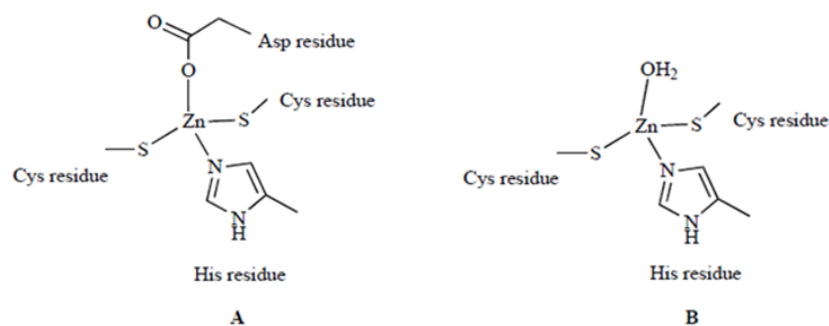


**Figure 6.** Coordination of Zn (II) in the  $\beta$ -CAs. A: *Porphyridium purpureum* and *Escherichia coli*; B: *Pisum sativum* and *Methanobacterium thermoautotrophicum*.

It has been demonstrated that at a pH of 7.5 or lower, the active site of carbonic anhydrase  $\beta$  is "locked", since the carboxyl group of an aspartic acid coordinates the zinc ion as a fourth ligand. At pH values higher than 8.3 the enzyme active site is converted in an open one, since the aspartate forms a salt bridge with residue Arg46 (numbering hp $\beta$ CA) stored in all the carbonic anhydrase from  $\beta$  class (Nishimori I., *et al.*, 2007). In this way, the molecule of water/hydroxide ion has the possibility to coordinate the metal ion to the completion of its tetrahedral geometry. As a result, the catalytic mechanism of  $\beta$ -CAs with the active site "open" is rather similar to the enzymes of  $\alpha$  class. Respect to the  $\alpha$ -class,  $\beta$ -CAs are oligomers formed by two or more identical subunits. Generally,  $\beta$ -CAs are dimers, tetramers and octamers. The monomeric subunit has a molecular weight of 25-30 kDa and the active form of the enzyme requires two subunits to reconstitute the catalytic site. Among the  $\beta$ -classes are available the crystal structures of the CA isolated from red alga *Porphyridium purpureum*, from chloroplasts of *Pisum sativum*, and prokaryotic CAs isolated from *Escherichia coli* and the archaeobacterium *Methanobacterium thermoautotrophicum* (Cronk J.D., *et al.* 2001; Strop P., *et al.* 2001).

### 1.5.3 $\gamma$ -CAs

The first  $\gamma$ -class carbonic anhydrase identified was isolated from the methanogenic archaeobacterium *Methanosarcina thermophila* and is indicated by the acronym "Cam" (Smith K.S. & Ferry J.G. 2000; Kisker C., *et al.* 1996; Iverson T.M., *et al.*, 2000; Innocenti A., *et al.* 2004; Alber B.E. & Ferry J.G. 1994). Compared with the  $\alpha$ -CA and  $\beta$ -CA Cam has a number of characteristics that differentiate it from these. In particular, the monomer Cam self-assembles

forming an active homo-trimer with an approximate molecular weight of 70 kDa (Figure 7).

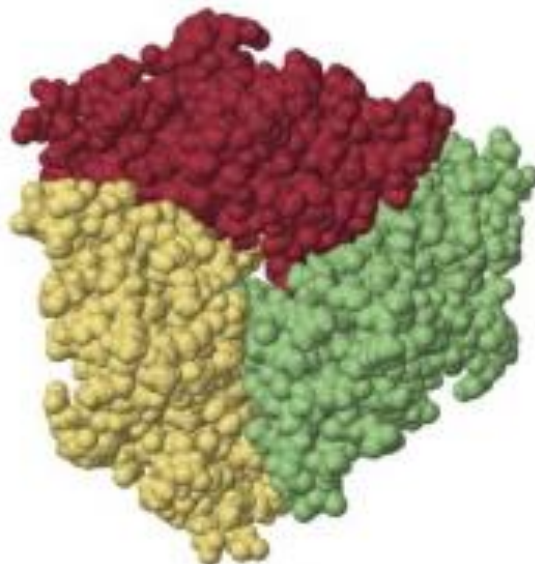


**Figure 7.** Tridimensional structure of g-CA. The monomers are indicated by red, yellow and green colors.

The single monomers of the  $\gamma$ -CAs, with molecular weight of about 20 kDa, did not show catalytic activity. The active sites are localized at the interface between the monomers and the ion Zn(II) is coordinated by three histidine residues each coming from a monomer.  $\gamma$ -CA active site assumed a trigonal bi-pyramidal geometry in the Cam containing zinc ion, and an octahedral geometry in enzyme binding cobalt. The catalytic mechanism is similar to that proposed for the  $\alpha$ -CA. At present, the mechanism zinc hydroxide, suggested for  $\gamma$ -CA is valid, but it is likely that in the active site of the enzyme may also be a balance between trigonal bi-pyramidal and tetrahedral metal ion species. The ligands in the active site of the enzyme, are in contact with the side chain of the residue Glu62, which suggests that this side chain can be protonated. In Cam, which has zinc uncomplexed, the side chains of residues Glu62 and Glu84 seem to share a proton and the residue Glu84 can be in multiple conformations. This suggests that the residue Glu84 performs a function similar to that of residue His64 in  $\alpha$ -CA (Supuran C.T. 2008).

#### 1.5.4 $\delta$ - e $\zeta$ -CAs

Unlike  $\delta$ -CAs, which are widely distributed throughout the marine phytoplankton, the  $\zeta$ -CAs are present only in diatoms. Recently in the marine diatom *Thalassiosira weissflogii* have been identified two CA, TweCA (or TWCA1) and CDCA1, belonging respectively to classes  $\delta$  and  $\zeta$  (Alterio V., *et al.* 2012). TweCA is a 27 kDa protein, probably a monomer, which does not show significant sequence similarity with other carbonic anhydrases. It is an example of convergent evolution, even if the crystallographic studies show that the active site is similar to that of  $\alpha$ -CA, with zinc ion coordinated by three histidine residues and one water molecule (Supuran C.T. 2008). The location of this enzyme in *T. weissflogii* and other diatoms it is not known, although recent studies suggest that TweCA has a cytoplasmic localization and catalyzes the reaction of dehydration of  $\text{HCO}_3^-$  to  $\text{CO}_2$ , increasing the concentration in the cytoplasm (Lee R.B.Y., *et al.* 2013).

CDCA1 is a protein belonging to the family of the  $\zeta$ -CA, is composed of three identical subunits named R1, R2, and R3 that form an active enzyme of 69 kDa. CDCA1 contains in the catalytic site ion Cd(II), although it is able to operate even with the ion Zn(II) (Figure 8). The rapidity of the exchange between the metal ion Zn(II) ion and Cd(II) depends on the availability of the metal ions in the marine environment. In literature is reported the crystallographic structure of the three subunits that comprise it. (Xu Y., *et al.* 2008).

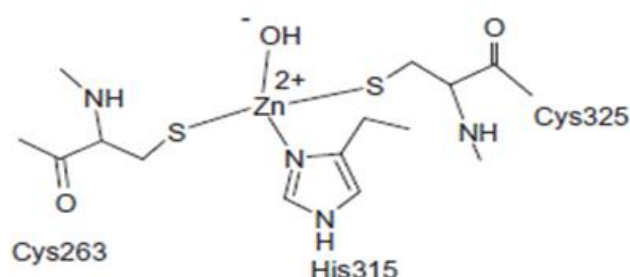


**Figure 8.**  $\zeta$ -CA. Ion Cd (II) can be replaced by Zn (II) without losing the catalytic activity (numbering of the R1 subunit of the enzyme of *T. weissflogii*).

In the subunit R2, the Cd(II) of the active site it is located in a pocket in the shape of funnel, coordinated by residues Cys263, His315, Cys325 and by a molecule of water. In the R1 subunit of CDCA1, the Cd(II) has a coordination identical to the R2 subunit (Figure 8). Since all three subunits have sequence

homology rather high, it is possible that the coordination geometry of the metal ion is similar also for the subunit R3. Since *T. weissflogii* grows in a marine habitat characterized by zinc salts and cadmium, it was hypothesized that the carbonic anhydrase CDCA1 containing cadmium, replace the enzyme TweCA in the mechanism of carbon concentration, when the concentration of marine zinc is very low. The mechanism of carbon concentration has developed in many species of phytoplankton to compensate for the low availability of CO<sub>2</sub> present in the water. In fact, carbonic anhydrases have the function of increasing the CO<sub>2</sub> concentration in proximity of ribulose 1,5-bisphosphate carboxylase / oxygenase (RuBisCo), the primary enzyme involved in carbon fixation, by allowing the enzyme to work efficiently (Xu Y., *et al.* 2008). Therefore, the carbonic anhydrases are key enzymes regarding the acquisition of inorganic carbon for photosynthesis in the phytoplankton.

### 1.5.5 $\eta$ -CAs, the last discovered class.

The causative agent of human malaria, *Plasmodium falciparum*, was one of the first protozoa to be investigated for the presence of CAs. The open reading frame of the malarial CA enzyme encodes a 600 amino acid polypeptide chain. In 2004, Krungkrai and coworkers cloned a truncated form of *Plasmodium falciparum* CA gene (GenBank: AAN35994.2) encoding for an active CA (named PfCA1) with a primary structure of 235 amino acid residues [77]. The metalloenzyme showed a good esterase activity with 4-nitrophenylacetate as a substrate. The authors observed that the highly conserved  $\alpha$ -CA active site residues, responsible for binding of the substrate and for catalysis, were present also in PfCA1 and considered thus the Plasmodium enzyme belonging to the  $\alpha$ -CA class. (Figure 9).

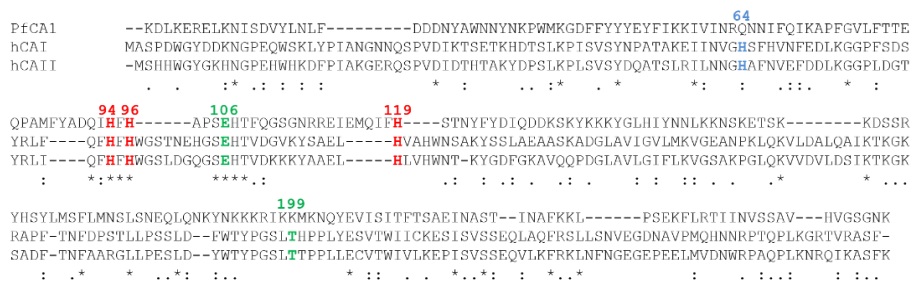
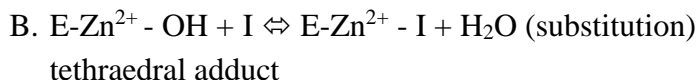
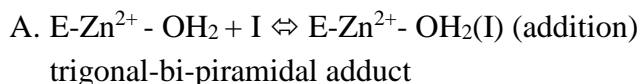


**Figure 9.** Multialignment of the amino acid sequence of the truncated form of the gene encoding for the PfCA1 with the amino acid sequences of the human isoforms (hCA I and II).

In the present thesis has been showed that *PfCAI* is a new CA-class, denominated with the Greek letter  $\eta$ -CA (Capasso C. & Supuran C.T., 2015). In fact, the alignment of the three-dimensional structures related to PfCA1 and several members of the  $\alpha$ -CAs, allowed us to reveal the unique characteristics of the  $\eta$ -CA (De Simone G., *et al.* 2015): the metal ion is coordinated by two histidine residues (His94, His96) and a residue of glutamine (Glu 119).

## 1.6 Inhibitors

There are two main classes of CA inhibitors (CAIs). The first class comprises the inorganic anions complexing metals, the second class includes organic ligands represented by the sulfonamides and related bioisosteres (sulfamates, sulfamides, hydroxamate and xanthates). Both classes of inhibitors work by coordinating the metal ion in the active site of the enzyme or through a replacement mechanism, forming tetrahedral adducts, or by an addition mechanism, generating trigonal-bi-pyramidal adducts (Figure 10) (Supuran C.T. 2008) according the following single reactions:



Since the thirties of the last century, it was known that inorganic ions more effective in inhibiting the activity of CA were cyanate and thiocyanate ions (Meldrum N.U. & Roughton F.J. 1933). Generally, anion inhibitors bind to zinc for addition thereby generating the trigonal-bipyramidal adduct (Figure 10A). The inorganic inhibitors complexing metals find no application in therapy because of their poor selectivity as well as the resulting numerous side effects. Moreover, having a reduced size, it is very complicated, if not impossible, to perform an optimization of their structure (Supuran C.T. 2008).

The sulfonamides derivatives even in this case their activity has long been known. In 1948, Krebs was the first to recognize its inhibitory action on CAs (Krebs HA, 1948) and, as of that date, the CAI entering treatment were dozens, even if, for some of these, the activities anti-CAs was not known. (Dogne J.M., *et al.* 2006; Knudsen J.F., *et al.* 2004; Supuran C.T. 2008). The primary

sulfonamides (R-SO<sub>2</sub>-NH<sub>2</sub>) are the classic inhibitors of CA and are used for the past half-century as diuretic and anti-glaucoma medications. Recently, they have also been found anticonvulsant, anti-obesity, anti-cancer, anti-infection and anti-panic properties, (Supuran C.T. *et al.* 2009; Winum J. *et al.* 2008; Domsic J.F., *et al.* 2008; Supuran C.T., *et al.* 2008; De Simone G. *et al.* 2008; Mincione F., *et al.* 2009; Krungkrai J. *et al.* 2008).

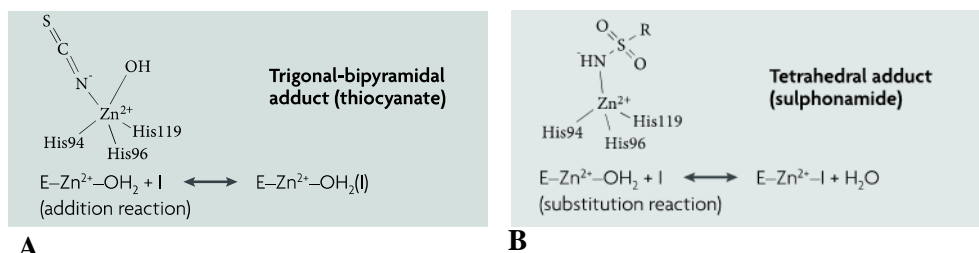


**Figure 10.** CAs inhibition mechanisms.

As discussed for the anions inhibitors, the mechanism of action of sulfonamides is based on the interaction of the inhibitor with the metal ion (Figure 10). In fact, the sulfonamide group, in contact with the acid environment of the catalytic site, loses a proton and forms a dative bond with the Zn (II) by substitution of the hydroxide ion (Figure 10 B). The inhibitor-metal complex is stabilized by two hydrogen bonds between the sulfonamide group and the residue of Thr199 (Figure 11).

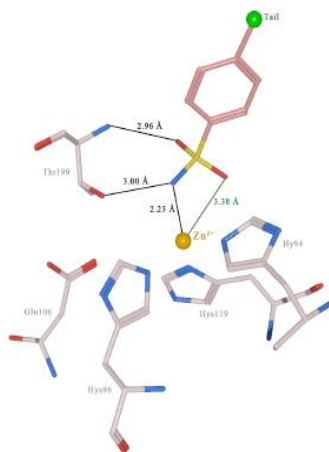


**Figure 11.** Binding of sulphonamidic CAI.

Some of CAI having significant inhibitory activity, such as sulfonamide derivatives used in clinical (acetazolamide, methazolamide, ethoxzolamide, diclorofenamide, dorzolamide and brinzolamide) are able to form a second bond with the metal cofactor through one of the sulfonamide oxygen (Supuran C.T. 2008).

The difficulties and problems founded in designing new CAs inhibitors as therapeutical agents are mainly due to the large number of human isoforms (16 human CAs, 13 of which have catalytic activity), the widespread location of the CA in many tissues/organs as well the lack of selectivity of the currently available inhibitors.

## 1.7 Activators

Activators of the CAs (CAAs) unlike CAIs, who have been extensively studied and are used in the clinic for prevention and treatment of various diseases, still represent an almost entirely unexplored field. There is a multitude of compounds such as biogenic amines (histamine, serotonin, catecholamines), amino acids, oligopeptides and small proteins, that are capable of effectively activate many CA isoenzymes. Several CAA design studies, considered as lead molecules histamine or carnosine (Temperini C., *et al.* 2006; Nishimori I., *et al.* 2007). Through the use of techniques, such us electron spectroscopy, X-ray crystallography and kinetics measurements that activators bind at the cavity of the active site, while CA inhibitors bind to metal core. CAAs participate in the displacement of the protons between the metal ion, bound to a water molecule, and the environment. This determines an increase of the hydroxylated forms of the metal, which corresponds to the catalytically active form of the enzyme (Clare B.W. & Supuran C.T. 1994). In the last few years, have been reported the crystal structures of the adducts formed by human isoforms hCA, hCAII and their activators (Temperini C., *et al.* 2007) in addition to those of histamine, dating to 1997 (Briganti F., *et al.* 1997). CAAs participate in a network of hydrogen bonds and hydrophobic interactions with specific amino acid residues or water molecules present in the active site. This explains their different power and ways of interaction with the various isoenzymes.

## **Chapter 2. Biotechnological and Biomedical application of CAs**

### **2.1 Carbon capture and storage (CCS)**

Has been repeatedly said that CAs are involved in a lot of physiological processes and relevant biochemical reactions, one of these is the carbon cycle and it is not surprising since the carbon is present in earth's atmosphere mainly as gas, the CO<sub>2</sub> (about 1,500 billion tons of carbon are present in the biosphere) (Revelle R. & Munk W. 1977). The carbon cycle is closely related to the flow of energy and productivity that crosses the biosphere. Photosynthesis and respiration are the two fundamental processes that govern this cycle and, are the main responsible for the major energy transfers, too. Photosynthesis is the first step of the carbon cycle. It allows that the carbon, present in the atmosphere as carbon dioxide, is fixed into organic compounds such as carbohydrates, fats, proteins and other biological molecules. The photosynthetic process is the anabolic phase of the carbon cycle and takes place out of the ground. In the soil, instead, it is realized the second step of the carbon cycle, i.e. the demolition of the organic substances produced by photosynthesis plant. In fact, organic debris, dead organisms containing carbon compounds, including sugars, cellulose, starch and others, are subject to the degradation, which corresponds to the catabolic phase of the carbon cycle. The catabolism of the carbon finally ends with the final processing into CO<sub>2</sub>, which in part is fixed in the ground in the form of calcium carbonate, in part in the water in form of carbonic acid and partly back into the air (Falkowski P., *et al.* 2000). Environmental CO<sub>2</sub> is the primary source of carbon and, in recent years, has increased from about 280 ppm to 390 ppm (Dlugokencky E. 2016). This increase was related to human activities during and after the industrial revolution, which began in 1850. In addition, from 1970 to 2004, CO<sub>2</sub> emissions increased by an average of 9% a year. The amount of CO<sub>2</sub> produced by human activities was higher than those assimilated from biomasses. Energy production, in fact, requires fossil fuels, which release about 24 billion tons of CO<sub>2</sub> per year (Huesemann M.H., *et al.* 2009; Falkowski P., *et al.* 2000). The production of CO<sub>2</sub> is linked to the industrial development that must necessarily reduce its production and/or reuse. To stabilize CO<sub>2</sub> in the atmosphere, a number of CO<sub>2</sub> sequestration methods have been proposed (Reichle D., *et al.* 1999). Most of them expect that the CO<sub>2</sub> captured from the flue gases is compressed, transported to the sequestration site

and injected within specific areas for long-term storage. This procedure determines an increase of the costs of the capture and storage processes (CCS). (Gentziz T., *et al.* 2000, Abadie L.M. & Chamorro J.M. 2008). In the last years, an industrial process very active is the biomimetic capture of CO<sub>2</sub>. This approach relies on use of the carbonic anhydrase, which is able to selectively bind the CO<sub>2</sub> and transform it into carbonate ion (Borchert, M. & Saunders P. 2008; Forsman C., *et al.* 1988). However, the biomimetic approach is greatly limited by the harsh conditions required in these processes, i.e., high temperatures and high concentrations of organic ions and metals. (Bond G.M., *et al.* 2001; Fisher Z., *et al.* 2012; Kanbar B. & Ozdemir, E. 2010). In order to capture CO<sub>2</sub> have been developed different techniques, such as absorption into a liquid, adsorption on a solid, gas phase separation, and membrane systems (Yang H., *et al.* 2008), and among these the use of thermostable CAs has been described for chemical absorption (Wang M., *et al.* 2011).

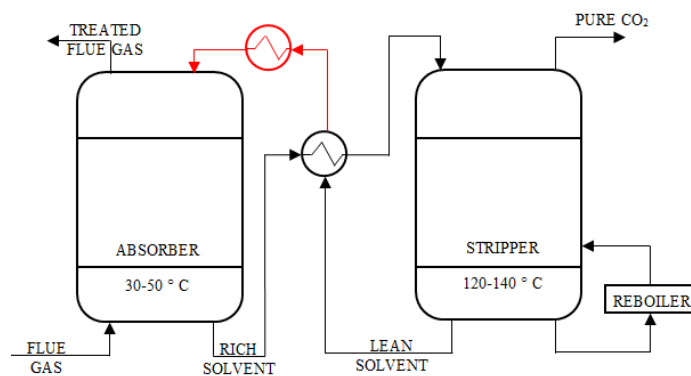


**Figure 12.** Schematic representation of a chemical absorption process. Red lines corresponds to absorber regeneration path.

This process involves the reaction of CO<sub>2</sub> with a chemical solvent to form an intermediate compound, which is then treated with heat, regenerating the original solvent and a CO<sub>2</sub> stream. In a typical chemical absorption process (Figure 12), the flue gas containing CO<sub>2</sub> enters from the bottom into a packed absorber column at low temperature (30–50 °C) and then contacts a CO<sub>2</sub> absorber; after absorption, the CO<sub>2</sub>-rich solvent is sent to a stripper operating at high temperatures (120–140 °C) to recover the absorber and CO<sub>2</sub>. After regeneration, the CO<sub>2</sub>-lean solvent is pumped back to the absorber for cyclic use, while the pure CO<sub>2</sub> is compressed for the subsequent transportation and storage (Wang M., *et al.* 2011; Yu C.H., *et al.* 2012). The main energy cost

associated to this process is due to the heat required for the desorption and the pumping of the absorbing solution around the system.

The biomimetic approach represents an interesting strategy for CO<sub>2</sub> capture. It, in fact, allows CO<sub>2</sub> conversion to water-soluble ions, offering many advantages over other methods, for example its eco-compatibility and the possibility to use the enzyme for multiple cycles. Moreover, thermophilic enzymes are thermostable and thermoactive respect to the mesophilic counterpart, and their use is preferred in environments characterized by hard conditions, such as those of the carbon capture process (high temperature, high salinity, extreme pH). Additionally, there are some disadvantages using free enzyme in solution because the repeatable usage is limited, and generally is not possible to recover the enzyme from the reaction environment. Fortunately, these disadvantages can be eliminated immobilizing the enzyme on specific supports.

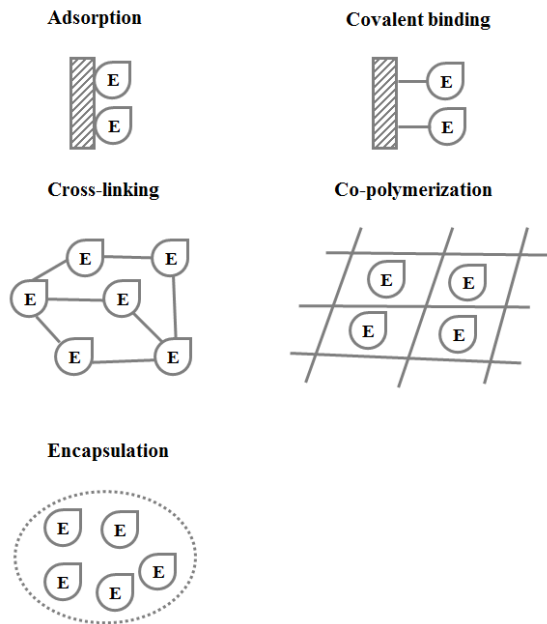


**Figure 13.** Immobilization methods.

In literature have been described different immobilization techniques schematized in figure 13, such as adsorption (ionic interaction, hydrogen bonds, Van der Waal forces), covalent binding, crosslinking, copolymerization, encapsulation (membrane confinement).

**Table I.** Attributes of immobilized enzymes.

| <b>Advantages</b>                                  | <b>Disadvantages</b>                          |
|--|---|
| Amenable to continuous and batch formats           | Loss of enzyme activity upon immobilization   |
| Reuse over multiple cycles possible                | Unfavorable alterations in kinetic properties |
| Improved stability over soluble enzyme forms       | Cost of carrier and fixing agents             |
| Favorable alterations in pH and temperature optima | Cost of immobilization process                |
| Sequester enzyme from product stream               | Mass transfer limitations                     |
| Co-immobilization with other enzymes possible      | Subject to fouling                            |

All of these processes have different advantages or disadvantage depending to the final application (Di Cosimo R., *et al*, 2013) (Table I) even if among all these methods, covalent immobilization generally ensures the highest strength of the bonding between support and enzyme. It, in fact, minimize the leakage issues, usually does not interfere with reagents/products mass transfer, and allows the highest enhancement of operational stability.

**Table II.** Immobilization matrix classification.

| <b>Classification of Supports</b> |   |
|-----------------------------------|---|
| <b>Organic</b>                    |   |
| Natural polymers                  | Polysaccharides: cellulose, dextrans, agar, agarose, chitin, alginate<br>Proteins: collagen, albumin<br>Carbon                          |
| Synthetic polymers                | Polystyrene<br>Other polymers: polyacrylate<br>polymethacrylates, polyacrylamide,<br>polyamides, vinyl, and allyl-polymers              |
| <b>Inorganic</b>                  | Natural minerals: bentonite, silica<br>Processed materials: glass (nonporous and controlled pore), metals, controlled pore metal oxides |

As shown in Table II, the matrixes or supports commonly used for immobilization of enzymes or whole cells are grouped in two major categories: 1) Organic (natural polymers and synthetic polymers) and 2) Inorganic materials.

The characteristics of the matrix are crucial in determining the performance of the enzyme and the system functionality. For example, an ideal support should have properties that include physical resistance to compression, hydrophilicity, inertness toward enzymes ease of derivatization, biocompatibility, resistance to microbial attack, and availability at low cost. (Trevan M., *et al.* 1980; Brodelius P. & Mosbach K. 1987; Bucholz K. & Klein J. 1987).

## **2.2 Carbonic anhydrases from pathogens as druggable enzymes**

### ***2.2.1 Pathogens***

The microorganisms that normally do not cause disease in humans, are in a state of commensalism or mutualism with the host (Roux O., *et al.* 2011; Joyce S.A., Watson R.J., Clarke D.J. 2006; Soto W., Punke E.B., Nishiguchi M.K. 2012). This non-harmful condition occurs when the immune system works well, but the same organisms can cause infection when the latter fails. All microorganisms that cause diseases or illnesses to their host are defined as pathogens (Cardoso T., *et al.* 2012).

Pathogens can be distinct into viruses, bacteria, fungi and protozoa. The pathogenicity of microorganisms is defined by the virulence, which is the ability of a pathogen to cause a damage more or less severe in the host (Webb S.A. & Kahler C.M. 2008; Grosso-Becera M.V., *et al.* 2015). Genetic characteristics, biochemical and structural properties of the pathogen influence the pathogen virulence, which allows the microorganism to cause disease through a set of actions on the host (Cardoso T., *et al.* 2012). These actions may be its ability to evade and/or fight the immune system, to assimilate nutrients from the host or to perceive environmental changes. All these abilities implicate the action of numerous enzymes. Enzymes considered as virulence factors are generally active against host components and contribute to virulence by damaging host tissues (Schaller M., *et al.* 2005; Alp S. 2006; Bostanci N. and

Belibasakis G.N. 2012).(Cox G.M., Mukherjee J., Cole G.T., *et al.* 2000; Cox G.M., McDade H.C., Chen S.C., *et al.* 2001).

Cloning the genomes of many pathogenic microorganisms offered the possibility of exploring alternative pathways for inhibiting virulence factors or proteins essential for their life cycle. (Sainsbury P.D., *et al.* 2015). Using this approach, carbonic anhydrase has been identified in the genome of bacteria, fungi and protozoa, as a new class of enzymes related to microbial virulence (Capasso C. & Supuran C.T. 2013).

### **2.2.2 Bacterial CAs**

Prokaryotes include several kinds of microorganisms, such as archaea, bacteria and cyanobacteria (Tibayrenc M. & Ayala F.J. 2012). It has been demonstrated that CAs are enzymes encoded by the genome of many pathogenic organisms. Recently, CAs started to be investigated in detail in several pathogenic bacteria, in the search for antibiotics with a novel mechanism of action, since it has been demonstrated that in many bacteria, CAs are essential for the life cycle of the organism. As reported in Table III, bacteria encode for enzymes belonging to the  $\alpha$ -,  $\beta$ -, and  $\gamma$ -CA classes (Vullo D., *et al.* 2014; Nishimori I., *et al.* 2014; Alafeefy A.M., *et al.* 2014; Vullo D., *et al.* 2013). Thus, the  $\alpha$ -CAs from *Neisseria spp.*, *Helicobacter pylori* and *Vibrio cholerae* as well as the  $\beta$ -class enzymes from *Escherichia coli*, *Helicobacter pylori*, *Mycobacterium tuberculosis*, *Brucella spp.*, *Streptococcus pneumoniae*, *Salmonella enterica* and *Haemophilus influenzae* have been cloned and characterized in detail in the last few years.

**Table III.** CAs from bacteria cloned and characterized so far, and their inhibition studies.

| Bacteria  | Class    | Acronym       | Inhibition studies   |                       |
|---|----------|---------------|----------------------|-----------------------|
|   |          |               | In vitro             | In vivo               |
| <i>Neisseria gonorrhoeae</i>                          | $\alpha$ | NgoCA         | Sulfonamides, anions | Sulfonamides          |
| <i>Neisseria sicca</i>                                | $\alpha$ | NsiCA         | Sulfonamides         | Sulfonamides          |
| <i>Helicobacter pylori</i>                            | $\alpha$ | hpaCA         | Sulfonamides, anions | Sulfonamides          |
| <i>H. pylori</i>                                      | $\beta$  | hp $\beta$ CA | Sulfonamides, anions | Sulfonamides          |
| <i>Escherichia coli</i>                               | $\beta$  | EcoCA         | -                    | -                     |
| <i>Haemophilus influenzae</i>                         | $\beta$  | HICA          | Bicarbonate          | -                     |
| <i>Mycobacterium tuberculosis</i>                     | $\beta$  | mtCA 1        | Sulfonamides         | Sulfonamides, phenols |
|   | $\beta$  | mtCA 2        | Sulfonamides         | Sulfonamides, phenols |
|   | $\beta$  | mtCA 3        | Sulfonamides         | Sulfonamides, phenols |
| <i>Brucella suis</i>                                  | $\beta$  | bsCA 1        | Sulfonamides         | Sulfonamides          |
|   | $\beta$  | bsCA 2        | Sulfonamides         | Sulfonamides          |
| <i>Streptococcus pneumoniae</i>                       | $\beta$  | PCA           | Sulfonamides, anions | Sulfonamides          |
| <i>Salmonella enterica</i>                            | $\beta$  | stCA 1        | Sulfonamides, anions | -                     |
|   | $\beta$  | stCA 2        | Sulfonamides, anions | -                     |
| <i>Vibrio cholerae</i>                                | $\alpha$ | VchCA         | Sulfonamides, anions | Sulfonamides          |
| <i>Sulfurihydrogenibium yellostonense</i>             | $\alpha$ | SspCA         | Sulfonamides, anions | -                     |
| <i>Sulfurihydrogenibium azorense</i>                  | $\alpha$ | SazCA         | Sulfonamides, anions | -                     |
| <i>Clostridium perfringens</i>                        | $\beta$  | CpeCA         | Sulfonamides, anions | -                     |
| <i>Porphyromonas gingivalis</i><br>(-) to investigate | $\gamma$ | PgiCA         | Sulfonamides, anions | -                     |

Within the Bacteria domain, the enzymes from *Neisseria gonorrhoeae*, *Neisseria sicca*, *H. pylori* and *V. cholerae* belong to the  $\alpha$ -class. The *N. gonorrhoeae* CA has a molecular mass of 28 kDa, being rather homologous to mammalian CAs and showing high CO<sub>2</sub> hydratase activity (similar to the human isoforms hCA II) as well as esterase activity for the hydrolysis of p-NpA. Instead, the *H. pylori*  $\alpha$ -CA displayed an activity similar to that of the human isoform hCA I for the CO<sub>2</sub> hydration reaction, being thus less efficient catalytically (see Table VI). (Cardoso T., *et al.* 2012; Cox G.M., *et al.* 2000; Cox G.M., *et al.* 2001; Bostanci N. & Belibasakis G.N. 2012; Alp S. 2006; Schaller M., *et al.* 2005; Tibayrenc M., & Ayala F.J. 2012; Roux O., *et al.* 2011; Joyce S.A., *et al.* 2006; Nishiguchi MK. 2012; Krungkrai S.R., *et al.* 2001; Sein K.K. & Aikawa M. 1998; Joseph P., *et al.* 2011; Supuran C.T. 2008).

The thesis has been focalized the attention on the carbonic anhydrases encoded by the genome of *Vibrio cholerae*. This gram-negative bacterium is the causative agent of cholera. The microorganism colonizes the upper small intestine where sodium bicarbonate is present at a high concentration. It has been demonstrated that sodium bicarbonate is an inducer of virulence gene expression in *Vibrio* (Cash R.A., *et al.* 1974). Since *V. cholerae* lacks of bicarbonate transporter proteins in its genome, it has been hypothesized that the pathogen utilizes the CAs system to accumulate bicarbonate into the cell to activate its virulence.

### **2.2.3 Protozoan CAs**

Malaria, a mosquito-borne disease of humans and other animal species, is caused by parasitic protozoa species belonging to the genus *Plasmodium*. Six different *Plasmodium* species infect humans: *Plasmodium falciparum*, *Plasmodium vivax*, *Plasmodium ovale*, *Plasmodium malariae* and the zoonotic *Plasmodium knowlesi*. Malaria parasites follow a complex lifecycle that involves an intermediate host such as humans and the definitive host, the mosquito vector. Following injection of sporozoite stage parasites from an infected female Anophelene mosquito into a human host, *Plasmodium* parasites move to the liver and invade hepatocytes where they replicate to form merozoites that are ultimately released into the blood circulation.

Few protozoan parasites have been investigated for the presence and druggability of CAs. The malaria-provoking organism *Plasmodium falciparum* was undoubtedly the first one. Protozoa utilize purines and pyrimidines for DNA/RNA synthesis during its exponential growth and replication. Plasmodia synthesize pyrimidines de novo from  $\text{HCO}_3^-$ , adenosine-5'-triphosphate (ATP), glutamine (Gln), aspartate (Asp) and 5-phosphoribosyl-1-triphosphate (PRPP).  $\text{HCO}_3^-$  is the substrate of the first enzyme involved in the Plasmodia pyrimidine pathway, which is generated from  $\text{CO}_2$  through the action of CA. Studies from Krungkrai's and our laboratories showed that *Plasmodium spp.* encode for several  $\alpha$ -class CAs, and these enzymes have significant catalytic activity (as esterase with 4-nitrophenyl acetate as substrate) and are inhibited by primary sulfonamides, the main class of CAIs. The best investigated such enzyme has been denominated PfaCA1. Here, we showed thereafter that the situation is rather different: PfaCA1 is not an  $\alpha$ -CA but it belongs to the  $\eta$ -class, being however sensitive to sulfonamide inhibitors.

## Chapter 3. Materials and Method

### 3.1 Identification of the CA genes in thermophilic and pathogenic bacteria

To determine the presence of carbonic anhydrases have been used similarity searching programs, such as BLAST and FASTA. As query sequences were used the amino acid sequences of CAs belonging to  $\alpha$ -,  $\beta$ - or  $\gamma$ -class. The search showed that the genome of *Sulfurihydrogenibium yellowstonense* YO3AOP and *Sulfurihydrogenibium azorense* encoded for  $\alpha$ - and  $\gamma$ -CAs. We focalized our attention on the most active class of CAs, the  $\alpha$ -class. The  $\alpha$ -CAs *S. yellowstonense* and *S. azorense* were named SspCA and SazCA, respectively.

The analysis performed on *Vibrio cholerae* genome identified three classes of carbonic anhydrase: the  $\alpha$ -CA, indicated with the acronym VchCA; the  $\beta$ -CA, named VchCA $\beta$ ; and the  $\gamma$ -CA, called VchCA $\gamma$ .

The gene encoding for PfCA1 identified in the genome of the protozoan *Plasmodium falciparum*, were cloned into the pET-43.1a expression vector and kindly provided by Prof. Sally-Ann Poulsen Griffith University, Brisbane, Australia.

### 3.2 Bacterial strains used for heterologous protein expression

#### 3.2.1 *E. coli* BL21(DE3)

*E. coli* BL21 host strain is the most used in standard applications of recombinant expression. *BL21-Gold (DE3)* (Agilent) is a robust strain of *E. coli*, able to grow vigorously in minimal media (Chart *et al.*, 2000). This strain presents the Hte phenotype, which increases the efficiency of transformation of the cells. In addition, the strain lacks of proteases OmpT and Leon, which can degrade the recombinant protein intact; and of endonuclease (endA), which can degrade the plasmid DNA isolated from mini preparations. The table IV shows other details of the cell genotype. The host strain lysogenized from the phage DE3 fragment, presents a copy of the bacteriophage T7 gene 1 integrated in the genome, which encodes the T7 RNA polymerase. Such gene is under the control of the promoter lacUV5 (derivative of the lac promoter) sensitive to the

adjustment by the cAMP-CRP complex and inducible by isopropyl- $\beta$ -D-1-thiogalattopyranoside (IPTG) (Studier & Moffat 1986). The T7 RNA polymerase drives the expression of the gene encoding for the recombinant protein.

### **3.2.2 *E. coli ArcticExpress (DE3)***

The strain of competent cells *ArcticExpress (DE3)* (Agilent) has the characteristics described above for the strain *BL21-Gold (DE3)* (Agilent). In addition, these cells are designed to deal with the problem of the insolubility of proteins, which may occur during the expression of the recombinant proteins. *Arctic Express (DE3)* cells, in fact, express proteins chaperone Cpn10 and Cpn60 of the psychrophilic bacterium *Oleispira antarctica*. These chaperonins have an amino acid identity with the chaperonins GroEL and GroES of *E. coli* by 74% and 54%, respectively, and show a good activity of protein folding at temperatures between 4 ° C and 20 ° C. These chaperonins, once expressed in cells ArcticExpress, optimize production of the heterologous protein at low temperatures and, presumably increase the amount of soluble and active recombinant protein produced. See table IV for more details on the genotype.

### **3.2.3 *E. coli DH5 $\alpha$***

Competent Cells *Subcloning Efficiency*™ *DH5 $\alpha$* ™ (Life Technologies) are generally used to propagate plasmids and have good processing efficiency. This strain carries a mutation that inactivates the endonuclease I (endA1) that could degrade the plasmid DNA during the extraction, and a mutation which inactivates the endonuclease EcoK I, but not the methylase activity (hsdR17 (RK, mk +)). These cells lack the recombinase recA1 that is responsible for the recombination between the plasmid and the *E. coli* genome, making the plasmid more stable. They can also be used to blue/white screen for bacterial plates containing Bluo-gal or X-Gal. More details on the genotype are shown in table IV.

**Table IV.** Host strain genotype

| <b>Host strain</b>           | <b>Genotype</b>   |
|------------------------------|---|
| BL21-Gold (DE3)              | <i>E. coli</i> B F <sup>-</sup> <i>ompT hsdS</i> (r <sub>B</sub> <sup>-</sup> m <sub>B</sub> <sup>-</sup> ) <i>dcm</i> <sup>+</sup> Tet <sup>r</sup> <i>gal</i> λ(DE3) <i>endA</i> The  |
| ArcticExpress (DE3)          | <i>E. coli</i> B F <sup>-</sup> <i>ompT hsdS</i> (r <sub>B</sub> <sup>-</sup> m <sub>B</sub> <sup>-</sup> ) <i>dcm</i> <sup>+</sup> Tet <sup>r</sup> <i>gal</i> λ(DE3) <i>endA</i> Hte [ <i>cpn10 cpn60 Gent</i> <sup>r</sup> ] |
| Subcloning Efficiency™ DH5α™ | F <sup>-</sup> Φ80 <i>lacZ</i> ΔM15Δ( <i>lacZYA-argF</i> ) U169 <i>recA1 endA1 hsdR17</i> (r <sub>k</sub> <sup>-</sup> , m <sub>k</sub> <sup>+</sup> ) <i>phoA supE44 thi-1 gyrA96 relA1</i> λ <sup>-</sup>                     |

### 3.3 Culture medium: LB (Luria-Bertani)

The culture medium LB (Luria-Bertani), nutritionally rich and designed for the growth of pure cultures of recombinant strains, is prepared by dissolving 20g of the prepared powder (LB BROTH, LENNOX-Laboratorios Conda) per liter of distilled water and sterilized by autoclaving at 121 ° C for 20 minutes. Heat-labile substances, such as antibiotics and IPTG, are added after sterilization and filtered with Millipore Millex-GP filter (0,22μm) during the preparation.

### 3.4 Expression vector: pET15b (Novagen)

The expression vector pET-15b (5708 bp) is constituted by an origin of replication and the gene for β-lactamase, which confers resistance to the antibiotic ampicillin, in addition to the viral T7 promoter, a multiple cloning site (MCS) for the enzymes restriction most common and a sequence that encodes a tag of histidines. The recombinant protein is expressed with the tag of histidines at the N-terminal (Figure 14), which allows the rapid purification of the recombinant protein by affinity chromatography using a specific resin loaded with metal ions. Furthermore, in the vector a cutting sequence recognized by the enzyme thrombin allows removal of the fusion tag. The expression of the gene cloned into the vector is controlled by the T7 promoter and recognized specifically by the T7 RNA polymerase of *E. coli*. Its expression is induced by 'isopropyl-β-D-1-thiogalattopiranoside (IPTG). Once the polymerase has reached a sufficient expression level, it binds to the promoter and initiates transcription.

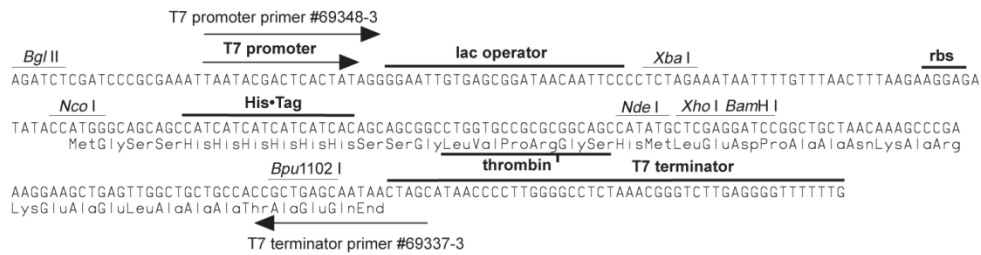


**Figure 14.** pET-15b Novagen cloning/expression region

## 3.5 Cloning procedure

### 3.5.1 Construct preparation

The CA gene encoding for the recombinant protein have been designed using the Life Technologies software. All the genes encoding for a  $\alpha$ -CAs were devoid of the signal peptide (first twenty amino acid residues of the peptide sequence) and fused at the N-terminal with a tag of histidines essential for the subsequent purification of the protein. These genes were synthesized and inserted by Life Technologies in the plasmid pMK-T, containing cleavage sites for the restriction enzymes NdeI and XhoI at the 5' end and 3' of the genes, respectively. Subsequently, it was shipped to the laboratory. The 5  $\mu$ g of plasmid aforementioned in lyophilized form were resuspended in 15  $\mu$ l RNase free water. The concentration was determined using the NanoDrop™ 1000 Spectrophotometer (Thermo Scientific). The DNA was stored at -20 °C.

### 3.5.2 Plasmid DNA amplification into *E. coli* DH5 $\alpha$ cells

The pMK-T cloning vector prepared as above was amplified using competent cells of *E. coli* DH5 $\alpha$ . An aliquot of 50  $\mu$ l of cells, stored at -80 °C, was thawed on ice for 2-5 minutes and transformed with 100 ng of plasmid DNA. The cell suspension was mixed gently and placed on ice for 30 min. and then subjected to heat shock (42 °C for 20 sec). After the addition of 950  $\mu$ l of LB medium preheated, the mixture of transformation was incubated for 1 h at 37 °C on a horizontal shaker (CERTOMAT® BS-1), at a speed of 200 rpm. Then, a quantity  $\geq$  200 L of the mixture of transformation, were plated on solid medium (LB-Agar + kanamycin 50  $\mu$ g / ml) and the plates were incubated overnight at 37 °C. To obtain higher quantities and a better purity of the plasmid

DNA, it was set up a maxi preparation, for which a single bacterial colony was inoculated into 200 ml of LB containing ampicillin 100 mg/ml and made to grow at 37 ° C for 16 hours. The culture was then centrifuged at 5000xg for 5 minutes and the pellet treated using The PerfectPrep EndoFree™ Plasmid Maxi Kit (5 PRIME), following the procedures described in the manual. Briefly, the plasmid DNA was then adsorbed on a column of silica gel and separated from RNA, proteins and other cellular components. The final elution was achieved with ribonuclease free water. The DNA was stored at -20 ° C.

### ***3.5.3 Vector digestion***

The expression vector pET-15b was digested with the restriction enzymes NdeI and XhoI (Biolabs, New England). The digestion of the plasmid DNA was carried out for 60 minutes at 37 ° C using 50 U of enzyme NdeI, and 50 U of XhoI enzyme in a reaction mixture containing 3 micrograms of BSA in Tris-HCl 6mM pH 7.5 containing 6 mM MgCl<sub>2</sub>, 50 mM NaCl and 1 mM DTT. The reaction was conducted in a final volume of 30 µl. After digestion, the linearized plasmid was treated with 0.1 U of bovine alkaline phosphatase and incubated at 37 ° C for 30 minutes. The alkaline phosphatase determines the dephosphorylation of the linearized plasmid to prevent it can reclose on itself. The sample was then loaded on 1% agarose gels in TAE buffer (Tris-acetate-EDTA). The run was conducted using a horizontal electrophoresis apparatus for 40 minutes at 90V. As molecular weight marker was used a mixture of DNA fragments of known size (1 Kb Plus DNA Ladder™ Thermo Fisher Scientific). Agarose gel was prepared adding ethidium bromide to a final concentration of 1µg/ml, to visualize the fragments of DNA by irradiation of the gel with ultraviolet light. The band corresponding to the linearized plasmid with NdeI and XhoI was excised from the gel and purified using Agarose GelExtract Mini Kit (5 Prime). The concentration of the purified plasmid was determined using the NanoDrop™ 1000 Spectrophotometer (Thermo Scientific). Similarly, the pMK-T cloning vector, containing the genes coding for the CAs, was digested with the restriction enzymes NdeI and XhoI (Biolabs, New England). The band corresponding to the DNA encoding for CAs (SspCA or SazCA or VchCA or VchCAβ or VchCAγ) was excised from the gel and purified using Agarose GelExtract Mini Kit (5 PRIME). The concentration of the purified fragment was determined by NanoDrop™ 1000 Spectrophotometer (Thermo Scientific).

### ***3.5.4 Ligation Reaction***

50 ng of the fragment corresponding to the DNA encoding for CAs (SspCA or SazCA or VchCA or VchCA $\beta$  or VchCA $\gamma$ ) was ligated into the expression vector pET-15b (100 ng). Constructs pET-15b / SspCA, pET-15b / SazCA, pET-15b / VchCA, pET-15b / VchCA $\beta$  and pET-15b / VchCA $\gamma$  were generated. The ligation reaction was carried out at 16 °C for 16 hours in the presence of 400 U of T4 DNA ligase supplied in 10 mM Tris-HCl, pH 7.4, 0.1 mM EDTA, 1 mM DTT, 200 mg / ml BSA and 50% glycerol, and 1X T4 DNA ligase buffer (50 mM Tris-HCl pH 7.5, 10 mM MgCl<sub>2</sub>, 10 mM DTT, 1 mM ATP, 25 mg / ml BSA) (New England BioLabs).

Three  $\mu$ L of the ligation reaction were used to transform XL10-Gold Ultracompetent cells (Stratagene) with high efficiency of transformation. The transformation was performed by thermal shock, and the cells plated on medium containing as ampicillin 100  $\mu$ g/ml (pET-15b contain the gene for ampicillin resistance)

### ***3.5.5 Clone identification***

Ten colonies grown on LB-agar plate with ampicillin 100  $\mu$ g/ml were analyzed to verify the presence of the gene encoding the CA of interest in the construct prepared as described above. For this purpose, the plasmid DNA was extracted from the colonies selected using the “The PerfectPrep EndoFree Plasmid Maxi” kit (5 PRIME) based on the method of lysis with alkali as described by Sambrook *et al.* 1992. Each bacterial colony was inoculated in 200 ml of LB containing ampicillin 100  $\mu$ g/ml and grown at 37 °C overnight. The cultures were then centrifuged at 6000xg for 5 min at 4 ° C and the resulting pellet suspended in Tris-HCl 10 mM pH 8.3. The bacterial suspension was lysed under alkaline conditions and the lysate neutralized in a buffer with a high salt concentration. The plasmid DNA was then adsorbed on a column of silica gel and separated from RNA, proteins and other cellular components. The final elution was achieved by water ribonuclease free. To verify that the gene encoding for SspCA or SazCA or VchCA or VchCA $\beta$  or VchCA $\gamma$  was correctly inserted, the purified plasmid DNA (100 ng/ $\mu$ L) was sequenced using the PRIMM service.

### ***3.5.6 Construct amplification***

The amplification of the expression plasmid pET-15 b containing the gene encoding for the CA of interest (SspCA or SazCA or VchCA or VchCA $\beta$  or VchCA $\gamma$  or PfCA1) was performed as described previously.

## **3.6 Expression of heterologous proteins in *E. coli* cells**

### ***3.6.1 Small-scale optimization***

To optimize the conditions for the expression of recombinant proteins, growth was performed in a small scale. After the addition of IPTG, the production of proteins of interest was monitored at different times of incubation (2h, 4h, 6h, and overnight). Moreover, it has also been used different concentrations of IPTG (0.1 mM, 0.5 mM, 1 mM). Aliquots of samples were analyzed by SDS-PAGE.

### ***3.6.2 Large scale expression***

For the heterologous expression of SspCA, SazCA, VchCA and VchCA $\beta$  it has been used *E. coli* BL21 (DE3) cells; while for the expression of VchCA $\gamma$  and PfCA1 it has used ArcticExpress (DE3) cells. Competent expression cells were transformed using the thermal shock technique, which facilitates the passage of DNA through bacterial wall. Briefly, 50  $\mu$ l of competent cells stored at -80 ° C, was thawed on ice for approximately 5 minutes. Then, the cells were incubated with for 10 minutes on ice in presence 1  $\mu$ l of  $\beta$ -mercaptoethanol (1.42 M) and subsequently transformed with 100 ng of plasmid DNA. The cell suspension was mixed gently and placed on ice for 30 min. After the addition of 950  $\mu$ L of LB medium preheated, the mixture of transformation was incubated (1 h at 37 ° C on a horizontal shaker at a speed of 200 rpm). Then, a quantity  $\geq$  200 L of the mixture of transformation, were plated on solid medium (LB-Agar + Ampicillin, 100 $\mu$ g/ml) and the plates were incubated overnight at 37 ° C. Two-three bacterial colonies were inoculated into 100 ml of LB containing ampicillin and grow at 37 ° C for 16 hours. The culture was diluted 10 times with fresh LB medium containing ampicillin and incubated at 37 ° C and grown to the value of optical density at 600 nm of 0.6. Differently, ArcticExpress (DE3) cells were pre-incubated at 30 ° C and once reached the 0.6 optical densities at 600 nm shifted to 20 ° C. Then the cells transformed with the

construct pET-15b/SspCA, pET-15b/SazCA, pET-15b/VchCA and pET-15b/VchCA $\beta$  were induced with 1 mM IPTG, while those transformed with the construct pET-15b/VchCA $\gamma$  and pET-43.1a/PfCA1 were induced with IPTG 0.5 mM. After half an hour from the induction with IPTG, ZnSO<sub>4</sub> was added to the culture at a concentration of 0.5 mM. The metal ion was added because the zinc ion is essential for the catalytic activity and for the folding of the CA. Depending on the type of construct containing the CA of interest, after 4, 5, 6 or 20 hours cells were harvested by centrifugation at 6000xg for 30 minutes in Sorvall RC 6 Plus <sup>TM</sup> (Thermo Scientific).

### 3.7 Purification of the recombinant CA

#### 3.7.1 Affinity chromatography

Bacterial cells previously collected were suspended in 10 mM Tris-HCl pH 8.3 (Vf = 50 ml), lysed by sonication using a Branson Digital Sonifier using 15 cycles of 10sec with a 50 % of power. The sonicate was centrifuged at 10000xg for 45 minutes in Sorvall RC 6 Plus <sup>TM</sup> (Thermo Scientific). All operations were performed at 4 °C. The supernatant was collected and purified by affinity chromatography on column HisTrap<sup>TM</sup> FF crude 1 ml (GE Healthcare Biosciences) connected to an AKTA FPLC system. The column resin (Chelatin Sepharose<sup>TM</sup> High Performance) is agarose linked to iminodiacetic acid, able to chelate metal ions such as Ni<sup>2+</sup> ions capable of coordinating the imidazole groups of the His-tag of our proteins (Figure 15).

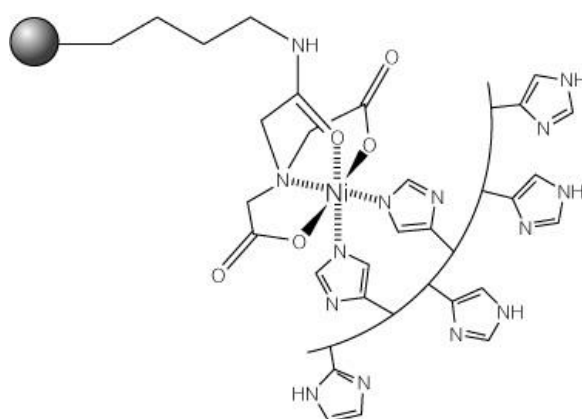


**Figure 15.** Schematic representation of His-Tag bounded to the beads of HisTrap<sup>TM</sup> FF column.

The column was prepared by passing approximately 20 ml of Milli-Q H<sub>2</sub>O (0.5 ml / min) and equilibrated with 10 column volumes of buffer A (20 mM imidazole, 20 mM phosphate buffer, 0.5 M NaCl pH 8 to a flow of 1 ml/min). Sample was loaded on the column at a constant flow of 1ml/min. Subsequently, washing was performed with 40 ml of buffer A. The protein, bound to the resin, was specifically eluted using an elution buffer (250 mM imidazole, 20 mM phosphate buffer, 0.5 M NaCl, pH 8) at a flow rate of 1 ml/min. Fractions were collected by recording the absorbance at 280 nm and dialyzed against 10 mM Tris-HCl, pH 8.3. Dialysis was performed at 4 ° C and using tubes with a cut-off of 12000 Daltons, in order to remove the high concentration of imidazole used for the elution. The dialyzed protein was collected and analyzed by SDS-PAGE.

### ***3.7.2 SDS-PAGE analysis of protein fractions***

The SDS-PAGE analysis of protein fractions obtained as described in the previous section was conducted according to the method described by Laemmli (1970). Each sample was dissolved in SDS Sample Buffer (62.5 mM Tris-HCl pH 6.8; 10% glycerol; 2% SDS; 10% β-mercaptoethanol; Bromophenol Blue 0.05%) and heated for 7 minutes at 100 °C to denature proteins. After this treatment, samples were subjected to vertical electrophoresis by loading 20 μl of each sample on a polyacrylamide gel at 12.5%. The electrophoretic run was performed on Mini-PROTEAN® Tetra Vertical Electrophoresis Cell (BioRad) at a constant voltage of 150 V for about an hour, using the running buffer 1X Tris-Glycine SDS buffer, pH 8.3 (250 mM Tris base, 192 mM glycine and 1% SDS). A molecular weight marker ranging from 10-250 kDa (Precision Plus Protein™ Dual Color Standards, BioRad) was used as standard. The protein bands were visualized by soaking the gel in the Staining Solution (0.025% Coomassie R-250; 50% methanol; 10% acetic acid; Milli-Q H<sub>2</sub>O to a volume of 1 L) and subsequently in destaining Solution (10% methanol; acid 10% acetic; Milli-Q H<sub>2</sub>O to a volume of 1 L). To calculate the molecular mass of the protein in question has been used the program Compute pI/Mw (Gasteiger et al., 2005), accessible from the server of Molecular Biology ExPASy.

### ***3.7.3 Determination of protein concentration***

The protein concentration was determined by the Bradford assay (Bio-Rad Laboratories, Hercules, USA) that is based on the color variation of an acidic

solution of Coomassie Brilliant Blue G-250 (Bio-Rad mix, max of absorption at 465 nm) in presence of protein. The color change results in an increase in absorbance from 465 nm to 595 nm, which is proportional to protein concentration. The calibration curve was constructed using known amounts of bovine serum albumin (BSA). For each sample (20  $\mu$ L) were added 200  $\mu$ L of the coloring solution Quick Start Bradford Dye Reagent 1x (BioRad) and water to reach the final volume of 1 ml. The blank was prepared with 20  $\mu$ l of the buffer used for harvesting the cells. The samples thus prepared were incubated 5 minutes at room temperature and read in a spectrophotometer at a wavelength of 595 nm. A three points calibration curve was prepared using known amounts of BSA. The sample unknown concentration was calculated using the first-degree equation determined from the BSA calibration curve.

### **3.8 Biochemical characterization**

#### ***3.8.1 Determination of the CA hydratase activity in solution***

The CAs activity assay is a modification of the procedure described by Chirica (Chirica L.C., *et al.* 1997) and is based on monitoring the change in pH due to the catalytic conversion of CO<sub>2</sub> into bicarbonate. The indicator of the variation of pH is bromothymol blue (BTB) (Sigma-Aldrich). The assay was performed at 0 °C in a final volume of 1 ml. The CO<sub>2</sub> saturated water was prepared by bubbling CO<sub>2</sub> into 100 mL of distilled water for about 3 h. To test the activity of the enzyme, 100  $\mu$ L of 250 mM Tris-HCl pH 8.3 containing BTB (to give a distinct and visible blue color), were placed in two tubes cooled in ice. Ten to 50  $\mu$ l of enzyme solution (purified enzyme in 10 mM Tris-HCl pH 8.3) were added to a test tube and, an equivalent amount of buffer was added to the second tube as a control. Immediately have been added 500  $\mu$ l of water saturated with CO<sub>2</sub> and 400  $\mu$ l of Milli-Q water and simultaneously a stopwatch was started. The time taken for the color change of the solution from blue (alkaline pH) to yellow (acidic pH) was recorded (the range of color change is between pH 6.0 and pH 7.6). The production of H<sup>+</sup> during the reaction of hydration of CO<sub>2</sub> lowers the pH of the solution up to the transition point of the dye. The time required for the color change is inversely proportional to the quantity of CA present in the sample. Next, we have calculated the Wilbur-Anderson units (WAU). One WAU of activity is defined as:  $(T_0 - T) / T$ , where T<sub>0</sub> (reaction not catalyzed) and T (reaction catalyzed) represent the time (in

seconds) necessary so that the pH falls from 8, 3 up to the transition point of the dye, in the control buffer, and in the sample in which is present enzyme respectively.

### **3.8.2 $\alpha$ -CA esterase activity assay**

Differently from the other CA classes, the  $\alpha$ -CAs are able to hydrolyze the ester p-nitrophenyl acetate (p-NpA) in p-nitrophenolate and acetate. The activity of hydrolysis of p-NpA was determined using a modification of the method proposed by Armstrong (Armstrong J.M., *et al.* 1966). The reaction mixture was composed as follows: 300  $\mu$ l of p-NpA 3mM, 700  $\mu$ l 15mM Tris Sulfate buffer at pH 7.6 and 10 $\mu$ l of enzyme. The hydrolysis of p-NpA was monitored by the increase of p-nitrophenolate, which was measured at 348nm for 5 minutes using a spectrophotometer Varian's Cary 50 (Agilent Technologies). The catalyzed reactions were corrected for the non-enzymatic reaction. One unit of enzyme was defined as the amount of enzyme capable of producing an  $OD_{348nm} = 0.03$  in 5 minutes.

### **3.8.3 Protonography**

It was set up a simple and inexpensive method, similar to zymography, which allowed the detection of CA activity on the polyacrylamide gel following the formation of H<sup>+</sup> ions produced by hydratase of CAs. The technique was called "protonography" (De Luca V., *et al.* 2015). Briefly, samples were run on SDS-PAGE at a concentration of about 4  $\mu$ g per well. The commercial bovine CA (bCA) was used as a control. SDS-Page was carried out as described in the section "SDS-PAGE analysis of protein fractions", with the exception that the SDS sample buffer didn't contain the  $\beta$ -mercaptoethanol and samples were not heated. Two SDS-PAGE gels were prepared: one was stained with Coomassie blue; the other was used to develop the protonogram. The last one was, in fact, treated with Triton X-100 at 2.5% and kept under stirring for one hour to remove the SDS. The gel was subjected to a washing step of 20 min with 100 mM Tris-HCl, pH 8.3, containing 10% isopropanol. It was washed two times for 10 minutes. Finally, the gel was incubated for 30 minutes at 4 °C under stirring with 0.1% bromothymol blue (BTB) in 100 mM Tris-HCl pH 8.3. BTB is a pH indicator. To detect the hydratase activity, the gel was immersed in distilled water saturated with CO<sub>2</sub> prepared by bubbling CO<sub>2</sub> into 200 mL of distilled water for about 3 h. The localized decrease of the pH value, due to the

presence of the enzymatic activity of CAs, was detected through the formation of yellow band due to the change of color of the BTB from blue (alkaline pH) to yellow (acidic pH).

#### ***3.8.4 Thermoactivity***

The temperature dependence activity of SspCA, SazCA and VchCA was determined using the p-NpA as substrate. The results were compared with that obtained for the bovine CA (bCA). In the assay were used 300 ng of protein. The reaction mixture was set up as described in the previous paragraph and the activity was measured at the temperatures ranging from 25 to 100 °C.

#### ***3.8.5 Thermostability***

The CA thermal stability was evaluated through experiments of thermal inactivation. The recombinant CAs were incubated at 25, 40, 50, 60, 70, 80, 90 and 100 ° C and aliquots were withdrawn at different times (30, 120 and 180min). Enzyme concentration was 3µg/mL in a buffer composed of Tris-HCl 10 mM, pH 8.3. The enzyme residual activity, expressed in percent of WAU, was measured at 0 °C using CO<sub>2</sub> as a substrate. The results were compared with those obtained for a mesophilic enzyme (bCA)

#### ***3.8.6 Determination of the kinetic and inhibition constants***

The kinetic and inhibition constants were obtained using the “stopped flow” apparatus. The apparatus (Applied Photophysics) is positioned in the laboratory direct by Prof. Claudiu Supuran, where have been collected all the kinetic results. The apparatus is made up of two main components: the mixing chamber and the observation chamber. As pH indicator it has been used phenol red (0.2mM), which operates at a maximum absorbance of 557 nm with HEPES buffer (acid 4-2-hydroxyethyl-1-piperazinyl-ethanesulfonic acid, an organic substance used to maintain the stable pH) 10 mM at pH 7.5 (for the α-CAs) or 20 mM Tris (pH 8.3 for β- and γ- CA) and 0.1 M NaClO<sub>4</sub> (to maintain ionic strength constant) at 20 ° C. The reaction was followed for a period of 10-100 sec (the reaction is not catalyzed needs about 60-100 sec under the test conditions, while the reactions catalyzed need about 6-10 sec). For the determination of kinetic parameters and inhibition constants, the concentrations of CO<sub>2</sub> are comprised between 1.7 and 17 mM. Stock solutions of inhibitor (10-

50 mM) were prepared in deionized-distilled water and then, with the Assay Buffer were made dilutions to 0.01  $\mu$ M. The inhibitor and the enzyme solutions were pre-incubated for 15 minutes at room temperature before assay, in order to allow the formation of the E-I complex (enzyme-inhibitor) or to the possible hydrolysis of the inhibitor, mediated by the active site. The kinetic parameters were determined using the diagram Lineweaver-Burk plot (or diagram of the double reciprocal), while the inhibition constants were obtained by the method of nonlinear least squares using PRISM 3 and represent the average of at least three different determinations.

### **3.9 Immobilization**

#### ***3.9.1 Enzyme immobilization on polyurethane foam***

10 mg of SspCA were dissolved in 3mL of distilled water and added to 3 g of viscous prepolymer HYPOL2060 (a gift from Dow Chemical Co., Italy) in a 50mL falcon tube. The solution was mixed vigorously for 30 s to achieve a homogeneous distribution of the enzyme within the prepolymer. The polymerization of the polyurethane is induced by the presence of water: the carbonyl group undergoes a nucleophilic attack by an OH<sup>-</sup> followed by a process of protonation, which causes release of CO<sub>2</sub> and the conversion of an isocyanate group in an amino group (NH<sub>2</sub>). The latter group reacts instantly with the isocyanate group of a nearby molecule, giving rise to a cross-link between two polymer chains. In the presence of the enzyme, it is favored cross-linkage between this and the pre-polymer given the availability of free amino groups on the surface of the enzyme. The CO<sub>2</sub> gas generated by the process gives the foam cured a porous texture with spongy appearance. The solution started to polymerize as result of a CO<sub>2</sub> release during the polymerization, which developed in 3–5 min. The polymer with the immobilized enzyme (PU-SspCA) was left at room temperature for an additional 15 min before being used (Kanbar B. & Ozdemir E. 2010). After completion of the enzyme immobilization, PU-SspCA foam was chopped using an IKA Ultra-Turrax® T25 and assayed for CA activity using CO<sub>2</sub> as substrate. The reaction was started by addition of the foam to the substrate-containing mixture under stirring. All the experiments were carried out in parallel with the mammalian enzyme. For studies on stability, foam slices containing the immobilized SspCA or bCA II were incubated at 100°C. The immobilized enzyme activity was

determined every 12 h over a total of 48 h. The assay was carried out using SspCA or bCA II and CO<sub>2</sub> as substrate.

### **3.9.2 Bioreactor**

The foam obtained as described in previous paragraph was placed inside a three-phase bioreactor (gas, liquid, solid) and was monitored the consumption of CO<sub>2</sub> using a CO<sub>2</sub> analyzer equipped with IR measuring cell (ABB URAS 17). The bioreactor (length 30 cm, i.d. 4 cm), realized in Pyrex glass, was designed according to the three-phase trickle-bed configuration, and was able to operate in both concurrent down-flow and countercurrent flow. In order to separate both inlet and outlet currents of gas and liquid were inserted two porous septa (40-100 μm) and the lower septum working also as a packed bed support. In the countercurrent operation, the measuring pump allowed the bi-distilled water to be fed from the top and the gas from the bottom (Migliardini F., *et al.* 2014).

### **3.9.3 Preparation of Magnetic Particles**

Magnetic particles (MP) were prepared dissolving 8.1 g of FeCl<sub>3</sub>·6H<sub>2</sub>O in 150 mL of distilled water, the resulting solution was kept under stirring at 70 °C in a conical flask. Subsequently, it has been added FeSO<sub>4</sub>·7H<sub>2</sub>O and 25% of NH<sub>3</sub>·H<sub>2</sub>O with shaking. After 1 min., were added 5 g of oleic acid dropwise and the reaction was conducted under stirring for 1 h. (Figure 16 A). The mixture was washed with ethanol three times and then, four times with distilled water. At the end of the washing procedure were added 0.016 mmol of H<sub>2</sub>SO<sub>4</sub>, 160 mL of distilled water and 1.6 g of KMnO<sub>4</sub>. The solution was stirred at 200 rpm for 4 h. (Figure 16 B). The material produced was washed with distilled water and air-dried at room temperature (Figure 16 C).

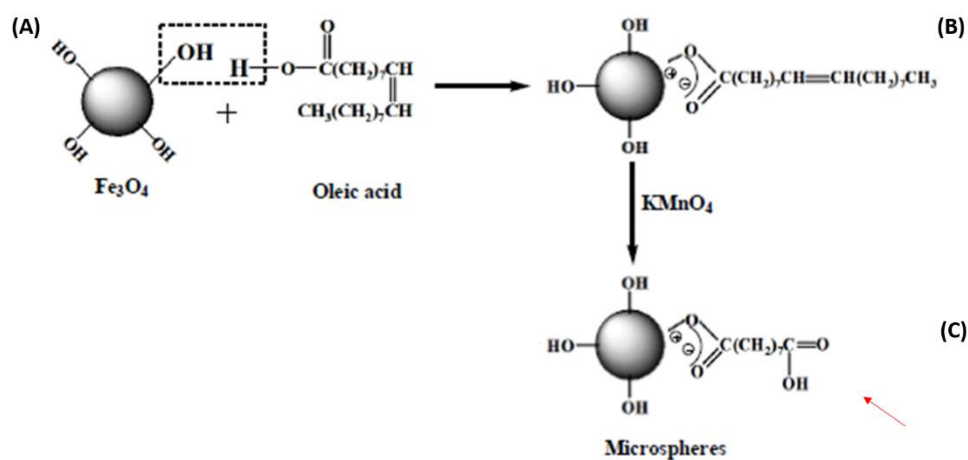


**Figure 16.** Magnetic Particles (MP) preparation.

### 3.9.4 Immobilization of CA on MP

30 mg of carboxyl-functionalized  $\text{Fe}_3\text{O}_4$  magnetic particles were incubated with the 0.12 mg of free enzyme. The mixture was stirred at 120 rpm for 4 h in presence of 10 mL of Tris-HCl, pH 8.0.

### 3.9.5 Activity measurement of immobilized CA on MP

The activity of the immobilized CAs on the paramagnetic nanoparticles was determined using the method described in paragraph 2.8.2.

## Chapter 4. Biotechnological application results

### 4.1 Biomimetic capture of CO<sub>2</sub>

Recently, CAs began to be considered for biotechnological applications of enzymatic CO<sub>2</sub> capture especially in relation to its increased emission in the atmosphere due to the anthropogenic activity (Huessemann M.H., *et al.* 2008; Greer T., *et al.* 2010; Fisher Z., *et al.* 2012). CAs, in fact, are very valid catalysts of the conversion of CO<sub>2</sub> to bicarbonate, such enzymes may lead to the capture/sequestration of CO<sub>2</sub> from combustion gases, and alleviate the global warming effects through a reduction of CO<sub>2</sub> emissions in the atmosphere. CAs from mesophilic organism are subject to denaturation during the CO<sub>2</sub> capture process characterized by extreme conditions, such as high temperature, high concentrations of salts, etc. For this reason, CAs present in the genome of extremophiles bacteria started to be investigated in detail ultimately. (Reysenbach, A.L., *et al.* 1992; Nakagawa S., *et al.* 2005; Aguiar P., *et al.* 2004; Takai K., *et al.* 2003; Tu C., *et al.* 2001; Moya A., *et al.* 2008; Domsic J.F., *et al.* 2008; Supuran C.T. 2008; Xu Y., *et al.* 2008; Viparelli F., *et al.* 2010; Alterio V., *et al.* 2012; Pastorekova S., *et al.* 2004). Generally, enzymes from thermophilic organisms, respect to the mesophilic counterpart, are thermostable and thermoactive representing good candidates in industrial processes characterized by extreme operating conditions.

### 4.2 Protein identification

Using as reference protein the amino acid sequence of the  $\gamma$ -CA from *Methanosarcina thermophila*, a moderate thermophilic methanogenic archaeon (Smith K.S. & Ferry J.G. 2000), and performing with “FASTA” program a search of sequences with significant similarity scores, we identified an  $\alpha$ -CA encoded by the the genome of the extremophilic bacteria *Sulfurihydrogenibium yellowstonense* YO3AOP1 and *Sulfurihydrogenibium azoreense* (Nakagawa S. 2005; Aguiar P. 2004). The genus *Sulfurihydrogenibium* comprises chemolithotrophic bacteria able to survive in extremely harsh conditions of temperature (up to 110 °C) and in the presence of high concentrations of hydrogen sulfide (between 1 – 100  $\mu$  M). The two carbonic anhydrases were named respectively SspCA and SazCA. The recombinant enzymes, whose

nucleotide sequences were synthesized by Life Technologies, were heterologously expressed in *Escherichia coli*.

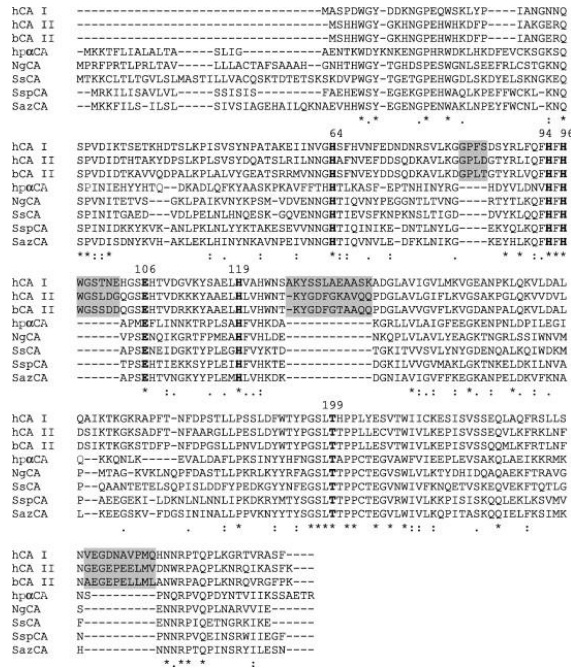


**Figure 17.** Multialignment of the amino acid sequences of  $\alpha$ -CAs from different organisms performed with the program Clustal W, version 2.1. Legend: hCA I, *Homo sapiens*, isoform I; hCA II, *Homo sapiens*, isoform II; bCA II, *Bos Taurus*, isoform II; hp $\alpha$ CA, *Helicobacter pylori* J99 CA; NgCA, *Neisseria gonorrhoeae* enzyme; SsCA, *Streptococcus salivarius* PS4 CA; SspCA, *Sulfurihydrogenibium sp.* YO3AOP1; SazCA, *Sulfurihydrogenibium azorense*. Asterisk (\*) indicates identity at all aligned positions; symbol (:, .) relates to conserved substitutions; (.) indicate semi-conserved substitutions. In bold are indicated the residues involved in the enzyme CO<sub>2</sub> hydratase. The zinc ligands (His94, 96 and 119 in bold), the proton shuttle residue (His64, in bold) and the gatekeeper residues (Glu106 and Thr199, in bold) are conserved in all these enzymes. The four loops absent in the bacterial enzymes are highlighted in grey. The numbering system used is that one from hCAI.

### 4.3 Primary structure analysis

The alignment of the SspCA and SazCA sequences, compared with that from other species (eukaryotic and prokaryotic) (Figure 17), indicated that the two bacterial polypeptide chains showed all the typical features of a  $\alpha$ -CAs.

#### **4.4 Cloning sequencing and production of expression vector**

In order to study the biochemical properties and chemical-physical properties of the CA identified, the two CAs, SspCA and SazCA were prepared using recombinant DNA techniques (see section “Materials and Methods”).

#### **4.5 Optimal expression conditions and production of the recombinant proteins**

Bacterial cells were transformed with the appropriate expression vectors, grown in rich medium and, after induction with IPTG and addition of the metal, samples were collected at various time points as described in "Materials and Methods". The induced cells synthesized the fusion protein, consisting of the HIS tag and the CA. The SDS-PAGE showed that the increased amount of SspCA and SspCA in the soluble fraction after sonication and centrifugation is obtained in about 5 hours after the induction with 1 mM IPTG. Defined the optimal conditions for growth, has been prepared the bacterial culture of 2.0 L by using the bacteria transformed with the construct of interest (pET-15b/SspCA or pET-15b/SazCA). Cells were grown for 5 hours, resuspended in Tris-HCl 10 mM pH 8.3 and disrupted by sonication.

#### **4.6 Purification of the recombinant proteins**

The recombinant proteins (SspCA and SazCA) were isolated and purified to homogeneity at room temperature from *Escherichia coli* BL21(DE3) cell extracts. CAs activities were recovered in the soluble fraction of cell extract obtained after sonication and centrifugation. The heterologously expressed SspCA and SazCA enzymes were purified by use of the affinity column (His-select HF nickel affinity gel). The subunit molecular mass of about 26.4 kDa and 25.6kDa for SspCA and SazCA respectively, were calculated on the basis of the amino acid sequence translated from the gene. The molecular weight estimated by SDS–PAGE was 26.0 kDa (Figure 18). For both the proteins it was calculated purity of about 85% (Figure 18).

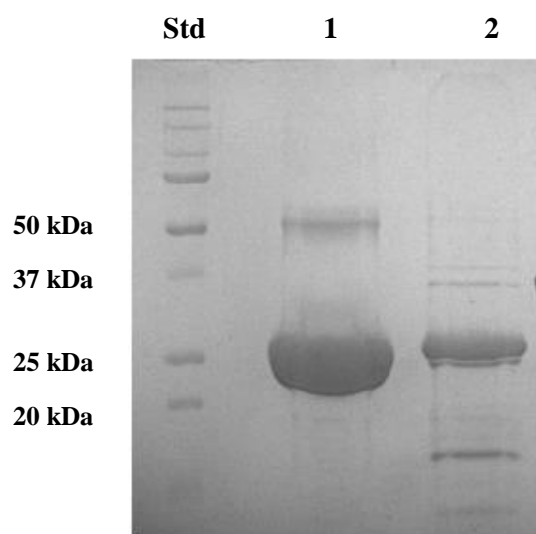


**Figure 18.** SDS-PAGE after affinity chromatography. Line 1: SazCA; Line 2: SspCA.

## 4.7 Characterization

### 4.7.1 Activity

The recombinant proteins were assayed in solution using CO<sub>2</sub> as a substrate using the procedure described by Chirica *et al.* (see “Materials and Methods”). Enzyme activity was expressed in Wilbur-Anderson units (WAU) (see experimental section). The table V showed specific activities of SspCA and SazCA compared with that obtained for the commercial bovine enzyme bCA ( $\alpha$ -CA). Interesting to note as the SazCA specific activity is higher respect to those of the SspCA and bCA.

$\alpha$ -CAs also catalyze the hydrolysis of esters, such as p-nitrophenyl acetate (p-NpA). Using this ester as substrate, we investigated the presence of esterase activity of the two bacterial enzymes comparing it with that of bCA enzymes. (Ferry J.G. 2010). SazCA showed a rather low specific activity towards p-NpA compared to SspCA and the mesophilic bovine  $\alpha$ -CA (bCA). The SazCA esterase activity (62 U/mg protein) was 5 and 21 times lower than that of SspCA and bCA, ‘respectively’(Table V).

**Table V.**

|       | Class    | Hydrase Specific activity<br>(WAU/mg protein) | Esterase Specific Activity<br>(U/mg protein) |
|-------|----------|---|--|
| SspCA | $\alpha$ | 6670  | 322  |
| SazCA | $\alpha$ | 50540   | 62   |
| bCA   | $\alpha$ | 4845  | 1282   |

#### 4.7.2 Kinetic Constants

The specific activities for SazCA, SspCA, hp $\alpha$ CA and hCA II were determined using CO<sub>2</sub> as substrate, by a stopped-flow assay method (Khalifah R.G.J. 1971). As reported in Table, the CO<sub>2</sub> hydrase activity of SazCA was the highest among all CAs known to date, being 2.33 times higher than that of hCA II (considered the most active CA up until now). In table VI are also shown the inhibition constant ( $K_I$ ) obtained using acetazolamide the classic CAs inhibitor.

**Table VI.** Comparison of the CO<sub>2</sub> hydrase activities and inhibition constant with acetazolamide of SazCA, SspCA (from thermophilic bacteria), hp $\alpha$ CA (from *Helicobacter pylori*) and hCA II. All constants were determined to "stopped-flow" at 20 ° C and pH 7.5 in the laboratories headed by Prof. Claudiu Supuran of the University of Florence, Department of Chemistry.

| Enzyme         | $k_{cat}$ (s <sup>-1</sup> ) | $K_M$ (mM) | $k_{cat}/K_M$ (M <sup>-1</sup> s <sup>-1</sup> ) | $K_I$ (nM)<br>(acetazolamide) |
|----------------|------------------------------|------------|--|-------------------------------|
| SazCA          | $4.40 \times 10^6$           | 12.5       | $3.5 \times 10^8$                                | 0.90                          |
| SspCA          | $9.35 \times 10^5$           | 8.4        | $1.1 \times 10^8$                                | 4.5                           |
| hCA II         | $1.40 \times 10^6$           | 9.3        | $1.5 \times 10^8$                                | 12                            |
| hp $\alpha$ CA | $2.5 \times 10^5$            | 16.6       | $1.5 \times 10^7$                                | 21                            |

All these enzymes were effectively inhibited by the sulfonamide acetazolamide, with inhibition constants in the range of 0.9 –21 nM. It may be observed that acetazolamide is an excellent, subnanomolar inhibitor of SazCA, being much more effective against this isoform than against hCA II (Table VI). Intriguingly, SazCA resulted more active than the hCAII considered the most active CA investigated until now.

#### 4.7.3 Thermoactivity and Thermostability

We performed studies of thermoactivity and thermostability. The first measures the enzyme activity at a determined temperature; while the second

measures the enzyme activity after that it was incubated at a specified temperature for a determined time.

The thermoactivity of SspCA and SazCA was determined at the temperatures of 25, 30, 40, 50, 60, 70, 80, 90 and 100 °C using as substrate the p-NpA. The results were compared with those obtained for the bovine enzyme (bCA). The results showed that that SazCA and SspCA were active in the temperature range from 0 to 100 °C, unlike the mammalian enzymes which was denatured at temperatures higher than 60 °C (Figure 19 A). The optimal temperature for the bovine enzyme activity was found to be 60 °C and, as expected for thermophilic enzymes, SazCA and SspCA, showed an optimum of temperature at 80–90 °C. These enzymes were still active at 100 °C (Figure 19 A). In Figure 19 B is reported the thermostabilities of SazCA, SspCA and bCA II at the temperatures indicated on the X-axis using CO<sub>2</sub> as substrate and considering 30 min and 180 min as incubation time. The mesophilic enzyme (bCA II) was inactivated at temperature higher than 60 °C (Figure 19 B) for all the incubation times considered. Enzymes from extremophiles were active at the temperature up to 100 °C. Interesting to note SazCA was more stable than the mesophilic enzyme and slightly less stable than SspCA. Our studies indicated that CAs from extremophiles were more stable at high temperature and retained their activity for a longer time (e.g., 180 min) when compared to the mammalian enzyme.

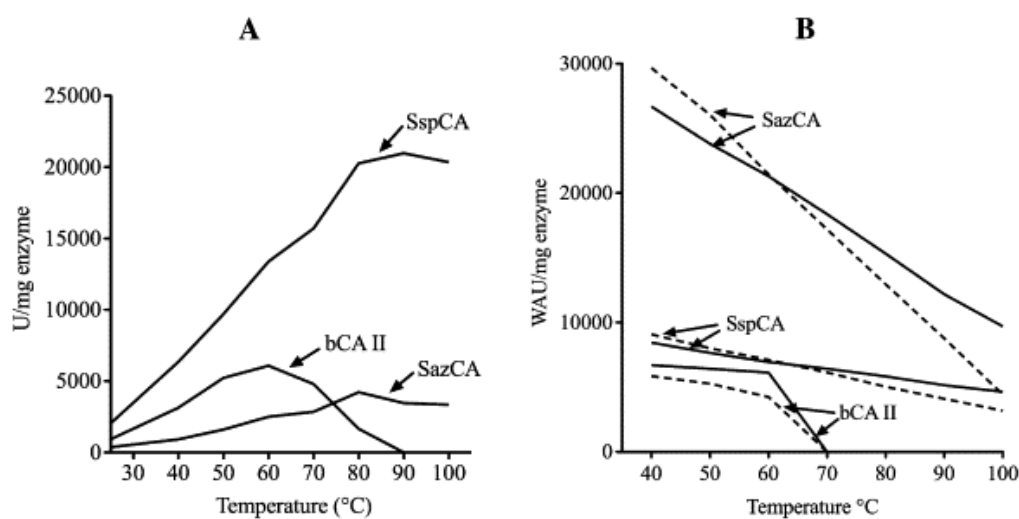


**Figure 19.** (A) Determination of optimal activity temperature of SazCA, SspCA and bCA. The enzyme activity was measured at the temperatures in the range from 25 to 100 °C using p-NpA as substrate. (B) Thermostability of SazCA, SspCA and bCA II. The enzymes were incubated for 30 and 180 min at the indicated temperatures on the X-axis and assayed using CO<sub>2</sub> as substrate. Each point is the mean  $\pm$  SEM of three independent determinations.

The CAs investigated show a very high stability at various temperature, and survive to denaturation even after various cycles of heating at temperatures as high as 100 °C. These two robust enzymes may have important applications in biotechnological processes, such as the CO<sub>2</sub> capture due to their thermoactivity and (we stress again, SazCA is the most active CA known to date and SspCA the most stable) and thermostability (De Simone G. & Supuran C.T. 2012). It is important to note that there is massive industrial/biotechnological interest in using CAs as bio-catalysts for carbon sequestration and biofuel production (Fisher Z., *et al.* 2012).

## 4.8 X-ray structure

### 4.8.1 SspCA

The determination of the SspCA crystallographic structure clarified the molecular basis of its exceptional thermostability (Di Fiore, A., *et al.* 2013). In particular, SspCA, like other  $\alpha$ -CAs (Alterio V., *et al.* 2012), showed a fold characterized by a central ten-stranded  $\beta$ -sheet surrounded by several helices and additional  $\beta$ -strands (Figure 20 A). The active site is located in a deep conical cavity, which extends from the protein surface to the center of the

molecule, with the catalytic zinc ion positioned at the bottom of this cavity. The metal ion is tetrahedrally coordinated by three histidine residues (His89, His91 and His108) and by the nitrogen atom of the inhibitor acetazolamide (AAZ), which was co-crystallized with the enzyme (Figure 20 B).

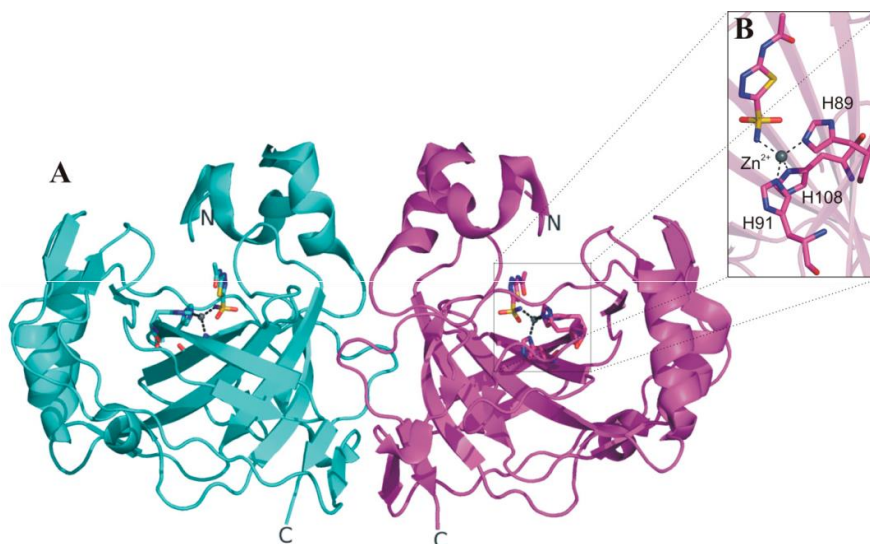


**Figure 20.** (A) SspCA dimer structure (PDB code 4G7A) with one monomer shown in cyan and the other one in magenta; (B) enlarged view of SspCA active site showing the zinc ion coordination.).

Interestingly, SspCA forms a dimer characterized by a large interface area and stabilized by several polar and hydrophobic interactions. This dimeric arrangement is a peculiar feature of all bacterial  $\alpha$ -CAs so far structurally characterized (James P., *et al.* 2014, Huang S., *et al.* 1998, De Simone G., *et al.* 2015).

#### 4.8.2 SazCA

SazCA is the other thermostable  $\alpha$ -CA isolated from the *Sulfurihydrogenibium* species and has been demonstrated to be the most catalytically active CA ever investigated so far (De Luca V., *et al.* 2013). Its CO<sub>2</sub> hydration activity is 2.33 times higher than that of the highly active hCA II, with a  $k_{\text{cat}}$  value of  $4.40 \times 10^6 \text{ s}^{-1}$  and a  $k_{\text{cat}} / K_{\text{M}}$  value of  $3.5 \times 10^8 \text{ M}^{-1} \cdot \text{s}^{-1}$  (De Luca V., *et al.* 2013). Thermoactivity studies revealed that this enzyme presents an esterase activity in a temperature range of 0 to 100 °C, with an optimum working temperature at 80 °C. Thermal stability studies showed that SazCA is able to retain CO<sub>2</sub> hydration activity after incubation at 100 °C for 3

h, even though it is less stable than SspCA (De Luca V., *et al.* 2013). The crystallographic structure of SazCA was recently determined (De Simone G., *et al.* 2015) (Figure 21).

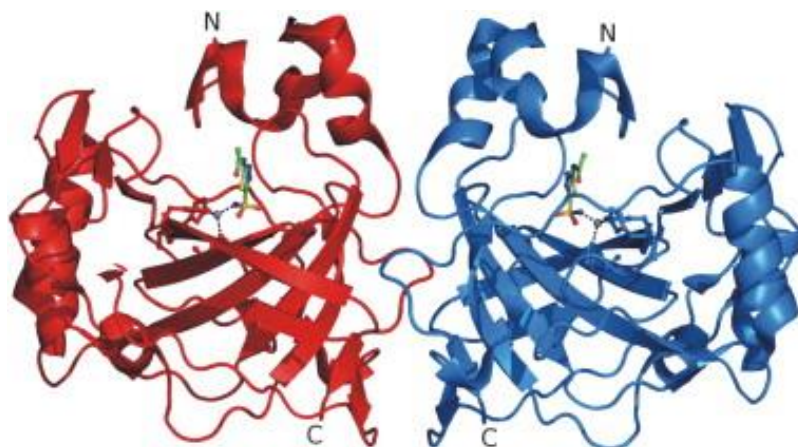


**Figure 21.** SazCA dimeric structure with one monomer shown in red and the other in blue.  $Zn_2^+$  ion coordination and the inhibitor AZM are also shown.

The analysis of this structure revealed the classical dimeric arrangement of bacterial  $\alpha$ -CAs (James P., *et al.* 2015; Di Fiore A., *et al.* 2013; Huang S., *et al.* 1998) and a substantial similarity with SspCA structure (Figure 22), in fact, the two enzymes have a sequence identity of 61.3%. (Di Fiore A., *et al.* 2013). However, a more detailed comparison allowed the identification of minor differences probably responsible of the difference in catalytic activity between SspCA and SazCA. Most of the residues of the active site are conserved in the two enzymes, however the substitution of the SspCA residues Glu2 and Gln207, located on the rim of the cavity, with His2 and His207 in SazCA, has been proposed to be responsible of the higher SazCA catalytic activity. These mutations might affect the pKa of His64 and consequently its ability to transfer the proton (De Simone G., *et al.* 2015). These results offer interesting prospects for the design of CA variants showing higher stability and catalytic activity than all other  $\alpha$ -CAs known to date.

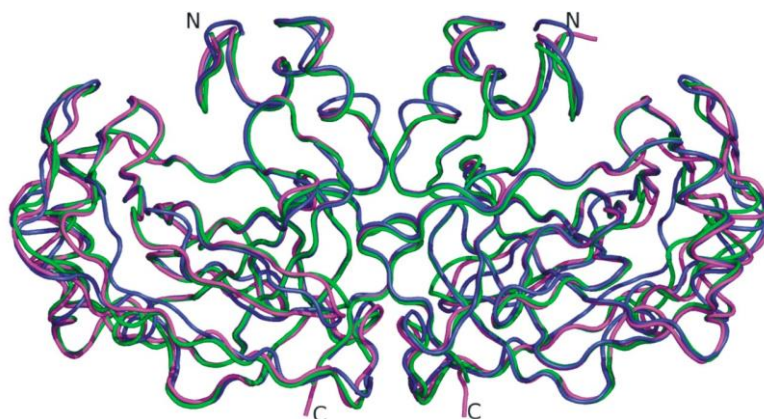


**Figure 22.** Superposition of the dimeric structure of SazCA (PDB code 4X5S, green) with those of SspCA (PDB code 4G7A, magenta) and TaCA (PDB code 4C3T, blue). TaCA dimer was generated using PISA program (<http://www.ebi.ac.uk>) [Krissinel, E.; Henrick, K. Inference of macromolecular assemblies from crystalline state. *J. Mol. Biol.* 2007, 372, 774–797.] on the crystallographic coordinates (PDB entry 4C3T).

## 4.9 Immobilization

### 4.9.1 Polyurethane

From the results obtained, we have selected SspCA as a potential candidate to use in the CO<sub>2</sub> capture process. We realized three-phase bioreactor (gas, liquid, solid) filled with the recombinant SspCA immobilized on polyurethane foam, a pre-polymer of polyethylene glycol. The polymerization of the polyurethane is induced by the presence of water: the carbonyl group undergoes a nucleophilic attack by an OH<sup>-</sup> followed by a process of protonation, which causes release of CO<sub>2</sub> and the conversion of an isocyanate group in an amino group (NH<sub>2</sub>). The latter group reacts instantly with the isocyanate group of a nearby molecule, giving rise to a cross-link between two polymer chains. In the presence of the enzyme, it is favored cross-linkage between this and the pre-polymer given the availability of free amino groups on the surface of the enzyme (Figure 23).

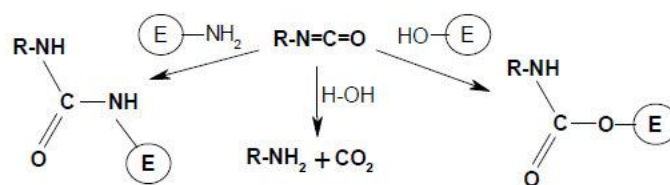


**Figure 23.** Polyurethane enzyme binding reaction

The CO<sub>2</sub> gas generated by the process gives the foam cured a porous texture with spongy appearance (Figure 24). The foam with the immobilized SspCA (PU-SspCA) was placed inside the bioreactor.



**Figure 24.** Chopped polyurethane foam with immobilized enzyme

The calculated specific activity of the PU-SspCA was similar to that of the free enzyme. Moreover, the dry polyurethane foam containing the immobilized SspCA or the free enzyme were stored at 25 ° C for several days. The free enzyme was stored in a buffer solution of 10mM Tris-HCl, pH 8.3. The PU-SspCA specific activity was measured after 1, 6 and 30 days and compared with that of the free enzyme. PU-SspCA specific activity remained constant up to one month, while that of the free enzyme decreased slightly. These results are reported in table VII.

**Table VII.** Comparison of the hydratase activity for the immobilized and free enzyme incubated for several days at 25 ° C.

| Incubation time | Hydratase Activity WAU/mg protein. |            |
|-----------------|------------------------------------|------------|
|                 | Pu-SspCA                           | SspCA free |
| 1 day           | 1900                               | 3250       |
| 6 day           | 1934                               | 3123       |
| 30 day          | 1910                               | 2756       |

Once immobilized the enzyme adsorption capacity has been verified in laboratory. The experiments were realized using a laboratory plant based on a three-phase trickle-bed reactor formed by a solid phase, which corresponds to the immobilized catalyst, liquid and gas phases. This bioreactor was realized in collaboration with Dr. Migliardini and Dr. Corbo CNR. Istituto Motori (IM). (Migliardini F., *et al.* 2014).

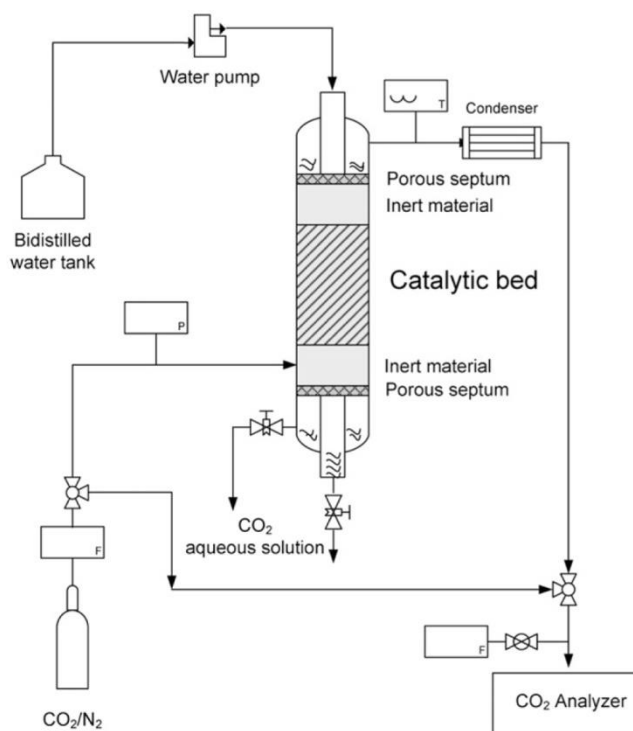


**Figure 25.** Schematic representation of a three-phase bioreactor

The gas phase was a mixture of N<sub>2</sub>/CO<sub>2</sub> (20% by volume) injected from the bottom of the bioreactor (Figure 25), the aqueous phase was the distilled water inject from the top and the solid phase was the enzyme immobilized on polyurethane foam. The CO<sub>2</sub> consumption was monitored using a CO<sub>2</sub> analyzer. In Figure 26 are reported the results obtained using the lab-scale bioreactor described above. It has been shown that the immobilized PU-SspCA is capable of converting about 15% of CO<sub>2</sub> from a gas mixture whose initial concentration was 20% (Figure 26). In the absence of catalyzer, (see yellow line in the graph of Figure 26) the spontaneous CO<sub>2</sub> conversion was about 18%. These results confirm that the CA from extremophile is good candidate for use in the processes of CCS.

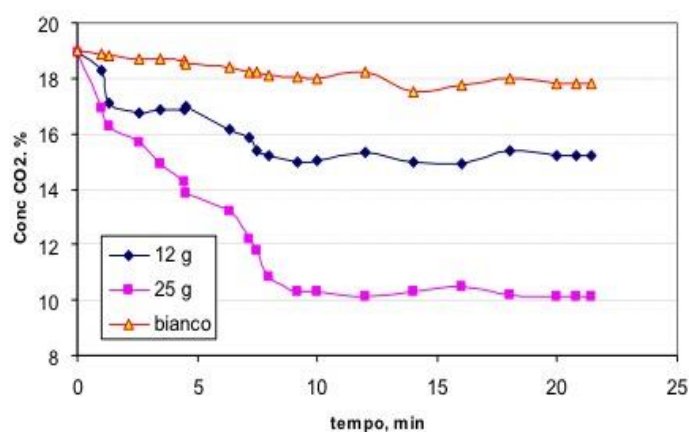


**Figure. 26** Conversion of CO<sub>2</sub> in presence of 25 g of PU-SspCA (pink line) or 12 g PU-SspCA (blue line) and PU without biocatalyst (yellow line).

#### 4.9.2 Paramagnetic particles

It was decided to immobilize SspCA on a magnetic support for recovering the catalyzer from the bioreactor in a very easy and practical way, for example through the use of a magnet. For this purpose, SspCA was immobilized on paramagnetic particles (MP). The immobilization yield on this new support prepared as described in “Materials and Methods” was about 95%. Interesting, the residual enzymatic activity of the immobilized enzyme was of 80% compared to that determined for the free enzyme in solution. This immobilization was better than done using PU as support. In fact, the enzyme immobilized on polyurethane, retained about 60% of its original activity. This

is due to the type of binding that is formed between the matrix and the immobilized enzyme. In fact, the immobilization PU-SspCA was covalent, while the immobilization on paramagnetic particles was ionic. As described in literature, the covalent immobilization of an enzyme forces the molecule into a rigid conformation, which could alter the enzyme activity. The ionic binding (obtained using the paramagnetic particles) gives more degrees of freedom the immobilized molecule. Unfortunately, the ionic bond is more sensible to the stringent working industrial conditions, characterized for example by high temperatures and high alkaline concentrations.

#### **4.10 Inhibition studies**

We have investigated the inhibition profiles of SazCA and SspCA with some of the main representatives of the CA inhibitors (CAIs), such as inorganic anions, dithiocarbamate, sulfonamide and several small molecules incorporating zinc-binding moieties of the sulfonamide/dithiocarbamate type (Table VIII). Moreover, we also considered sulfur-containing compounds such as hydrogen sulfide, hydrogen sulfite, sulfate anions, halides and bicarbonate, which are present in the environment colonized by these extremophiles (Kubo K., *et al.* 2011; Yang T., *et al.* 2011).

**Table VIII.** Inhibition of hCA II, SspCA, SazCA and hp $\alpha$ CA with several anions, sulfonamides and a dithiocarbamate. AAZ = acetazolamide, 5-acetamido-1,3,4-thiadiazole-2-sulfonamide.

| Inhibitor                                     | $K_I$ ( $\mu$ M) |         |        |                |
|---|------------------|---------|--------|----------------|
|   | hCA II           | SspCA   | SazCA  | hp $\alpha$ CA |
| F <sup>-</sup>                                | > 300,000        | 417,000 | 980    | 4080           |
| Cl <sup>-</sup>                               | 200,000          | 8300    | 850    | 2700           |
| Br <sup>-</sup>                               | 63,000           | 49,000  | 940    | 2410           |
| I <sup>-</sup>                                | 26,000           | 860     | 870    | 6050           |
| HCO <sub>3</sub> <sup>-</sup>                 | 85,000           | 33,200  | 15,700 | 750            |
| HSO <sub>3</sub> <sup>-</sup>                 | 89,000           | 21,100  | 950    | 990            |
| HS <sup>-</sup>                               | 40               | 580     | 380    | 690            |
| SCN <sup>-</sup>                              | 1600             | 710     | 580    | 4100           |
| SeCN <sup>-</sup>                             | 86               | 70      | 490    | 730            |
| CS <sub>3</sub> <sup>2-</sup>                 | 8.8              | 60      | 39     | 380            |
| Et <sub>2</sub> NCS <sub>2</sub> <sup>-</sup> | 3100             | 4.0     | 3.1    | 5.0            |
| SO <sub>4</sub> <sup>2-</sup>                 | > 300,000        | 820     | 10,000 | 820            |
| H <sub>2</sub> NSO <sub>3</sub> H             | 390              | 42      | 4.8    | 80             |
| AAZ   | 0.012            | 0.004   | 0.0009 | 0.021          |

Errors in the range of  $\pm 5\%$  of the reported data from three different assays.

Data shown in Table VIII reported that the halides were sub-millimolar inhibitors of SazCA (inhibition constants in the range of 0.87–0.98 mM with the four halide anions). SazCA has much higher affinity for these anions compared to SspCA or the human isoform hCA II, which were scarcely inhibited by these anions. The ‘extremo- $\alpha$ -CAs’ were strongly inhibited by the iodide ion respect to the mammalian hCA II and bacterial hp $\alpha$ CA. The structural modifications in the active site of the  $\alpha$ CAs from extremophiles constitute the possible explanation for the difference in binding of the iodide ion. Bicarbonate was also a better SazCA and SspCA inhibitor compared to hCA II, whereas hydrogen sulfide inhibited better hCA II ( $K_I$  of 40  $\mu$ M) compared to the two bacterial enzymes ( $K_I$  in the range of 380–580  $\mu$ M). This may be an evolutionary adaptation of the bacterial enzymes from these extremophiles which survive in the presence of high concentrations of H<sub>2</sub>S, and the corresponding anions is thus less inhibitory for their catalytic activity compared to the human isoform hCA II.

## Chapter 5. Biomedical application results

### 5.1 *Vibrio Cholerae*

Bacteria can increase cytosolic levels of bicarbonate through the transporters of the bicarbonate or through the action of enzymes, the carbonic anhydrase, which convert the CO<sub>2</sub> to bicarbonate or metabolic than atmospheric entry into the cells by simple diffusion (Smith K.S. & Ferry J.G. 2000). The analysis of the genome of *Vibrio cholerae* through the use of the program FASTA (Pearson W.R., 1994) has evidenced the absence of nucleotide sequences of the bicarbonate transport system similar to those identified in *S. elongates*. It was hypothesized that *V. cholerae* uses the enzymatic system of the carbonic anhydrase to accumulate bicarbonate inside the cell. (Del Prete S., *et al.* 2014). From the inspection of the *V. cholerae* genome, carried out using the BLAST program, it was found that the pathogen encoded for three classes of carbonic anhydrase: the  $\alpha$ -class CA, encoded by the gene *cah* (VC0395\_0957), indicated by the acronym VchCA; the  $\beta$ -CA derived from the gene VC0395\_A 0118, indicated by the acronym VchCA $\beta$  and a  $\gamma$ -CA encoded by the gene VC0395\_A2463, indicated with the acronym VchCA $\gamma$ . In prokaryotes, the existence of genes encoding CAs from at least three classes ( $\alpha$ -,  $\beta$ - and  $\gamma$ -class) suggests that these enzymes play an important role in the prokaryotic physiology.

#### 5.1.1 VchCA

VchCA is a carbonic anhydrase belonging to  $\alpha$  class and consists of 239 amino acid residues. The figure 27 shows the alignment of VchCA with human (isoform hCA I and II) and bacterial  $\alpha$ -CAs (hpyCA identified in the bacterium *Helicobacter pylori*; NgonCA identified in *Neisseria gonorrhoeae*).





## **5.2 Cloning sequencing and production of expression vector**

The three classes of CAs belonging to *V. cholerae* (VchCA, VchCA $\beta$  and VchCA $\gamma$ ) have been prepared using the DNA recombinant technology. The synthetic genes encoding for VchCA (657bp) or VchCA $\beta$  (669bp) or VchCA $\gamma$  (552bp) were cloned into the expression vector pET-15b (see “Material and Methods”)

## **5.3 Optimal growing condition and recombinant protein production**

Time course experiments were performed to optimize the protein expression. For this propose, bacterial cells were transformed with the appropriate expression vectors, grown in rich medium and, after induction with IPTG and metal addition, samples were collected at various time points as described in the experimental section. Compute pI/MW program calculated a theoretical molecular weight of 25 kDa for VchCA, of 29 kDa and 24 kDa for VchCA $\beta$  for VchCA $\gamma$ . In this calculation was included also the His-Tag fragment. After the induction with IPTG, the SDS-PAGE showed that most of protein present in the soluble fraction was obtained after 5 hours for VchCA, 4 hours for VchCA $\beta$  and 6 hours for VchCA $\gamma$ .

Once defined the optimum growth conditions a bacterial culture of 2.0 L has been prepared by using the bacteria transformed with the construct of interest (pET-15b/VchCA, pET-15b/VchCA $\beta$ , pET-15b/VchCA $\gamma$ ). Protein expression was performed as described in the experimental section. After having grown cells, the bacterial pellet was resuspended in Tris-HCl 10 mM pH 8.3 and sonicated.

## **5.4 Purification**

The bacterial extract obtained by sonication was purified by Nichel affinity chromatography as described in “Materials and Methods”. The fractions containing the protein of interest were dialyzed against 10 mM Tris-HCl pH 8.3. The yield of the protein at the end of the purification process was 30 mg VchCA and VchCA $\beta$  28 mg, while for VchCA $\gamma$  it was recovered about 0.7 mg of total protein. The recombinant proteins were analyzed by SDS-PAGE. Vibrio CAs showed a single band of about 26 kDa (Figure 30).

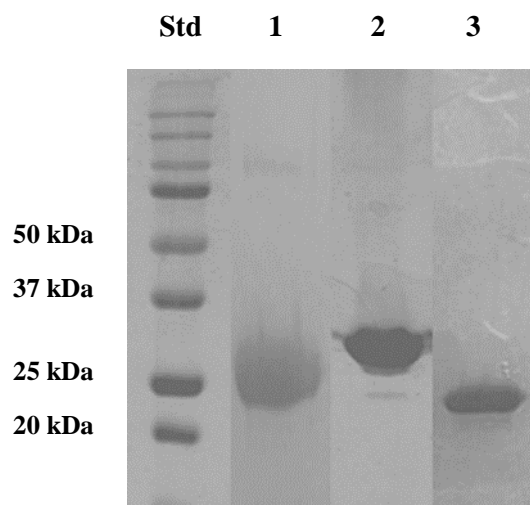


**Figure 30.** SDS-PAGE after affinity chromatography. Std: standards; 1: VchCA; 2: VchCA $\beta$ ; 3: VchCA $\gamma$ .

## 5.5 Biochemical characterization

### 5.5.1 Activity

The *Vibrio* CAs produced as described above were assayed in solution using CO<sub>2</sub> as a substrate and following the procedure described by Chirica *et al.* Enzyme activity was expressed as Wilbur-Anderson units (WAU). Table IX shows specific activities of VchCA, VchCA $\beta$  and VchCA $\gamma$  compared with that obtained for the bovine enzyme bCA ( $\alpha$ -CA). The specific activity of VchCA is 5.4 times higher than the commercial bovine enzyme (bCA), 16 times greater than that calculated for VchCA $\beta$  and 8 times that of VchCA $\gamma$ . The results obtained demonstrate that the VchCA ( $\alpha$ -CA) was the most active. Interestingly VchCA $\gamma$ , is more active than VchCA $\beta$  (respectively the  $\gamma$ -class and  $\beta$ -class CAs founded in *V. cholerae* genome). Generally,  $\gamma$ -CA are reported to be less active than  $\beta$ -CAs

**Table IX.** Specific activity of the three classes of CAs identified in the genome of *V. cholerae* and of bovine  $\alpha$ -CA.

|                                 | Class    | Specific activity<br>(WAU/mg protein) |
|---------------------------------|----------|---------------------------------------|
| <b>VchCA</b>                    | $\alpha$ | 26232                                 |
| <b>VchCA<math>\beta</math></b>  | $\beta$  | 1600                                  |
| <b>VchCA<math>\gamma</math></b> | $\gamma$ | 3200                                  |
| <b>bCA</b>                      | $\alpha$ | 4845                                  |

As described in literature  $\alpha$ -class CAs, in addition to the hydration reaction of CO<sub>2</sub>, catalyze such as secondary reaction the reversible reaction of hydrolysis of esters. The esterase activity of VchCA, identified in the genome of *V. cholerae*, was determined using as substrate the p-NpA. VchCA presents a very low esterase activity (19 U/mg) compared with that of the commercial bCA (Table X).

**Table X.** Esterase activity of VchCA and bCA.

|              | Class    | Specific activity<br>(WAU/mg protein) |
|--------------|----------|---------------------------------------|
| <b>VchCA</b> | $\alpha$ | 19                                    |
| <b>bCA</b>   | $\alpha$ | 1100                                  |

### 5.5.2 Kinetic constants

In Table XI are shown the rate constants ( $k_{cat}$ ,  $K_M$  and  $k_{cat} / K_M$ ) of the three classes of CA identified in the genome of *V. cholerae* and the inhibition constant ( $K_I$ ) using the inhibitor acetazolamide. These constants were compared with the kinetic parameters of other CA belonging to  $\alpha$ -,  $\beta$ - and  $\gamma$ -classes identified in different organisms.

**Table XI.** Kinetic constants determination for the hydratase reaction catalyzed by CAs identified in the genome of *V. cholerae*. The results were compared with those obtained for CAs identified in other organisms. The inhibition constant was obtained for the classical sulfonamide inhibitor, acetazolamide.

| Class    | Enzyme                          | Organism        | $k_{cat}$ ( $s^{-1}$ )               | $K_M$ (M)                               | $k_{cat}/K_M$ ( $M^{-1}s^{-1}$ )    | $K_I$ (nM)<br>(acetazolamide) |
|----------|---------------------------------|-----------------|--------------------------------------|---|-------------------------------------|-------------------------------|
| $\alpha$ | hCA I                           | Mammal          | $2,00 \times 10^5$                   | $4,0 \times 10^{-3}$                    | $5,0 \times 10^7$                   | 250                           |
|          | hCA II                          | Mammal          | $1,40 \times 10^6$                   | $9,3 \times 10^{-3}$                    | $1,5 \times 10^8$                   | 12                            |
|          | hp $\alpha$ CA                  | Bacteria        | $2,5 \times 10^5$                    | $16,6 \times 10^{-3}$                   | $1,5 \times 10^7$                   | 21                            |
|          | SazCA                           | Bacteria        | $4,40 \times 10^6$                   | $12,5 \times 10^{-3}$                   | $3,5 \times 10^8$                   | 0,90                          |
|          | SspCA                           | Bacteria        | $9,35 \times 10^5$                   | $85 \times 10^{-3}$                     | $1,1 \times 10^8$                   | 4,5                           |
|          | <b>VchCA</b>                    | <b>Bacteria</b> | <b><math>8,23 \times 10^5</math></b> | <b><math>11,7 \times 10^{-3}</math></b> | <b><math>7,0 \times 10^7</math></b> | <b>6,8</b>                    |
| $\beta$  | FbiCA I                         | Plant           | $1,2 \times 10^5$                    | $1,6 \times 10^{-3}$                    | $7,5 \times 10^6$                   | 27                            |
|          | BsuCA219                        | Bacteria        | $6,4 \times 10^5$                    | $16,4 \times 10^{-3}$                   | $3,9 \times 10^7$                   | 63                            |
|          | BsuCA213                        | Bacteria        | $1,1 \times 10^6$                    | $1,2 \times 10^{-3}$                    | $8,9 \times 10^7$                   | 303                           |
|          | PgiCA $\beta$                   | Bacteria        | $2,8 \times 10^5$                    | $18,6 \times 10^{-3}$                   | $1,5 \times 10^7$                   | 214                           |
|          | hp $\beta$ CA                   | Bacteria        | $7,1 \times 10^5$                    | $14,7 \times 10^{-3}$                   | $4,8 \times 10^7$                   | 40                            |
|          | <b>VchCA<math>\beta</math></b>  | <b>Bacteria</b> | <b><math>3,34 \times 10^5</math></b> | <b><math>8,1 \times 10^{-3}</math></b>  | <b><math>4,1 \times 10^7</math></b> | <b>451</b>                    |
| $\gamma$ | PgiCA                           | Bacteria        | $4,1 \times 10^5$                    | $7,5 \times 10^{-3}$                    | $5,4 \times 10^7$                   | 324                           |
|          | CAM                             | Archea          | $6,1 \times 10^4$                    | $7,0 \times 10^{-3}$                    | $8,7 \times 10^5$                   | 63                            |
|          | <b>VchCA<math>\gamma</math></b> | <b>Bacteria</b> | <b><math>7,39 \times 10^5</math></b> | <b><math>11,5 \times 10^{-3}</math></b> | <b><math>6,4 \times 10^7</math></b> | <b>473</b>                    |

VchCA showed a  $k_{cat}$  of  $8.23 \times 10^5 s^{-1}$ , a  $K_M$  of 11.7 mM and a  $k_{cat}/K_M$  of  $7.0 \times 10^7 M^{-1} s^{-1}$ . VchCA was more active of the human isoform hCAI ( $k_{cat} = 2.0 \times 10^5 s^{-1}$ ) and hp $\alpha$ CA ( $k_{cat} = 2,5 \times 10^5 s^{-1}$ ), it has an activity of an order of magnitude lower than hCA II and SazCA, an extremophilic CA from the genome of *Sulfurihydrogenibium azorense*. Furthermore, VchCA was inhibited by acetazolamide ( $K_I = 6.8$  nM) better than the hCA II and hp $\alpha$ CA.

VchCA $\beta$  had a  $k_{cat}$  of  $3.34 \times 10^5 s^{-1}$  and a  $K_M$  of  $8.1 \times 10^{-3} s^{-1}$  and a catalytic efficiency of  $4.1 \times 10^7 M^{-1} s^{-1}$ . The enzyme showed a  $k_{cat}$  similar to that of the enzyme identified in plant (FbiCA1) and its catalytic efficiency is very similar to that of other bacterial enzymes, but it was two orders of magnitude lower compared to the  $\beta$ -class enzyme identified in the bacterium *Porphyromonas gingivalis* (PgiCA $\beta$ ). In addition,

acetazolamide was found to be a less effective inhibitor for VchCA $\beta$  than VchCA, showing an inhibition constant of 451 nM (Table XI).

VchCA $\gamma$  showed a  $k_{cat}$  of  $7.39 \times 10^5 s^{-1}$ , an order of magnitude higher than that of  $\gamma$ -CA (CAM) identified in the thermophilic Archeon *Metanosarcina thermophila* and, slightly higher than the  $k_{cat}$  of the bacterial  $\gamma$ -CA PgiCA. Interestingly, VchCA $\gamma$  resulted more active than VchCA $\beta$ , while the acetazolamide shows an inhibition constant of 473 nM.

### 5.5.3 Thermoactivity and Thermostability

Thermoactivity was only determined for VchCA because this is the unique class of CA ( $\alpha$ -CA) that possesses an esterase activity. The results were compared with those obtained for the bovine enzyme, bCA. In Figure 31 is shown that VchCA activity is shifted of 10 degrees respect to that of the mammalian enzyme. bCA, in fact, showed a maximum peak of enzyme activity at 60 ° C, while for VchCA this peak was at 70 ° C (Figure 31).

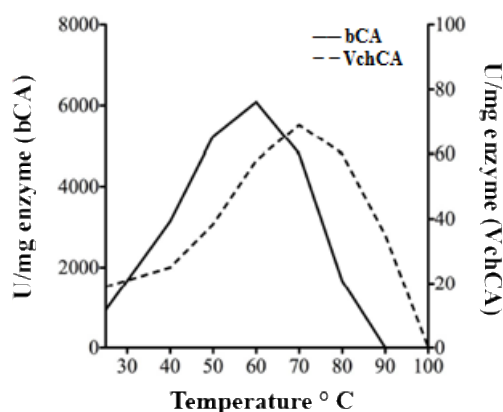


**Figure 31.** Comparison of the thermoactivity of VchCA and bCA. The enzyme activity was measured at the indicated temperatures on the x-axis using the p-NpA as a substrate. Each point is the mean  $\pm$  SEM of three independent determinations.

This variation may be due to the fact that the enzyme of *Vibrio cholerae* is characterized by an amino acid sequence shorter than bCA, which probably confers stability to the bacterial enzyme.

Thermostability of VchCA, VchCA $\beta$ , VchCA $\gamma$  and bCA were investigated incubating each enzyme at 30, 40, 50, 60, 70, 80 and 90 ° C. After 30 and 120

minutes of incubation, an aliquot of each enzyme was taken and assayed using CO<sub>2</sub> as a substrate. Figure 32 showed that after 30 minutes of incubation the activity of the bovine enzyme (bCA) decreases faster than that of VchCA. In fact, at 80 °C the residual activity for VchCA is 40%, while for bCA is 0. VchCA $\gamma$  and VchCA $\beta$  have a behavior very similar to the bovine enzyme (Figure 32). After 120 minutes of incubation, the bCA and VchCA $\beta$  are inactive at temperatures higher than 60 °C, VchCA $\gamma$  is inactivated at 70 °C, while VchCA is completely inactive at 80 °C. These results demonstrated that VchCA is more stable respect to the  $\beta$  and  $\gamma$ -CAs identified in the genome of *Vibrio cholerae*.

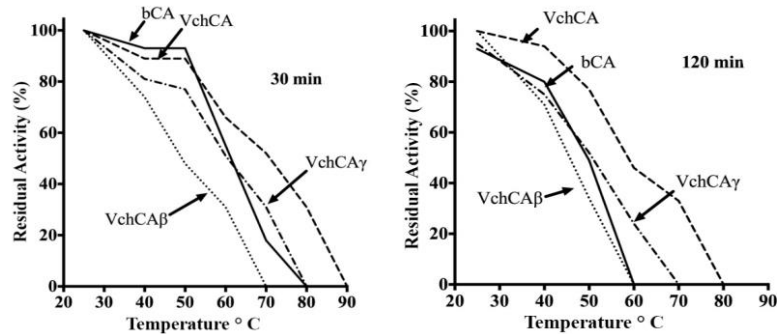


**Figure 32.** Thermostability of VchCA, VchCA $\beta$ , VchCA $\gamma$  and bCA. The enzymes were incubated for 30 to 120 minutes at the indicated temperatures on the x-axis and assayed using CO<sub>2</sub> as a substrate. Each point is the mean  $\pm$  SEM of three independent determinations.

#### 5.5.4 Protonography

The activity of proteolytic enzymes, capable of refold and acquire the proteolytic activity after treatment with SDS, can be determined by SDS-PAGE after the removal of the detergent. Such a technique is known with the name of zymography. It has developed a technique to identify the activity of CA hydratase on SDS-PAGE (see Materials and Methods), we named this technique protonography, because during the CO<sub>2</sub> hydratase reaction are produced protons, which are then responsible of the change of color that appears on the gel, in correspondence of the CA (see Material and Methods).

In figure 33 are reported the protonograms obtained using bovine bCA ( $\alpha$ -CA class) and the recombinant CAs ( $\alpha$ ,  $\beta$  and  $\gamma$ ) from *V. cholerae*. Protonograms of VchCA, VchCA $\beta$  and VchCA $\gamma$  showed the different behavior

that the three bacterial CAs assumed during the SDS-PAGE. It is known that mammal  $\alpha$ -CAs are monomeric and the protonogram of bCA showed a single band of activity corresponding to a monomer of 30 kDa (Figure 33 A). The bacterial  $\alpha$ -CAs are generally dimeric enzymes and the protonogram showed three bands of activity: a monomer (25 kDa), a dimer (50 kDa) and a tetramer (100 kDa) (Figure 33 A). Therefore, unlike bCA, VchCA is present in three different oligomeric states. The protonogram of VchCA $\beta$  (Figure 33 B) showed two bands of activity: a band corresponding to the monomeric form (29 kDa) and one at the dimeric form (58 kDa). The protonogram of VchCA $\gamma$  showed a band of activity in correspondence of the monomer (24 kDa) and the trimer (69 kDa) (Figure 33C). The yellow bands found in correspondence of the inactive monomeric form of VchCA $\beta$  or VchCA $\gamma$ , is due to the fact that at the end of the electrophoretic run, the SDS is removed from the gel. This procedure may lead to the rearrangement of  $\beta$ - or  $\gamma$ -CA monomers in the gel and the final result is the reconstitution of the active dimeric ( $\beta$  -CA) or trimeric forms ( $\gamma$  -CA). Protonography allowed us to distinguish not only the active enzyme, but also oligomeric states of the CA.

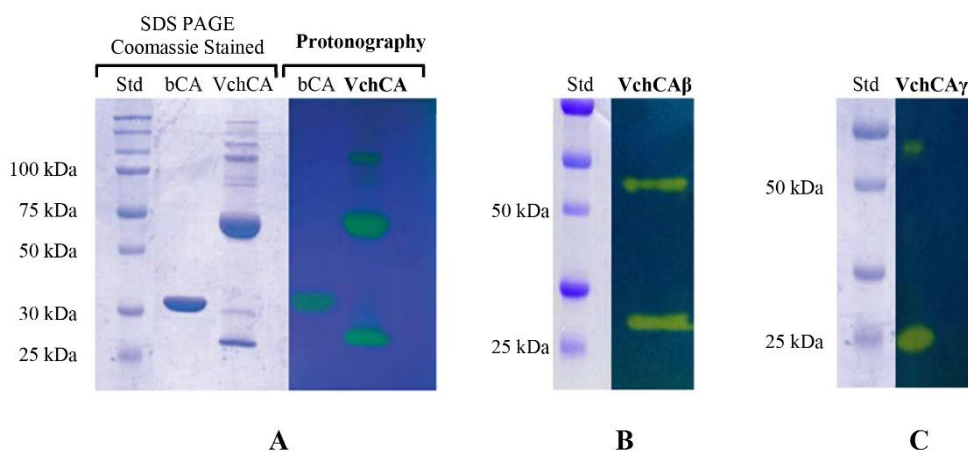


**Figure 33.** A: protonogram and SDS-PAGE stained with Coomassie compared. Both Gels were run in non-reducing denaturing conditions and loaded with 4 micrograms of bCA and VchCA. The appearance of the band occurred after 5 seconds of incubation in CO<sub>2</sub> saturated water. B: protonogram of VchCA $\beta$  with a molecular weight marker (Coomassie gel not shown). The band appeared after 40 seconds of incubation in CO<sub>2</sub> saturated water. C: protonogram of VchCA $\gamma$  with a molecular weight marker (Coomassie gel not shown). The band appeared after 25 seconds of incubation in CO<sub>2</sub> saturated water.

## 5.6 Inhibition

### 5.6.1 Sulfonamides and the bioisosteres

In collaboration with Prof. C. Supuran, University of Florence, a large number of sulfonamides and sulfamates were tested to evaluate their effectiveness on the inhibition of *V. cholerae* CA.

Simple aromatic and heteroaromatic sulfonamides of types **1-24** were among them, as well as derivatives **AAZ-IND**, which are clinically used drugs or agents in clinical development (Figure 34). Acetazolamide **AAZ**, methazolamide **MZA**, ethoxzolamide **EZA** and dichlorophenamide **DCP**, are the classical, systemically acting CAIs. Dorzolamide **DZA** and brinzolamide **BRZ** are topically-acting antiglaucoma agents, benzolamide **BZA** is an orphan drug belonging to this class of pharmacological agents, whereas topiramate **TPM** and zonisamide **ZNS** are widely used antiepileptic drugs. Sulpiride **SLP** and indisulam **IND** were recently shown by this group to belong to this class of pharmacological agents. Sulfonamides **1-24** and the clinically used agents investigated in this study were either commercially available, or were prepared as reported earlier by our group (Figure 34).

The study of inhibition profiles has the aim to identify the existence of selective inhibitors for the CA identified in the genome of *V. cholerae*. Some of these compounds are excellent inhibitors of bacterial enzymes (Table XIII). These results will be of great assistance for the realization of new inhibitors characterized by a high selectivity towards the bacterial CAs.

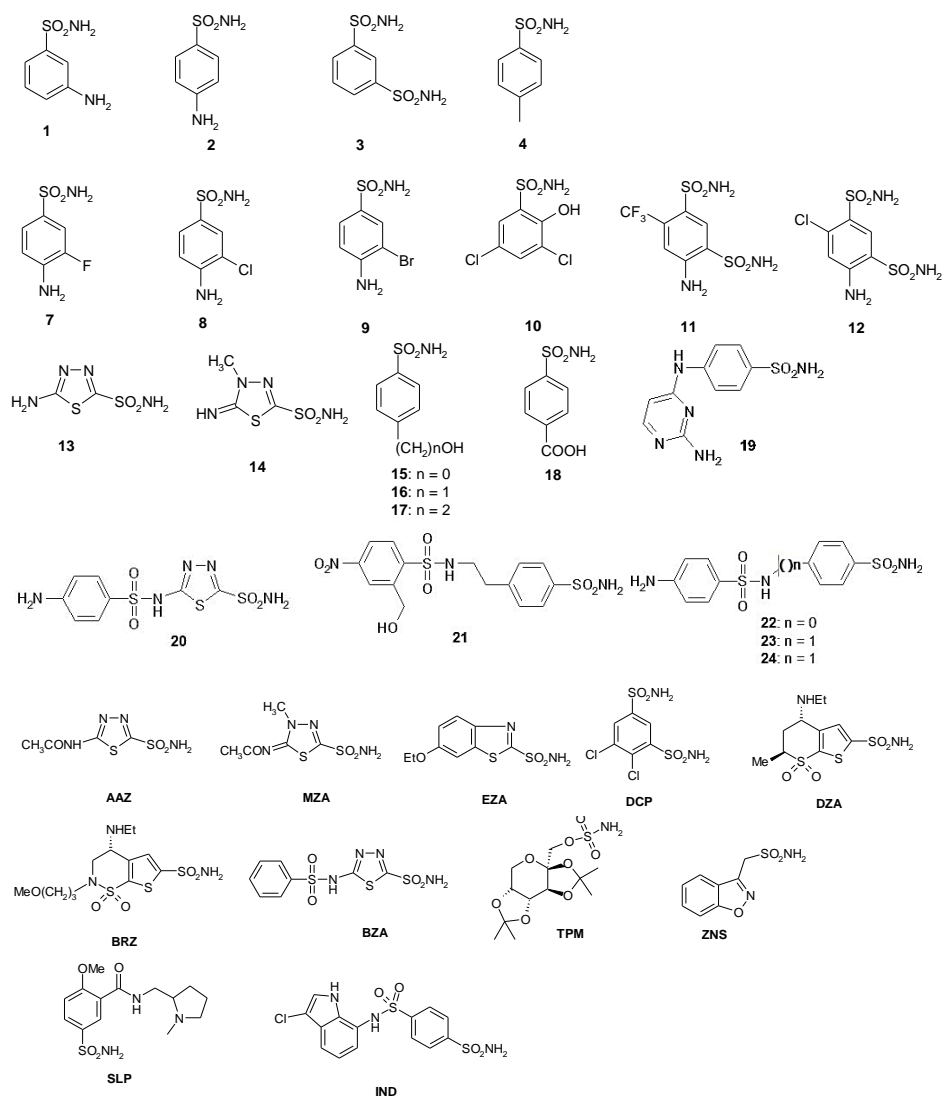


**Figure 34.** Sulfonamides and bisosteres inhibitors structures.

**Table XII.** Sulfonamides and bioisosteres inhibition constants for the human  $\alpha$ -CA isoforma I and II, the  $\alpha$ -CA of *H. pylori* (hp $\alpha$ CA) and the three classes of CA identified in the genome of *V. cholerae*, obtained with the technique of "stopped flow" at 20 ° C and pH 7.5.

| <b>K<sub>r</sub><sup>a</sup> (nM)</b> |              |               |                                |              |                                |               |
|---------------------------------------|--------------|---------------|--------------------------------|--------------|--------------------------------|---------------|
| <b>Inhibitor</b>                      | <b>hCA I</b> | <b>hCA II</b> | <b>hp<math>\alpha</math>CA</b> | <b>VchCA</b> | <b>Vch<math>\beta</math>CA</b> | <b>VchyCA</b> |
| 1                                     | 45400        | 295           | 426                            | 440          | 463                            | 672           |
| 2                                     | 25000        | 240           | 454                            | 471          | 447                            | 95,3          |
| 3                                     | 28000        | 300           | 316450                         | 125          | 785                            | 93,6          |
| 4                                     | 78500        | 320           | 873                            | 219          | >10000                         | 76,3          |
| 5                                     | 25000        | 170           | 1150                           | 447          | >10000                         | 80,6          |
| 6                                     | 21000        | 160           | 1230                           | 402          | >10000                         | 69,0          |
| 7                                     | 8300         | 60            | 378                            | 199          | >10000                         | 73,6          |
| 8                                     | 9800         | 110           | 452                            | 139          | 9120                           | 73,6          |
| 9                                     | 6500         | 40            | 510                            | 133          | >10000                         | 95,3          |
| 10                                    | 6000         | 70            | 412                            | 99,1         | >10000                         | 544           |
| 11                                    | 5800         | 63            | 49                             | 62,9         | 879                            | 87,1          |
| 12                                    | 8400         | 75            | 323                            | 45,3         | 4450                           | 563           |
| 13                                    | 8600         | 60            | 549                            | 23,5         | 68,1                           | 66,2          |
| 14                                    | 9300         | 19            | 268                            | 12,1         | 82,3                           | 69,9          |
| 15                                    | 6            | 2             | 131                            | 4,2          | 349                            | 88,5          |
| 16                                    | 164          | 46            | 114                            | 42,7         | 304                            | 556           |
| 17                                    | 185          | 50            | 84                             | 30,3         | 3530                           | 6223          |
| 18                                    | 109          | 33            | 207                            | 59,8         | 515                            | 5100          |
| 19                                    | 95           | 30            | 105                            | 4,7          | 2218                           | 4153          |
| 20                                    | 690          | 12            | 876                            | 0,59         | 859                            | 5570          |
| 21                                    | 55           | 80            | 1134                           | 54,5         | 4430                           | 764           |
| 22                                    | 21000        | 125           | 1052                           | 56,7         | 757                            | 902           |
| 23                                    | 23000        | 133           | 541                            | 71,5         | 817                            | 273           |
| 24                                    | 24000        | 125           | 21                             | 52,1         | 361                            | 73,3          |
| AAZ                                   | 250          | 12            | 225                            | 6,8          | 4512                           | 473           |
| MZA                                   | 50           | 14            | 193                            | 3,6          | 6260                           | 494           |
| EZA                                   | 25           | 8             | 378                            | 0,69         | 6450                           | 85,1          |
| DCP                                   | 1200         | 38            | 4360                           | 37,1         | 2352                           | 1230          |
| DZA                                   | 50000        | 9             | 210                            | 6,3          | 4728                           | 87,3          |
| BRZ                                   | 45000        | 3             | 315                            | 2,5          | 845                            | 93,0          |
| BZA                                   | 15           | 9             | 172                            | 4,2          | 846                            | 77,6          |
| TPM                                   | 250          | 10            | 231                            | >1000        | 874                            | 68,8          |
| ZNS                                   | 56           | 35            | 204                            | 982          | 8570                           | 725           |
| SLP                                   | 1200         | 40            | 413                            | >1000        | 6245                           | 77,9          |
| IND                                   | 31           | 15            | nt                             | 8,1          | 7700                           | 91,3          |
| VLX                                   | 54000        | 43            | nt                             | 89,7         | 8200                           | 817           |
| CLX                                   | 50000        | 21            | nt                             | >1000        | 4165                           | 834           |
| SLT                                   | 374          | 9             | nt                             | 88,4         | 455                            | 464           |
| SAC                                   | 18540        | 5959          | nt                             | >1000        | 275                            | 550           |
| HCT                                   | 328          | 290           | nt                             | 79,5         | 87,0                           | 500           |

<sup>a</sup> error in the range of 5-10% for the reported values; nt = not tested

Table XII showed inhibition data for this panel of sulfonamides (and one sulfamate, TPM) against the human  $\alpha$ -CAs (isoforms hCAI and hCAII) and the recombinant  $\alpha$ ,  $\beta$  and  $\gamma$  CAs from *Vibrio cholerae*. The following should be noted regarding a comparison of *V. cholerae* enzymes inhibition with the compounds investigated in this study: (i) Topiramate **TPM**, a sulfamate, sulpiride **SLP**, a primary sulfonamide, as well as saccharin **SAC**, an acylsulfonamide, were ineffective VchCA inhibitors ( $K_{IS} > 1000$  nM). Moreover, **SAC** was a bad inhibitor for VchCA $\beta$  and VchCA $\gamma$ , while **TPM** and **SLP** were effective inhibitors of VchCA $\gamma$ . These compounds (except saccharin) generally act as good inhibitors of other bacterial or mammalian  $\alpha$ -CAs. Zonisamide, **ZNS**, an aliphatic primary sulfonamide was also a very weak inhibitor for the bacterial enzymes but effective towards the human enzymes ( $K_{IS} \geq 725$  nM); (ii) A large number of simple aromatic sulfonamides, such as derivatives **1-9**, showed moderate VchCA and VchCA $\gamma$  inhibitory properties, with inhibition constants in the range of 125 – 672 nM (Table XIII). It may be observed that all these derivatives are benzenesulfonamides with one or two simple substituents in *ortho*-, *para*- or the 3,4-positions of the aromatic ring with respect to the sulfamoyl zinc-binding moiety. Most of these CAIs were ineffective towards VchCA $\beta$  with  $K_{IS} \geq 9120$  nM; (iii) Most of the sulfonamides investigated here showed a potent inhibitory effect against VchCA, VchCA $\beta$  and VchCA $\gamma$  with inhibition constants in the range of 23.5 – 88.5 nM. These derivatives include compounds **13-15**. It is interesting to note that compounds **10-13**, **16-18**, **21-24**, **DCP**, **VLX**, **SLT** and **HCT** showed a potent inhibitory effect against VchCA. Some of them are effective towards VchCA $\beta$  or VchCA $\gamma$  but never effective for all the three classes identified in the genome of *V. cholerae* (Table XII); (iv) Several very potent VchCA inhibitors were detected, such as compounds **14**, **15**, **19**, **20**, **AAZ**, **MZA**, **EZA**, **DZA**, **BRZ**, **BZA**, and **IND**, which showed  $K_{IS}$  in the range of 0.59 – 12.1 nM (Table XIII); (v) Most of the sulfonamides used were effective inhibitors of VchCA $\gamma$  but the  $K_{IS}$  was always  $\geq 69$  nM; (v) The inhibition profile of VchCA, VchCA $\beta$  or VchCA $\gamma$  was different from that of the

other bacterial or mammalian CAs investigated up until now, proving that probably it will be possible to design VchCA-, VchCA $\beta$ - or VchCA $\gamma$ -selective inhibitors using the scaffold of leads detected here.

### **5.6.2 Anions**

In addition to sulfonamides and bioisosteres, another class of CA inhibitors is represented by anions. In the table XIII is shown the inhibition profile of VchCA, VchCA $\beta$  and VchCA $\gamma$  with a series of simple and complex inorganic anions in comparison with those obtained for the human isoforms (hCA I and II) and the bacterial enzyme of *Helicobacter pylori* (hpaCA).

**Table XIII.** Anions inhibition constants for the human  $\alpha$ -CAs isoforms I and II,  $\alpha$ -CA of *H. pylori* and the three classes of CA identified in the genome of *V. cholerae*, obtained with the technique of "stopped- flow "at 20 ° C and pH 7.5.

| <b>K<sub>I</sub><sup>a</sup> (mM)</b>           |              |               |                                |              |                                |                                 |
|---|--------------|---------------|--------------------------------|--------------|--------------------------------|---------------------------------|
| <b>Inhibitor</b>                                | <b>hCA I</b> | <b>hCA II</b> | <b>hp<math>\alpha</math>CA</b> | <b>VchCA</b> | <b>Vch<math>\beta</math>CA</b> | <b>Vch<math>\gamma</math>CA</b> |
| F <sup>-</sup>                                  | >300         | >300          | 4,08                           | 0,80         | 8,7                            | 21,3                            |
| Cl <sup>-</sup>                                 | 6            | 200           | 2,70                           | 0,93         | 8,1                            | 8,8                             |
| Br <sup>-</sup>                                 | 4            | 63            | 2,41                           | 28,0         | 7,4                            | 8,7                             |
| I <sup>-</sup>                                  | 0,3          | 26            | 6,05                           | 9,73         | 9,0                            | 6,3                             |
| CNO <sup>-</sup>                                | 0,0007       | 0,03          | 0,60                           | 0,075        | 7,1                            | 2,6                             |
| SCN <sup>-</sup>                                | 0,2          | 1,60          | 4,10                           | 0,82         | 9,5                            | 13,1                            |
| CN <sup>-</sup>                                 | 0,0005       | 0,02          | 0,76                           | 0,033        | 5,7                            | 8,4                             |
| N <sub>3</sub> <sup>-</sup>                     | 0,0012       | 1,51          | 0,83                           | 0,76         | 20,5                           | 8,7                             |
| HCO <sub>3</sub> <sup>-</sup>                   | 12           | 85            | 0,75                           | 5,13         | 5,9                            | 3,0                             |
| CO <sub>3</sub> <sup>2-</sup>                   | 15           | 73            | 0,66                           | 4,64         | 6,7                            | 8,2                             |
| NO <sub>3</sub> <sup>-</sup>                    | 7            | 35            | 0,81                           | 0,67         | 8,4                            | 7,8                             |
| NO <sub>2</sub> <sup>-</sup>                    | 8,4          | 63            | 0,93                           | 34,1         | 9,1                            | 8,7                             |
| HS <sup>-</sup>                                 | 0,0006       | 0,04          | 0,69                           | 0,074        | 21,3                           | 7,9                             |
| HSO <sub>3</sub> <sup>-</sup>                   | 18           | 89            | 0,99                           | 0,068        | >200                           | >200                            |
| SnO <sub>3</sub> <sup>2-</sup>                  | 0,57         | 0,83          | 0,55                           | 5,32         | 3,1                            | 2,9                             |
| SeO <sub>4</sub> <sup>2-</sup>                  | 118          | 112           | 0,72                           | 60,8         | 3,4                            | 9,1                             |
| TeO <sub>4</sub> <sup>2-</sup>                  | 0,66         | 0,92          | 0,34                           | 14,5         | 2,3                            | 7,2                             |
| P <sub>2</sub> O <sub>7</sub> <sup>4-</sup>     | 25,8         | 48,5          | 0,66                           | 2,96         | 15,1                           | 7,3                             |
| V <sub>2</sub> O <sub>7</sub> <sup>4-</sup>     | 0,54         | 0,57          | 0,27                           | 0,84         | 7,9                            | 8,3                             |
| B <sub>4</sub> O <sub>7</sub> <sup>2-</sup>     | 0,64         | 0,95          | 0,56                           | 16,6         | 3,4                            | 7,2                             |
| ReO <sub>4</sub> <sup>+</sup>                   | 0,11         | 0,75          | 0,88                           | 5,11         | 6,3                            | >200                            |
| RuO <sub>4</sub> <sup>+</sup>                   | 0,101        | 0,69          | 0,36                           | 0,61         | 8,4                            | >200                            |
| S <sub>2</sub> O <sub>8</sub> <sup>2-</sup>     | 0,107        | 0,084         | 0,92                           | 84,1         | 3,4                            | >200                            |
| SeCN  | 0,0085       | 0,086         | 0,73                           | 0,76         | 5,3                            | 8,7                             |
| CS <sub>3</sub> <sup>2-</sup>                   | 0,0087       | 0,0088        | 0,38                           | 0,088        | 7,0                            | 8,8                             |
| Et <sub>2</sub> NCS <sub>2</sub> <sup>-</sup>   | 0,79         | 3,1           | 0,005                          | 0,043        | 0,73                           | 0,44                            |
| SO <sub>4</sub> <sup>2-</sup>                   | 63           | >200          | 0,82                           | 0,85         | >200                           | 9,6                             |
| ClO <sub>4</sub> <sup>-</sup>                   | >200         | >200          | 10,1                           | >200         | >200                           | >200                            |
| BF <sub>4</sub> <sup>-</sup>                    | >200         | >200          | >200                           | >200         | >200                           | >200                            |
| FSO <sub>3</sub> <sup>-</sup>                   | 0,79         | 0,46          | 0,91                           | 86,1         | 8,9                            | 7,5                             |
| NH(SO <sub>3</sub> ) <sub>2</sub> <sup>2-</sup> | 0,31         | 0,76          | 0,54                           | 88,2         | >200                           | 8,1                             |
| H <sub>2</sub> NSO <sub>2</sub> NH <sub>2</sub> | 0,31         | 1,13          | 0,073                          | 0,008        | 0,054                          | 0,084                           |
| H <sub>2</sub> NSO <sub>3</sub> H               | 0,021        | 0,39          | 0,080                          | 0,031        | 0,086                          | 0,087                           |
| PhB(OH) <sub>2</sub>                            | 58,6         | 23,1          | 0,097                          | 0,007        | 0,085                          | 0,081                           |
| PhAsO <sub>3</sub> H <sub>2</sub>               | 31,7         | 49,2          | 0,44                           | 0,023        | 0,079                          | 0,091                           |

<sup>a</sup> error in the range of 3 - 5% for the reported values

Interestingly, the carbonate and bicarbonate are not very effective inhibitors for *V. cholerae* CA ( $K_I = 3$  to 8.2 mM). This result is in agreement with the fact that *V. cholerae* colonizes the upper part of the small intestine characterized by high concentrations of bicarbonate, in turn considered a potent inducer of the expression of the genes involved in the virulence of the pathogen. This is an example of evolutionary adaptation of the *Vibrio* CAs to the high concentrations of bicarbonate. Interesting, also for two human isoforms (hCA I

and hCAII) carbonate and bicarbonate are not effective inhibitors ( $K_I = 12\text{-}85$  mM). In fact, these anions are present in the plasma at high concentrations.

### 5.7 *Plasmodium falciparum*

In 2004, in genome of the protozoan *Plasmodium falciparum*, the causative agent of malaria Krungkrai and coworkers identified a gene encoding for a CA. This gene was identified in the GeneBank with the following accession number AAN35994.2. The open reading frame of the malarial CA enzyme (*P. falciparum* CA, accession number AAN35994.2, PlasmoDB: PF3D7\_1140000) encodes a 600 amino acid polypeptide chain. In 2004, Krungkrai and coworkers cloned a truncated form of *Plasmodium falciparum* CA gene (GenBank: AAN35994.2) encoding for an active CA (named PfCA1) with a primary structure of 235 amino acid residues (Reungprapavut S., *et al.* 2004). The metalloenzyme showed a good esterase activity with 4-nitrophenylacetate as a substrate and was inhibited by known sulfonamide CA inhibitors (CAIs). The authors observed that the highly conserved  $\alpha$ -CA active site residues, responsible for binding of the substrate and for catalysis, were present also in PfCA1 and considered thus the Plasmodium enzyme belonging to the  $\alpha$ -CA class. Subsequent, it was showed that different Plasmodium spp. encoded CAs, all considered to belong to the  $\alpha$ -class, and that primary sulfonamides inhibited in vitro and in vivo the growth of Plasmodium parasites. Recently, in the laboratory where I did my PhD, it was reanalyzed and realigned the amino acid sequence of the truncated PfCA1 with the two human  $\alpha$ -CA isoforms, hCA I and II, in order to identify other features of the protozoan enzyme (Figure 9). We observed that to have three histidines aligned with the three zinc-coordinating histidines of the human isoforms, it was necessary to “force” the alignment, introducing in the PfCA1 sequence a five-residues insertion and a six-residues deletion between residues 96–119. Nevertheless, the other residues crucial for the catalytic mechanism of the  $\alpha$ -CAs, such as the proton shuttle His64 and one of the gatekeeper residues, Thr199, seemed to be not conserved in the Plasmodium enzyme (Del Prete S. *et al.* 2014; Vullo D. *et al.* 2015; Supuran C.T. & Capasso C. 2014) (Figure 9). The dyad Glu106-Thr199 is highly conserved in all  $\alpha$ -CAs investigated so far, being involved in the orientation of the substrate for the nucleophilic attack by the zinc hydroxide species of the enzyme. Thus, the proposed alignment showed important amino acid substitutions that differentiated the sequence of Plasmodium enzyme from those

of other  $\alpha$ -CAs. Hence, a phylogenetic tree was constructed to better investigate the relationship of the Plasmodia amino acid sequences with CAs from prokaryotic and eukaryotic species belonging to different classes ( $\alpha$ -,  $\beta$ -,  $\gamma$ -,  $\delta$ -, and  $\zeta$ -CAs). In Figure 35 has been represented only the branches with  $\alpha$ -,  $\delta$ -,  $\eta$  and  $\zeta$ -CAs). It was observed that Plasmodia CAs clustered in a branch different from that of the  $\alpha$ -CAs, although close to it, while they were well separated from the other CA classes (Figure 35). We hypothesized that the Plasmodia CAs were the result of modifications of an ancestral  $\delta$ -CA gene, which originated a new class of CA that we denominated  $\eta$ -class.

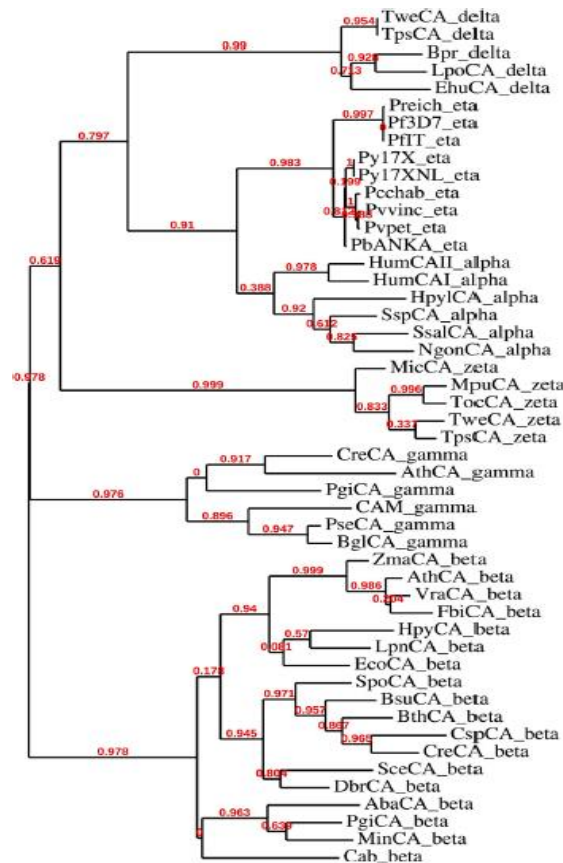


**Figure 35.** Phylogenetic tree that led to the discovery of  $\eta$  class in the genus Plasmodium, built using the amino acid sequences of the  $\alpha$ -,  $\beta$ -,  $\gamma$ -,  $\delta$ -,  $\zeta$ - and  $\eta$ -CA of prokaryotic and eukaryotic organisms. To build the tree was used PhyML 3.0 program.

In collaboration with Dr. Giuseppina De Simone, we constructed, for homology modeling, the three-dimensional structure model of *P. falciparum* CA, aligning the entire shape of the CA of the protozoan (600 aa) with different amino acid sequences of  $\alpha$ -CA with known crystallographic structure (De Simone G., *et al.* 2015) such as *Neisseria gonorrhoeae*, *Thermovibrio ammonificans*, *Homo sapiens*, *Chlamydomonas reinhardtii*, *Aspergillus oryzae* and *Dunaliella salina*. In figure 36 it is shown a detail of the structural model of *P. falciparum* CA catalytic site.

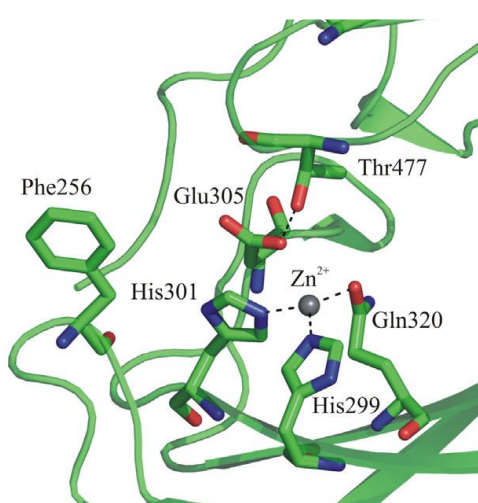


**Figure 36.** Particular of CA catalytic site of *Plasmodium falciparum* modeled on the three-dimensional structure of known CAs.

From that model, it shows that the metal is coordinated with two His residues (corresponding to residues 94 and 96 in the sequence of hCA I) and a residue of glutamine (which corresponds to residue His119 in sequence hCA I) (Figure 36). This coordination pattern was never observed in any of the CAs gene family. It is probable that the event, which triggered the separation of  $\eta$ - from  $\alpha$ -class, has been the mutation of one of the histidine residues that coordinate the zinc ion with the residue of glutamine. Moreover, the separation of the class  $\eta$ - from the  $\alpha$ -class, is also characterized by the replacement of the His residue in position 64 with a tyrosine residue (De Simone, G. et al, 2015).

In collaboration with Prof. Claudiu Supuran, were determined the kinetic constants of this new class of CA. PfCA1, showed the following kinetic

properties for the CO<sub>2</sub> hydration reaction to bicarbonate and protons:  $k_{\text{cat}}$  of  $1.4 \times 10^5 \text{ s}^{-1}$  and a  $k_{\text{cat}} / K_{\text{M}}$  of  $5.4 \times 10^6 \text{ M}^{-1} \times \text{s}^{-1}$ . In Table XIV were compared the kinetic constants of PfCA1 with those of other classes of CAs from different organisms. It can be noted as PfCA1 presents a significant catalytic action with a  $k_{\text{cat}}$  of value in the same order of magnitude of hCA I and of the CA from *Flaveria bidentis*, while it is about 28 times less efficient than the hCA II. Moreover, the activity of PfCA1 is effectively inhibited by acetazolamide ( $K_{\text{I}} = 170 \text{ nM}$ ). Although the  $\eta$ - and  $\alpha$ -CAs share many similar features, strongly suggesting the first ones to be evolutionary derived from the last, there are significant differences between the two families to allow some optimism for the drug design of selective inhibitors for the parasite over the host enzymes. However, these studies are still in their initial phase and further work by X-ray crystallography should validate the model proposed in order to detect inhibitors with high affinity and selectivity for the  $\eta$ -CAs over the  $\alpha$ -CAs

**Table XIV.** Kinetic parameters for the hydration reaction of CO<sub>2</sub> catalyzed by different CA belonging to different families.  $\alpha$  class : hCA I and II and the bacterial enzyme SazCA (*Sulfurihydrogenibium azorense*).  $\beta$  class : CH2 (*Cryptococcus neoformans*) and FbiCA1 (*Flaveria bidentis*).  $\gamma$  class : is represented by PgiCA (*Porphyromonas gingivalis*) and that of  $\eta$  class from PfCA1 of *Plasmodium falciparum*.

|               | Class    | Organism  | $k_{\text{cat}}$ (s <sup>-1</sup> ) | $k_{\text{cat}}/K_{\text{M}}$ (M <sup>-1</sup> s <sup>-1</sup> ) | $K_{\text{I}}$ (nM)<br>(acetazolamide) |
|---------------|----------|-----------|-------------------------------------|--|--|
| <b>hCA I</b>  | $\alpha$ | Mammal    | $2,0 \times 10^5$                   | $5,0 \times 10^7$  | 250                                    |
| <b>hCA II</b> | $\alpha$ | Mammal    | $1,4 \times 10^6$                   | $1,5 \times 10^8$  | 12                                     |
| <b>SazCA</b>  | $\alpha$ | Bacteria  | $4,4 \times 10^6$                   | $3,5 \times 10^8$  | 0,9                                    |
| <b>Can2</b>   | $\beta$  | Fungi     | $3,9 \times 10^5$                   | $4,3 \times 10^7$  | 10,5                                   |
| <b>FbiCA1</b> | $\beta$  | Plant     | $1,2 \times 10^5$                   | $7,5 \times 10^6$  | 27                                     |
| <b>PgiCA</b>  | $\gamma$ | Bacteria  | $4,1 \times 10^5$                   | $5,4 \times 10^7$  | 324                                    |
| <b>PfCA1</b>  | $\eta$   | Protozoan | $1,4 \times 10^5$                   | $5,4 \times 10^6$  | 170                                    |

### 5.7.1 $\eta$ -CA inhibition studies

I started to investigate the inhibition profile of the  $\eta$ -CA from *Plasmodium falciparum* against a panel of sulfonamides and one sulfamate compound, some of which are clinically used. The strongest inhibitors identified were ethoxzolamide and sulthiame, with  $K_{\text{Is}}$  of 131–132 nM, followed by acetazolamide, methazolamide and hydrochlorothiazide ( $K_{\text{Is}}$  of 153–198 nM).

Brinzolamide, topiramate, zonisamide, indisulam, valdecoxib and celecoxib also showed significant inhibitory action against  $\eta$ -CA, with  $K_{Is}$  ranging from 217 to 308 nM. Considering the small number of inhibition studies reported at this moment for the  $\eta$ -CAs, these results demonstrate it is quite probable that effective, low nanomolar inhibitors may be developed. Moreover, some dendrimers investigated showed a better inhibitory power compared to acetazolamide. The main conclusion is that this class of molecules may lead to important developments in the field of anti-infective CA inhibitors. Given that drug resistance has emerged against most antimalarial in clinical use, the discovery of  $\eta$ -CA -specific inhibitors may lead to a novel therapeutic approach for malaria once the biology of  $\eta$ -CA has been further investigated in different life cycle stages.

## Chapter 6. Evolutionary aspects

The analysis of the Gram-positive and Gram-negative genomes conducted by similarity sequence searching programs, such as Blasta and Fasta, revealed a very complex distribution of the different classes of CAs in the two groups of bacteria. In fact, the genome of some of them encodes for all three classes of CAs ( $\alpha$ ,  $\beta$  and  $\gamma$ ), while for others the genome encodes for two or one classes of CAs. Interestingly, the  $\alpha$ -CAs class are only present in the genome of Gram-negative and not in that of Gram-positive bacteria. By analyzing these results, in this thesis we will try to answer the following questions: 1) Why the  $\alpha$ -CA are present only in Gram-negative? 2) What is the physiological role of  $\alpha$ -CA in bacteria? 3) Why the  $\alpha$ -CAs are not present in all Gram-negative? 4) Why there are species of bacteria whose genome does not code for CA?

A characteristic common to the  $\alpha$ -CA identified in Gram-negative bacteria, it is the presence of a signal peptide to the N-terminal of the amino acid sequence (Figure 37 marked in red). This sequence directs the newly synthesized  $\alpha$ -CA towards the periplasmic space, i.e. the space between the inner and outer membrane, which is absent in Gram-positive bacteria. The presence, then, of the periplasmic space would explain why the  $\alpha$ -CA are present only in Gram-negative bacteria.

```

hCAI      -----MASP----DWGYDD-KNGPEQW-----SKL
hCAII     -----MSH----HWGYGK-HNGPEHW-----HKD
hCAVA     MLGRN----TWKTSAFSFLVEQHWAP----LWSR---SMRPGRWCSQRSCAWQTSNNTL
hCAVI     ---MR----ALVLLLSLFLGGQAQH--VSDWTYSEGALDEAHW-----PQH
HpyCA     ---MKKT---FLIALALTA SLIGAE NT---KWDYKNKENGPHRW-----DKL
VchCA     ---MKKT---TWVLAMVASMSFGTQAS----EWGYEG-EHAPEHW-----GKV
NgonCA    MPRFPRTLPRLTAVLLLACTAFSIAAHGNHWHWYTG-HDSPESW-----GNL
SspCA     ---MRKIL--ISAVLVLSISISFAEH----EWSYEG-EKGPEHW-----AQL

```

**Figure 37.** A detail of the multialignment of the  $\alpha$ -CA amino acid sequences identified in the genome of mammalian and Gram-negative bacteria. The signal sequence included in the red rectangle is absent in the two human isoforms hCA I and II, while it is present in the mitochondrial form (hCA VA) for localization in the intermembrane space, in the hCA VI for secretion in saliva, and in the  $\alpha$ -CA for bacterial localization in the periplasmic space.

To understand the role played by  $\alpha$ -CA in Gram-negative, need to refer to some bacteria characterized by the presence of periplasmic  $\alpha$ -CA. *Helicobacter pylori* is a pathogenic bacterium, Gram-negative, flagellated acidophilus, whose natural habitat is the gastric mucus of the human stomach. Its genome encodes for a  $\alpha$ -, a  $\beta$ - and a  $\gamma$ -CA (Nishimori I., *et al.* 2008; Morishita S., *et al.* 2008;

Chirica L.C., *et al.* 2002). The  $\alpha$ -CA has a periplasmic location, the  $\beta$ -CA has a cytoplasmic localization while still nothing is known about the expression and localization of  $\gamma$ -CA. *H. pylori* has developed unique adaptive mechanisms for growth in highly acidic environments such as the stomach. These mechanisms involve urease and CAs. In acidic conditions, urea penetrates into the cell through the channel and urea, in bacterial cytoplasm is hydrolyzed to  $\text{CO}_2$  and  $2\text{NH}_3$  (Supuran C.T. 2008) (Figure 38). In the bacterial cytoplasm, the  $\text{CO}_2$  is hydrated by  $\beta$ -CA, while the  $\text{CO}_2$  diffuses into the periplasm is converted to  $\text{HCO}_3^-$  by periplasmic  $\alpha$ -CA. The ions  $\text{H}^+$  products are used by  $\text{NH}_3$  to form  $\text{NH}_4^+$  in the periplasm and cytoplasm, respectively. Then, as shown in figure 38, the role of periplasmic  $\alpha$ -CA and cytoplasmic  $\beta$ -CA it is to produce  $\text{HCO}_3^-$  and protons to neutralize the acid input. In *H. pylori*, then, the periplasmic  $\alpha$ -CA is crucial for the acid acclimatization of the pathogen within the stomach. (Marcus E.A., *et al.* 2005; Sachs G., *et al.* 2005).

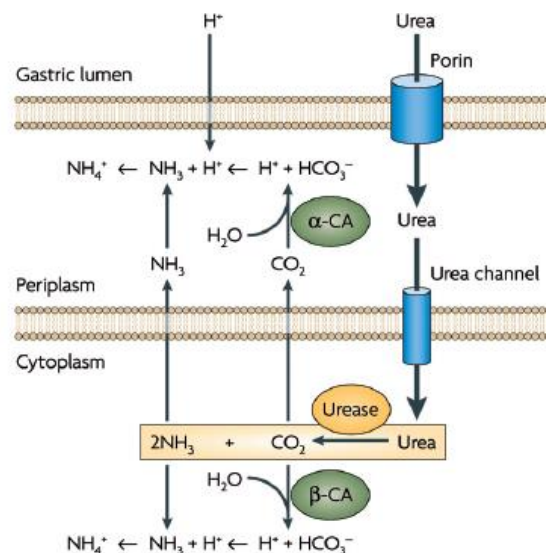


**Figure 38.** Schematization of the role of the  $\alpha$ - and  $\beta$ -CA in maintaining periplasmic pH in *Helicobacter pylori*.

A similar mechanism has been reported for the Gram-negative bacterium *Ralstonia eutropha* (Gai C.S., *et al.* 2014). The genome of this bacterium encode for an  $\alpha$ -, a  $\beta$ - and  $\gamma$ -CA. The  $\alpha$ -CA has a periplasmic localization and assists the transport of bicarbonate across the cell membrane (Gai C.S., *et al.* 2014). Concerning the bacterium *Vibrio cholerae*, the  $\alpha$ -CA, probably located in the periplasmic space, could be involved in the production of bicarbonate, an inducer of gene expression of the virulence of the pathogen. In addition, the two

bacteria belonging to the genus *Sulfurihydrogenibium*, *S. yellowstonense* and *S. azorense*, which live at temperatures up to 110 ° C, exhibit  $\alpha$ -CA characterized by a signal peptide for periplasmic localization of this enzyme. These observations allow assuming that in the course of evolution, in Gram-negative bacteria, a signal peptide placed at the 'N-terminal of a primordial CA, has generated a new class of CAs, namely the class  $\alpha$ , with localization in the periplasmic compartment. Dr. Clemente Capasso and Prof. Claudiu Supuran, have speculated that the  $\alpha$ -CA are able to convert the CO<sub>2</sub> to bicarbonate diffused in the periplasmic space, ensuring the survival and/or satisfying the metabolic needs of the microorganism. Instead, the  $\beta$ - and  $\gamma$ -CA localized in the cytoplasm are responsible for the supply of CO<sub>2</sub> to the carboxylase or for the homeostasis of intracellular pH and other functions (Capasso C. & Supuran C.T. 2014).

Not all Gram-negative bacteria, however, have  $\alpha$ -CAs. Probably the  $\alpha$ -CAs are not required when the Gram-negative bacteria colonize habitats defined as adverse to their survival or limiting for their metabolic needs (Capasso C. & Supuran C.T. 2014).

There are also bacteria whose genome does not code for any class of CAs. A very interesting study has shown that knockout mutants for the CAs of *Ralstonia eutropha*, *Escherichia coli* and *Saccharomyces cerevisiae* are able to grow only in the presence of atmosphere with a CO<sub>2</sub> level of between 2 and 5% (Ueda K., *et al.* 2012). High levels of CO<sub>2</sub>, in fact, generate high concentrations of bicarbonate spontaneously, through the reaction not catalyzed. These microorganisms lacking the CAs, at low concentrations of CO<sub>2</sub> (0.035%) are not able to grow, if not by providing a sufficient amount of bicarbonate. This shows that the CAs are not necessary for microbial growth in environments with high concentrations of CO<sub>2</sub> as the intestine, the sea water and in conditions of syntrophism and commensalism, but become necessary when this gas is present in low concentrations. The bacteria belonging to the genera *Buchnera* and *Rickettsia*, living in habitats with high concentration of CO<sub>2</sub>, such as soil, seawater or the intestine, do not need CAs.

We also wondered if there was a relationship between the evolutionary history of bacterial CAs and evolution of Gram-positive and Gram-negative bacteria. The phylogenetic tree (Figure 39) obtained by aligning the amino acid sequences of the  $\alpha$ -,  $\beta$ - and  $\gamma$ -CA identified in the genome of Gram-positive and

negative bacteria, showing that the  $\gamma$ -CA by Gram-positive and negative are closely associated to each other, as meaning that they form mixed groups of  $\gamma$ -CA from Gram-positive and Gram-negative bacteria.

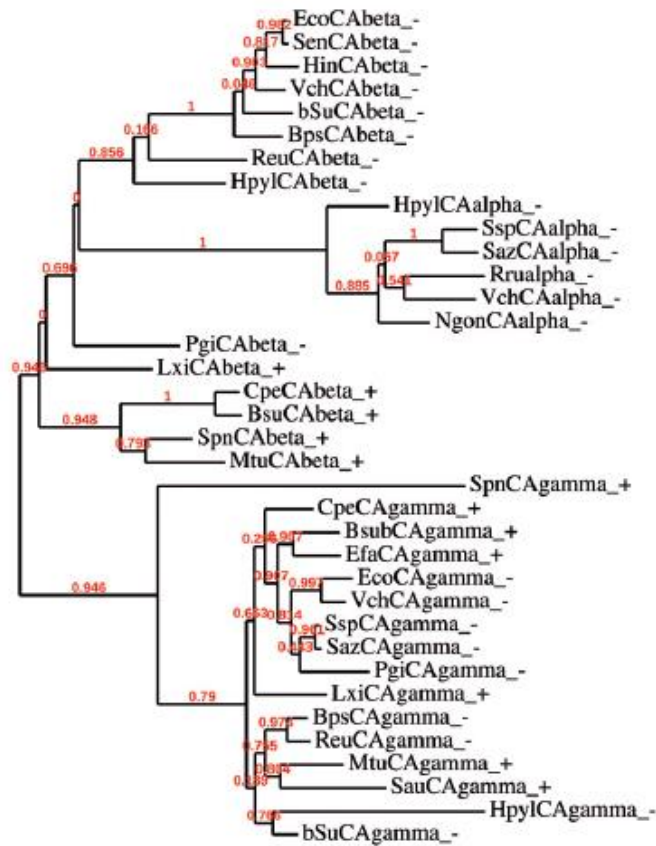


**Figure 39.** Phylogenetic analysis of  $\alpha$ -,  $\beta$  and  $\gamma$ -CA of Gram-positive and negative. For the construction of the dendrogram it was used the program PhyML 3.0.

The  $\beta$ -CAs, unlike the  $\gamma$ -CAs, with the exception of LxiCAbeta\_+ and PgiCAbeta\_-, form two separate clusters, one containing the  $\beta$ -CAs only from Gram-negative bacteria and the other containing  $\beta$ -CAs only from Gram-negative bacteria positive. This could be the result of a gene duplication event. The  $\alpha$ -CAs, found only in Gram-negative bacteria, form a separate cluster, located in the same cluster of  $\beta$ -CAs of Gram-negative bacteria (Capasso C. & Supuran C.T. 2014).

The results that come from the phylogenetic analysis is that the ancestral CAs are represented by the  $\gamma$ -class. In fact, even if the  $\gamma$ -class is widely distributed in all three domains, it is the only mainly identified in archaea, the

oldest living organisms on our planet (Zimmerman S., *et al.* 2004; Tripp B.C., *et al.* 2001 -2004; Smith K.S., *et al.* 1999).

This is in agreement with the theory that supports a close relationship between the archaea and bacteria Gram-positive and considers phylogenetically distinct the Gram-negative bacteria.

From the class  $\gamma$  would be originated the class  $\beta$  of Gram-positive and then that of the Gram-negative bacteria. Subsequently, from an ancestral  $\beta$ -CA of a Gram-negative bacterium, they would originate the  $\alpha$ -CAs, the latter exclusively present in Gram-negative bacteria. This hypothesis can also be corroborated by the theory of "enzyme promiscuity" (Baas B.J., *et al.* 2013; Chakraborty S., *et al.* 2013; Khersonsky O., *et al.* 2010), i.e. the ability of an enzyme to catalyze additional reactions to the primary role. Tawfik considers, in fact, promiscuity a key factor in the evolution of a new function of the same protein (Khersonsky O. & Tawfik D.S. 2010). In fact, it has been noted that the  $\gamma$ -CAs use only the  $\text{CO}_2$  as substrate, while the  $\beta$ -CAs can hydrolyze in addition to  $\text{CO}_2$ , also hydrogen sulfide and carbonyl sulfide. Instead, the  $\alpha$ CA not only catalyze the reaction of hydration of  $\text{CO}_2$  and carbon disulphide, but also possess esterase and thioesterase activity. Furthermore, by analyzing the size of the catalytic site bacterial of  $\alpha$ -,  $\beta$ - and  $\gamma$ - CAs, it has been seen that the catalytic pocket is rather small for the  $\gamma$ -CAs, a bit bigger for  $\beta$ -CAs and wide for  $\alpha$ -CAs (Figure 40).

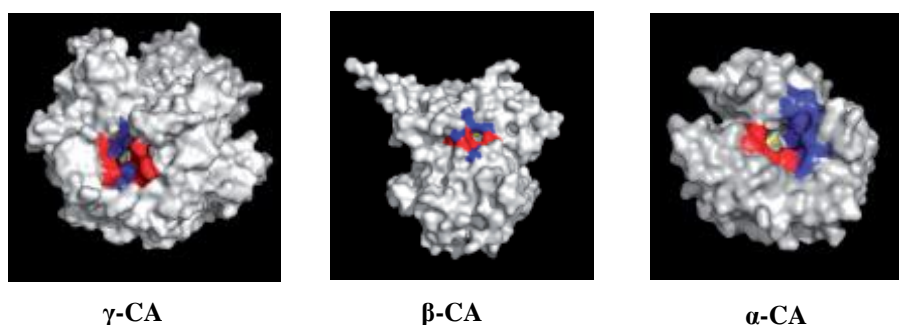


**Figure 40.** Three-dimensional structure of the catalytic site of the  $\gamma$ -(Cam),  $\beta$ -(Can2) and  $\alpha$ -(hCA II)-CAs.

Overall, the catalytic efficiency of  $\gamma$ -CA is lower than the  $\beta$ -CA, which in turn represent the catalysts less efficient than  $\alpha$ -CA (Capasso C. & Supuran C.T. 2014). We can conclude that phylogenetic analysis and theory of enzyme

promiscuity support the hypothesis that the most recent CA is that of class  $\alpha$  (with additional catalytic activities), while the  $\gamma$ -CA is the class ancestral, that catalyzes only the reaction of hydration of  $\text{CO}_2$  (with a catalytic efficiency rather low). These results are in agreement with the evolutionary theory according to which the Gram-positive bacteria, characterized by a simple cellular structure, have appeared before the Gram-negative bacteria with a more complex cell structure (outer membrane and inner membrane).

## Chapter 7. Discussion

### 7.1 Biotechnological application

Since CAs are very valid catalysts of the conversion of CO<sub>2</sub> to bicarbonate, such enzymes may lead to the capture/sequestration of CO<sub>2</sub> from combustion gases, and alleviate the global warming effects through a reduction of CO<sub>2</sub> emissions in the atmosphere. The interest of the study for the CAs from thermophilic microorganisms comes from the following consideration: the enzymes from thermophiles, compared to mesophilic counterpart, are characterized by high stability at high temperature and are resistant to the common denaturing agents. These features allowed their use in industrial processes characterized by extreme operating conditions, such as high temperature, high pH, high concentrations of salts etc. For this purpose, CAs present in the genome of extremophilic bacteria started to be investigated in detail ultimately. We have identified a  $\alpha$ -CAs in the genome of the extremophilic bacteria *Sulfurihydrogenibium yellowstonense* YO3AOP1 living in the Yellowstone National Park, and *Sulfurihydrogenibium azorense*, living in the Azores Islands (Nakagawa S. 2005; Aguiar P. 2004). The two CAs, named SspCA and SazCA, were extensively investigated. Two issues related to CO<sub>2</sub> capture process were examined: the CO<sub>2</sub> hydration kinetics and long-term stability at high temperature. The first documented carbonic anhydrase from a thermophile was purified from the thermophilic methanoarcheon *M. thermoautotrophicum*, but the enzyme was thermostable at temperatures up to 75 °C and belonged to the  $\beta$ -CA (Smith K.S, & Ferry J.G. 1999; Smith K.S. & Ferry J.G. 2000). Our results showed that SspCA was stable for 3 hr. at 100 °C, whereas the bovine enzyme (bCA) was fully inactivated after 60 °C. Instead, SazCA was less thermostable than SspCA, but it had a turnover number ( $k_{cat}$ ) higher than that of the human enzyme (hCAII) considered the most active CA to date. The analysis of the amino acid sequences and the crystallographic structures of the two CAs explained their main features, such as the higher activity and thermal stability. The present thesis demonstrated that SspCA resulted the most stable CA never investigated, while SazCA was the faster CA investigated up to now.

SspCA was efficiently immobilized within PU foam and on paramagnetic particles (MP) as biocatalyst to be used in the CO<sub>2</sub> capture process. SspCA

covalently bound to polyurethane showed the following characteristics: a) preserved its activity; b) enhanced its stability for long time (60 days); c) resulted an efficient enzyme in the biomimetic capture of CO<sub>2</sub>. It has been shown, in fact, that the immobilized PU-SspCA is capable of converting about 15% of CO<sub>2</sub> from a gas mixture whose initial concentration was 20%.

## 7.2 Biomedical application

Infectious diseases are still today the second leading cause of death worldwide, and the abuse and/or inappropriate use of antibiotics have led to a wide spread of the phenomenon of the antibiotic resistance of pathogenic microorganisms (Saccarlal J., *et al.* 2009; Nour N.M. 2012). As a general rule antibiotics inhibit the growth of the pathogen by acting on metabolic "pathways" such as cell wall biosynthesis, biosynthesis of proteins, biosynthesis of DNA and RNA, biosynthesis of folates (Gaynor M. & Mankin A.S. 2003). In recent years, many research groups have focused their interest of study on CAs of bacteria, fungi and protozoa, since they constitute a class of enzymes whose inhibition, as reported in literature, can slow or stop the growth of the pathogen through a different mechanism of action respect to those reported for antibiotics. CAs are target molecules of many antibacterial or antifungal drugs. It has been proved, in fact, that the CA are essential to the life cycle of the microorganisms (Capasso C. & Supuran C.T. 2013; Rusconi S., *et al.* 2004; Supuran C.T. 2012). In many pathogenic microorganisms have been identified and characterized CAs from at least four gene families  $\alpha$ ,  $\beta$ ,  $\gamma$  and  $\eta$ . Usually bacteria encode for CA belonging to the classes  $\alpha$ ,  $\beta$  and  $\gamma$ . It has been reported in literature that the *in vivo* inhibition with sulfonamides and phenolic derivatives of the bacterial CAs identified in *Helicobacter pylori*, *Mycobacterium tuberculosis* and *Brucella suis*, hindered the growth of microorganisms. The acetazolamide and ethoxzolamide have been used in the clinic in the 80<sup>th</sup> and 90<sup>th</sup> as anti-ulcer agents and has been shown that the inhibition of CA from *Helicobacter pylori* represented a valid alternative for the control of the disease. The crystallographic structure of *Helicobacter pylori*  $\alpha$ -CA complexed to acetazolamide or methazolamide represents a useful template for designing highly selective inhibitors for the bacterial CAs with few side effects. Fungi express  $\alpha$ - and  $\beta$ -CA and it was found that the inhibition of these enzymes with sulfonamides, thiols and dithiocarbamates, block the *in vivo* growth of *Malassezia globosa*, *Candida albicans* and *Cryptococcus*

*neoformans*. Protozoa, however, encode for  $\alpha$ -  $\beta$ - or  $\eta$ -CA. It has been shown that sulphonamidic inhibitors, thiols and idroxamates actually cause the death of some microorganisms *in vivo* such as *Trypanosoma cruzi*, *Leishmania donovani chagasi* and *Plasmodium falciparum*. In the present thesis it has been shown that the sulfonamides and their relative bioisosteres and, anions inhibited *in vitro*, the three classes of CAs identified in the genome of *Vibrio cholerae*. The inhibition study with a panel of sulfonamides and one sulfamate led to the detection of a large number of nanomolar VchCA $\gamma$  inhibitors, including simple aromatic/heterocyclic sulfonamides (compounds **2-9**, **11**, **13-15**, **24**) as well as **EZA**, **DZA**, **BRZ**, **BZA**, **TPM**, **ZNS**, **SLP**, **IND** ( $K_{IS}$  in the range of 66.2-95.3 nM). As it was proven that bicarbonate is a virulence factor of this bacterium and since ethoxzolamide was shown to inhibit this virulence *in vivo*, we propose that VchCA, VchCA $\beta$  and VchCA $\gamma$  may be a target for antibiotic development, exploiting a mechanism of action rarely considered up until now, i.e., interference with bicarbonate supply as a virulence factor. The inhibition profile of VchCA, VchCA $\beta$  or VchCA $\gamma$  was different from that of the other bacterial or mammalian CAs investigated up until now, proving that probably it will be possible to design VchCA, VchCA $\beta$  or VchCA $\gamma$  selective inhibitors using the scaffold of leads detected here.

For the treatment of diseases such as malaria, for example, several drugs are available, but over the years, their effectiveness is greatly diminished and, thus, remains the problem of antibiotic resistance. Protozoa, such as *Plasmodium falciparum*, utilize purines and pyrimidines for DNA/RNA synthesis during its exponential growth and replication. Plasmodia synthesize pyrimidines *de novo* from  $\text{HCO}_3^-$ , which is the substrate of the first enzyme involved in the Plasmodia pyrimidine pathway.  $\text{HCO}_3^-$  is generated from  $\text{CO}_2$  through the action of a CA. Our studies have shown that PfCA1, the CA identified in the genome of *Plasmodium falciparum*, belongs to a new class of CAs, called  $\eta$ . The metal ion coordination pattern of the  $\eta$ -CA from the malaria producing protozoa *P. falciparum* is unique among all six genetic families encoding for such enzymes, comprising two His and one Gln residues, in addition to the water molecule/hydroxide ion acting as nucleophile in the catalytic cycle. To date, few inhibitors were tested for  $\eta$ -CA. The attempt to selectively inhibit the CA of pathogenic organisms such as bacteria, protozoa and fungi, can represent an alternative approach for the design of antibacterial/pesticides/antifungal with a novel mechanism of action.  $\alpha$ -CAs are

potential drug targets, as shown by the use of sulfonamides in the clinic for the treatment of infection by *Helicobacter pylori* (Puscas I. 1984) and for the  $\beta$ -,  $\gamma$ - or  $\eta$ -class CAs there is a great interest in identifying selective inhibitors, since they are absent in humans and other mammals.

### 7.3 Phylogenetic analysis

The complex distribution of the various CA classes in Gram-positive and negative bacteria allowed us to find a correlation between the evolutionary history of the bacteria and the three CA classes ( $\alpha$ ,  $\beta$  and  $\gamma$ ) identified in their genome. Prokaryotes appeared on the Earth 3.5-3.8 billion years ago, while eukaryotes were dated 1.8 billion years ago. During the first 2.0-2.5 billion years the Earth's atmosphere not contained oxygen, thus the first organisms were anaerobic. Eukaryotic organisms almost aerobes developed on the Earth when the atmosphere was characterized by stable and relatively high oxygen content. All the oldest part of the evolutionary history of the planet and more than 90% of the phylogenetic diversity of life can be attributed to the microbial world. Moreover, the fact that the archaea are distinct from other prokaryotes is demonstrated by the existence of protein sequences that are present in archaea, but not in eubacteria (Gupta R.S. 1998). Many phylogenetic methods support a close correlation of archaea with Gram-positive bacteria, while Gram-negative bacteria form a separate clade, indicating their phylogenetic distinction. Gupta et al. believe that the Gram-positive bacteria occupy an intermediate position between archaea and Gram-negative bacteria, and that they evolved precisely from archaea. Phylogenetic analysis of carbonic anhydrases identified in bacteria Gram-positive and negative, showed that the ancestral CA is represented by  $\gamma$ -class. In fact, the  $\gamma$ -CA is the only CA class, which has been identified in archaea (Zimmerman S., et al. 2004; Tripp B.C., et al. 2001-2004; Smith K.S., et al. 1999). This is consistent with the theory that maintains a close relationship between the archaea and the Gram-positive bacteria, considering Gram-negative arising from the latter. Furthermore, phylogenetic analysis of bacterial CAs showed that the  $\alpha$ -CAs, exclusively present in Gram-negative bacteria, were the most recent CAs. These results have been corroborated by the enzymatic promiscuity theory, which is the ability of an enzyme to catalyze a side reaction in addition to main reaction (Torrance J.W., et al. 2007). In fact, as described in the Results section, the  $\alpha$ -CAs can catalyze

secondary reaction, such as the hydrolysis of p-NpA or thioester, in addition to its primary reaction consisting in the CO<sub>2</sub> hydration.

## **7.4 Conclusions**

My PhD project brought new insights in the field of carbonic anhydrases. It has been demonstrated: a) the thermostable and thermoactive CAs identified in thermophilic bacteria are good candidates in the CO<sub>2</sub> capture process; b) the studies carried out on the CAs from pathogens have identified selective inhibitors to be used as anti-infective; c) the discovery of the  $\eta$ -CA, a new genetic families of CAs; d) the introduction of a new technique, named protonography, useful for the identification of CA activity on a polyacrylamide gel; and to the phylogenetic analysis of the  $\alpha$ -,  $\beta$ - and  $\gamma$ -CAs identified in the genome of the Gram-positive and Gram-negative bacteria.

## Bibliography

- Abadie, L. M., & Chamorro, J. M. European CO<sub>2</sub> prices and carbon capture investments. *Energy Economics*, 2008, 30(6), 2992-3015.
- Adams M.W.W. Enzymes and proteins from organisms that grow near and above 100 degrees C. *Ann Rev Microbiol* 1993, 47:627–658,58;
- Aerosol Air Qual. Res.* 2012, 12, 745–769.
- Akdemir A., Vullo D., De Luca V., Scozzafava A., Carginale V., Rossi M., Supuran C.T., Capasso C. The extemo- $\alpha$ -carbonic anhydrase (CA) from *Sulfurihydrogenibium azorense*, the fastest CA known, is highly activated by amino acids and amines. *Bioorg Med Chem Lett.* 2013; 23(4):1087-90.
- Alber B.E., Ferry J.G. A carbonic anhydrase from the archaen *Methanosarcina thermophila*. *Proc Natl Acad Sci U S A.* 1994; 91(15):6909-13.
- Alp S. Putative virulence factors of *Aspergillus* species. *Mikrobiyoloji Bulteni* 2006; 40:109-119.
- Alterio V., Di Fiore A., D'Ambrosio K., *et al.* Multiple binding modes of inhibitors to carbonic anhydrases: how to design specific drugs targeting 15 different isoforms? *Chem Rev* 2012; 112:4421-68.
- Alterio V., Langella E., Viparelli F., Vullo D., Ascione G., Dathan N.A., Morel F.M., Supuran C.T., De Simone G., Monti S.M. Structural and inhibition insights into carbonic anhydrase CDCA1 from the marine diatom *Thalassiosira weissflogii*. *Biochimie.* 2012; 94(5):1232-41.
- Andrews K.T., Fisher G.M., Sumanadasa S.D., Skinner-Adams T., Moeker J., Lopez M., Poulsen S.A.. Antimalarial activity of compounds comprising a primary benzene sulfonamide fragment. *Bioorg Med Chem Lett.* 2013; 23(22):6114-7.
- Armstrong J.M., Myers D.V., Verpoorte J.A., Edsall J.T. Purification and properties of human erythrocyte carbonic anhydrases. *J Biol Chem.* 1966; 241(21):5137-49.
- Baas B.J., Zandvoort E., Geertsema E.M., Poelarends G.J. Recent advances in the study of enzyme promiscuity in the tautomerase superfamily. *Chembiochem.* 2013; 14(8):917-26.
- Badger M.R., Price G.D. The role of carbonic anhydrase in photosynthesis. *Annu Rev Plant Physiol Plant Mol Biol* 1994; 45: 369-92.

- Bond G.M., Stringer J., Brandvold D.K., Simsek F.A., Medina M.G. and Egeland, G. Development of integrated system for biomimetic CO<sub>2</sub> sequestration using the enzyme carbonic anhydrase. *Energy & Fuels*, 2001; 15(2), 309-316.
- Borchert, M., Saunders, P. Heat Stable Carbonic Anhydrases and Their Use. Patent WO 2008095057
- Boron W.F. Evaluating the role of carbonic anhydrases in the transport of HCO<sub>3</sub><sup>-</sup>-related species. *Biochim Biophys Acta*. 2010; 1804(2):410-21. Review.
- Bostanci N., Belibasakis G.N. *Porphyromonas gingivalis*: an invasive and evasive opportunistic oral pathogen. *Molecular Microbiology* 2012; 333:1-9.
- Boztas M., Çetinkaya Y., Topal M., Gülcin İ., Menzek A., Şahin E., Tanc M., Supuran C.T. Synthesis and Carbonic Anhydrase Isoenzymes I, II, IX, and XII Inhibitory Effects of Dimethoxybromophenol Derivatives Incorporating Cyclopropane Moieties. *Journal of medicinal chemistry*, 2015; 58(2):640-50.
- Briganti, F., Mangani, S., Orioli, P., Scozzafava, A., Vernaglione, G., Supuran C.T., Carbonic anhydrase activators: X-ray crystallographic and spectroscopic investigations for the interaction of isozymes I and II with histamine. *Biochemistry*, 1997; 36, 10384-10392.
- Brodelius, P. and Mosbach, K. (1987) Immobilization Techniques for Cells/Organelles. In: *Methods in Enzymology*, volume 135, (Mosbach, K., ed.), Academic Press, London, pp. 173–454.
- Buchholz, K. and Klein, J. (1987) Characterization of Immobilized Biocatalysts. In: *Methods in Enzymology* volume 135, (Mosbach, K., ed.), Academic Press, London, pp. 3–30.
- Capasso C., De Luca V., Carginale V., Cannio R., Rossi M. Biochemical properties of a novel and highly thermostable bacterial  $\gamma$ -carbonic anhydrase from *Sulfurihydrogenibium yellowstonense* YO3AOP1. *J Enzyme Inhib Med Chem* 2012; 27:892–897
- Capasso C., Supuran C.T. An overview of the alpha-, beta- and gamma-carbonic anhydrases from Bacteria: can bacterial carbonic anhydrases

- shed new light on evolution of bacteria? *J Enzyme Inhib Med Chem*. 2014; 30(2):325-32.
- Capasso C., Supuran C.T. Anti-infective carbonic anhydrase inhibitors: a patent and literature review. *Expert Opin Ther Pat*. 2013; 23(6):693-704.
- Capasso C., Supuran C.T. Bacterial Carbonic Anhydrases as Drug Targets. *The Carbonic Anhydrases as Biocatalyst* 2015; 271-281.
- Cardoso T., Ribeiro O., Aragao I.C., et al. Additional risk factors for infection by multidrug-resistant pathogens in healthcare-associated infection: a large cohort study. *BioMed Central Infectious Disease* 2012; 12:375.
- Cash R.A., Music S.I., Libonati J.P., Snyder M.J., Wenzel R.P., Hornick R.B. Response of man to infection with *Vibrio cholerae*. I. Clinical, serologic, and bacteriologic responses to a known inoculum. *J Infect Dis*. 1974;129(1):45-52.
- Cash R.A., Music S.I., Libonati J.P., Snyder M.J., Wenzel R.P., Hornick R.B. Response of man to infection with *Vibrio cholerae*. I. Clinical, serologic, and bacteriologic responses to a known inoculum. *J. Infect. Dis*. 1974; 129, 45–52.
- Chakraborty S., Minda R., Salaye L., Dandekar A.M., Bhattacharjee S.K., Rao B.J. Promiscuity-based enzyme selection for rational directed evolution experiments. *Methods Mol Biol*. 2013; 978:205-16.
- Chegwidden W.R., Carter N.D., Edwards Y.H. *The Carbonic Anhydrases: New Horizons*, 2000; 12-28.
- Chirica L.C., Elleby B., Jonsson B.H., Lindskog S. The complete sequence, expression in *Escherichia coli*, purification and some properties of carbonic anhydrase from *Neisseria gonorrhoeae*. *Eur J Biochem*. 1997; 244(3):755-60.
- Chirica L.C., Petersson C., Hurtig M., Jonsson B.H., Borén T., Lindskog S. Expression and localization of alpha- and beta-carbonic anhydrase in *Helicobacter pylori*. *Biochim Biophys Acta*. 2002; 1601(2):192-9.
- Clare B.W. and Supuran C.T. Carbonic anhydrase activators. 3: structure-activity correlations for a series of isozyme II activators. *J Pharm Sci*. 1994; 83(6):768-73.

- Cox G.M., McDade H.C., Chen S.C., Tucker SC, Gottfredsson M, Wright LC, Sorrell TC, Leidich SD, Casadevall A, Ghannoum MA et al. Extracellular phospholipase activity is a virulence factor for *Cryptococcus neoformans*. *Molecular Microbiology* 2001; 39:166-75.
- Cox G.M., Mukherjee .J, Cole G.T., et al. Urease as a virulence factor in experimental cryptococcosis. *Infection and Immunity* 2000; 68:443-487.
- Cronk J.D., Endrizzi J.A., Cronk M.R., O'Neill J.W., Zhang K.Y.J. Crystal structure of *E. coli* beta-carbonic anhydrase, an enzyme with an unusual pH-dependent activity. *Protein Sci* 2001; 10: 911-922.
- De Luca V., Del Prete S., Supuran C.T., Capasso C. Protonography, a new technique for the analysis of carbonic anhydrase activity. *J Enzyme Inhib Med Chem*. 2015; 30(2):277-82.
- De Simone G., Di Fiore A., Capasso C., Supuran C.T. The zinc coordination pattern in the  $\eta$ -carbonic anhydrase from *Plasmodium falciparum* is different from all other carbonic anhydrase genetic families. *Bioorg Med Chem Lett*. 2015; 25(7):1385-9.
- De Simone G., Supuran C.T. (In)organic anions as carbonic anhydrase inhibitors. *J Inorg Biochem*. 2012; 111:117-29.
- De Simone, G., Di Fiore, A., Supuran C.T., Are carbonic anhydrase inhibitors suitable for obtaining antiobesity drugs. *Current Pharmaceutical Design* 2008; 14, 655–660.
- Del Prete S., De Luca V., Scozzafava A., Carginale V., Supuran C.T., Capasso C. Biochemical properties of a new alpha-carbonic anhydrase from the human pathogenic bacterium, *Vibrio cholerae* . *J Enzyme Inhib Med Chem* 2014; 29 : 23 – 7.
- Del Prete S., De Luca V., Vullo D., Scozzafava A., Carginale V., Supuran C.T., Capasso C. Biochemical characterization of the  $\gamma$ -carbonic anhydrase from the oral pathogen *Porphyromonas gingivalis*, PgiCA. *J Enzyme Inhib Med Chem*. 2014; 29(4):532-7.
- Del Prete S., Isik S., Vullo D., De Luca V., Carginale V., Scozzafava A., Supuran C.T., Capasso C. DNA cloning, characterization, and inhibition studies of an  $\alpha$ -carbonic anhydrase from the pathogenic bacterium *Vibrio cholerae*. *J Med Chem*. 2012; 55(23):10742-8.

- Del Prete S., Vullo D., De Luca V., AlOthman Z., Osman S.M., Supuran C.T., Capasso C. Biochemical characterization of recombinant  $\beta$ -carbonic anhydrase (PgiCAb) identified in the genome of the oral pathogenic bacterium *Porphyromonas gingivalis*. *J Enzyme Inhib Med Chem*. 2014; 1-5.
- Del Prete S., Vullo D., De Luca V., Supuran C.T., Capasso C. Biochemical characterization of the  $\delta$ -carbonic anhydrase from the marine diatom *Thalassiosira weissflogii*, TweCA. *J Enzyme Inhib Med Chem*. 2014; 29(6):906-11.
- Del Prete S., Vullo D., Fisher G.M., Andrews K.T., Poulsen S.A., Capasso C., Supuran CT. Discovery of a new family of carbonic anhydrases in the malaria pathogen *Plasmodium falciparum*--the  $\eta$ -carbonic anhydrases. *Bioorg Med Chem Lett*. 2014 ; 24(18):4389-96.
- Di Fiore A., Alterio V., Monti S.M., De Simone G., D'Ambrosio K. Thermostable Carbonic Anhydrases in Biotechnological Applications. *Int J Mol Sci*. 2015; 8;16(7):15456-80. doi: 10.3390/ijms160715456.
- Di Fiore A., Capasso C., De Luca V., Monti S.M., Carginale V., Supuran C.T., Scozzafava A., Pedone C., Rossi M., De Simone G. X-Ray structure of the first "extremo- $\gamma$ -carbonic anhydrase", a dimeric enzyme from the thermophilic bacterium, *Sulfurihydrogenibium yellowstonense* YO3AOP1. *Acta Crystallographica Section D: Biological Crystallography*, 2013; 69.6: 1150-1159.
- DiCosimo R., McAuliffe J., J. Poulouse A. and Bohlmann G. Industrial use of immobilized enzymes *Chem. Soc. Rev.*, 2013; 42, 6437
- Dlugokencky E. Annual Mean Carbon Dioxide Data. Earth System Research Laboratory. National Oceanic & Atmospheric Administration. Retrieved 12 February 2016
- Dogne, J. M., Hanson, J., Supuran, C.T., Pratico, D. Coxibs and cardiovascular side-effects: from light to shadow. *Curr Pharm Des* 2006; 12, 8, 971-975.
- Domsic J. F., Avvaru B. S., Kim C.U., Gruner S.M., Agbandje-McKenna M., Silverman, D.N., McKenna R., Entrapment of carbon dioxide in the active site of carbonic anhydrase II. *J. Biol. Chem.*, 2008; 283, 30766-30771.

- Dudutienė V., Matulienė J., Smirnov A., Timm D.D., Zubrienė A., Baranauskienė L., Morkūnaite V., Smirnovienė J., Michailovienė V., Juozapaitienė V., Mickevičiūtė A., Kazokaitė J., Bakšytė S., Kasiliauskaitė A., Jachno J., Revuckienė J., Kišonaitė M., Pilipuitytė V., Ivanauskaitė E., Milinavičiūtė G., Smirnovas V., Petrikaitė V., Kairys V., Petrauskas V., Norvaišas P., Lingė D., Gibieža P., Capkauskaitė E., Zakšauskas A., Kazlauskas E., Manakova E., Gražulis S., Ladbury J.E., Matulis D. Discovery and characterization of novel selective inhibitors of carbonic anhydrase IX. *J Med Chem.* 2014; 57(22):9435-46.
- Edsall J.T. Multiple molecular forms of carbonic anhydrase in erythrocytes. *Ann N Y Acad Sci.* 1968; 151(1):41-63.
- Falkowski P., Scholes R.J., Boyle E., Canadell J., Canfield D., Elser J., Gruber N., Hibbard K., Höglberg P., Linder S., MacKenzie F.T., *et al* The Global Carbon Cycle: A Test of Our Knowledge of Earth as a System. *Science* 2000; 290 (5490): 291–296
- Forsman C., Behravan G., Osterman A., Jonsson B.H. Production of active human carbonic anhydrase II in *E. coli*. *Acta Chem Scand* 1988; 42:314–318.
- Gaynor M., Mankin A.S. Macrolide antibiotics: binding site, mechanism of action, resistance. *Curr Top Med Chem* 2003; 3:949-61.
- Grosso-Becera M.V., Servín-González L., Soberón-Chávez G. RNA structures are involved in the thermoregulation of bacterial virulence-associated traits. *Trends Microbiol.* 2015; pii: S0966-842X(15)00098-0. doi: 10.1016/j.tim.2015.04.004.
- Gupta R.S. What are archaeobacteria: life's third domain or monoderm prokaryotes related to gram-positive bacteria? A new proposal for the classification of prokaryotic organisms. *Mol Microbiol.* 1998; 29(3):695-707. Review.
- Harris J.B., LaRocque R.C., Qadri F., Ryan E..T, Calderwood S.B. Cholera. *Lancet.* 2012; 379(9835):2466-76.
- Huesemann M.H., Hausmann T.S., Bartha R., Aksoy M., Weissman J.C., Benemann J.R. Biomass productivities in wild type and pigment mutant of *Cyclotella* sp. (Diatom). *Appl Biochem Biotechnol* 2009; 157:507–526.

- Innocenti A., Zimmerman S., Casini A., Ferry J.G., Scozzafava A., Supuran C.T. Carbonic anhydrase inhibitors. Inhibition of the zinc and cobalt gamma-class enzyme from the archaeon *Methanosarcina thermophila* with anions *Bioorg Med Chem Lett* 2004; 14: 3327- 31.
- James P., Isupov M.N., Sayer C., Saneei V., Berg S., Lioliou M., Kotlar H.K., Littlechild J.A. The structure of a tetrameric alpha-carbonic anhydrase from *Thermovibrio ammonificans* reveals a core formed around intermolecular disulfides that contribute to its thermostability. *Acta Crystallogr. D Biol. Crystallogr.* 2014; 70, 2607–2618.
- Joseph P, Ouahrani-Bettache S, Montero JL, Nishimori I, Minakuchi T, Vullo D, Scozzafava A, Winum JY, Kohler S, Supuran CT. 2011. A new beta-carbonic anhydrase from *Brucella suis*, its cloning, characterization, and inhibition with sulfonamides and sulfamates, leading to impaired pathogen growth. *Bioorg Med Chem* 19: 1172-1178.
- Joyce S.A., Watson R.J., Clarke D.J. The regulation of pathogenicity and mutualism in *Photobacterium*. *Current Opinion in Microbiology* 2006;9:127-132.
- Kanbar B., Ozdemir E. Thermal stability of carbonic anhydrase immobilized within polyurethane foam. *Biotechnol Prog* 2010;26: 1474–1480.
- Khalifah R.G. The carbon dioxide hydration activity of carbonic anhydrase. I. Stop-flow kinetic studies on the native human isoenzymes B and C. *J Biol Chem.* 1971; 246(8):2561-73.
- Khersonsky O., Tawfik D.S. Enzyme promiscuity: a mechanistic and evolutionary perspective. *Annu Rev Biochem.* 2010; 79:471-505.
- Kimber M.S., Pai E.F. The active site architecture of *Pisum sativum*  $\beta$ -carbonic anhydrase is a mirror image of that of  $\alpha$ -carbonic anhydrases. *EMBO J* 2000; 19: 2323-2330.
- Knudsen J.F., Carlsson U., Hammarstrom P., Sokol G.H., Cantilena L.R. The cyclooxygenase-2 inhibitor celecoxib is a potent inhibitor of human carbonic anhydrase II. *Inflammation* 2004; 28, 5, 285-290.
- Köhler K. *et al.* Saccharin inhibits carbonic anhydrases: possible explanation for its unpleasant metallic aftertaste. *Angewandte Chemie International Edition* 46; 2007; 7697–7699.

- Krebs H. A. Inhibition of carbonic anhydrase by sulphonamides. *Biochem J* 1948; 43, 4, 525-528.
- Krissinel E. and Henrick K. Inference of macromolecular assemblies from crystalline state. *J. Mol. Biol.* 2007; 372, 774–797.
- Krungkrai J., Supuran C.T. The alpha-carbonic anhydrase from the malaria parasite and its inhibition. *Curr Pharm Des.* 2008; 14(7):631-40.
- Krungkrai SR, Suraveratum N, Rochanakij S, Krungkrai J. 2001. Characterisation of carbonic anhydrase in *Plasmodium falciparum*. *Int J Parasitol* 31: 661-668.
- Lee R. B.Y., Smith J A.C., Rickaby R.E.M.J. *Phycol.* 2013; 49, 170.
- Maeda S., Price G.D., Badger M.R., Enomoto C., Omata T.. Bicarbonate binding activity of the CmpA protein of the cyanobacterium *Synechococcus* sp. strain PCC 7942 involved in active transport of bicarbonate. *J Biol Chem.* 2000; 275(27):20551-5.
- Mandal S., Mandal M.D., Pal N.K. Cholera: a great global concern. *Asian Pac. J. Trop. Med.* 2011; 4, 573–580.
- Marcus E.A., Moshfegh A.P., Sachs G., Scott D.R. The periplasmic alpha-carbonic anhydrase activity of *Helicobacter pylori* is essential for acid acclimation. *J Bacteriol.* 2005; 187(2):729-38.
- Meldrum N.U., Roughton F.J. Carbonic anhydrase. Its preparation and properties. *J Physiol.* 1933; 80(2):113-42.
- Menlove K.J., Clement M., Crandall K.A. Similarity searching using BLAST. *Methods Mol Biol* 2009; 537:1–22.
- Mincione F., Scozzafava A. and Supuran C.T. (2009). Antiglaucoma carbonic anhydrase inhibitors as ophthalmologic drugs (pp. 139-154). Wiley: Hoboken (NJ).
- Mitsuhashi S, Mizushima T., Yamashita E., Yamamoto M., Kumasaka T., Moriyama H., *et al.* X-ray structure of beta-carbonic anhydrase from the red alga, *Porphyridium purpureum*, reveals a novel catalytic site for CO<sub>2</sub> hydration. *J Biol Chem* 2000; 275: 5521-6.
- Morishita S., Nishimori I., Minakuchi T., *et al.* Cloning, polymorphism, and inhibition of beta-carbonic anhydrase of *Helicobacter pylori*. *J Gastroenterol* 2008; 43:849–57.

- Nishimori I., Minakuchi T., Kohsaki T., Onishi S., Takeuchi H., Vullo D., *et al.* Carbonic anhydrase inhibitors: the beta-carbonic anhydrase from *Helicobacter pylori* is a new target for sulfonamide and sulfamate inhibitors. *Bioorg Med Chem Lett* 2007; 17: 3585-94.
- Nishimori I., Minakuchi T., Morimoto K., Sano S., Onishi S., Takeuchi H., *et al.* Carbonic anhydrase inhibitors: DNA cloning and inhibition studies of the alpha-carbonic anhydrase from *Helicobacter pylori*, a new target for developing sulfonamide and sulfamate gastric drugs. *J Med Chem* 2006; 49 : 2117 – 26.
- Nishimori I., Onishi S., Takeuchi H., Supuran C.T. The alpha and beta classes carbonic anhydrases from *Helicobacter pylori* as novel drug targets. *Curr Pharm Des* 2008; 14:622–30.
- Nishimori I., Onishi S., Vullo D., Innocenti A., Scozzafava A., Supuran C.T. Carbonic anhydrase activators: the first activation study of the human secretory isoform VI with amino acids and amines. *Bioorg. Med. Chem. Lett.* 2007; 17, 5351–5357.
- Nour N.M. Premature delivery and the millennium development goal. *Rev Obstet Gynecol* 2012; 5:100-5.
- Pearson W.R. Using the FASTA program to search protein and DNA sequence databases. *Methods Mol Biol.* 1994; 24:307-31.
- Pouwels J., Moracci M., Cobucci-Ponzano B., Perugino G., van der Oost J., Kaper T. *et al.* Activity and stability of hyperthermophilic enzymes: A comparative study on two archaeal  $\beta$ -glycosidases. *Extremophiles* 2000;4:157–164.
- Puscas I. Treatment of gastroduodenal ulcers with carbonic anhydrase inhibitors. *Ann NY Acad Sci* 1984; 429:587–91.
- Reichle D., *et al.* Carbon sequestration research and development, 1999 Rep. DOE/SC/FE-1, U.S. Dep. of Energy, Washington, D. C.
- Reungprapavut S., Krungkrai S.R., Krungkrai J. Plasmodium falciparum carbonic anhydrase is a possible target for malaria chemotherapy. *J Enzyme Inhib Med Chem.* 2004; 19(3):249-56.
- Revelle R. & MunkW. Chapter: 10. The Carbon Dioxide Cycle and the Biosphere. *Energy and Climate: Studies in Geophysics* 1977

- Rossi M. (1995). Proteins and enzymes from extremophiles: Academical and industrial prospects. New York: Plenum Press.
- Roux O., Cereghino R., Solano P.J., *et al.* Caterpillars and fungal pathogens: two co-occurring parasites of an ant-plant mutualism. PLoS One 2011; 6:e20538.
- Rusconi S., Scozzafava A., Mastrolorenzo A., *et al.* New advances in HIV entry inhibitors development. Curr Drug Targets Infect Disord 2004; 4:339-55.
- Sacaral J., Nhacolo A.Q., Sigauque B., *et al.* A 10 year study of the cause of death in children under 15 years in Manhica, Mozambique. BMC Public Health 2009; 9:67.
- Sachs G., Weeks D.L., Wen Y., Marcus E.A., Scott D.R., Melchers K. Acid acclimation by *Helicobacter pylori*. Physiology (Bethesda). 2005; 20:429-38. Review.
- Sainsbury P.D., Mineyeva Y., Mycroft Z., Bugg T.D.H. Chemical intervention in bacterial lignin degradation pathways: Development of selective inhibitors for intradiol and extradiol catechol dioxygenases. Bioorg Chem. 2015; 60:102-9.
- Schaller M., Borelli C., Korting H.C., *et al.* Hydrolytic enzymes as virulence factors of *Candida albicans*. Mycoses 2005; 48:365-377.
- Scozzafava A., Briganti F., Ilies M.A. & Supuran C.T. Carbonic anhydrase inhibitors. Synthesis of membrane-impermeant low molecular weight sulfonamides possessing *in vivo* selectivity for the membrane-bound versus the cytosolic isozymes. Journal of Medicinal Chemistry. 2000; 43, 292–300.
- Sein K.K., Aikawa M. 1998. The pivotal role of carbonic anhydrase in malaria infection. Med Hypotheses 50: 19-23.
- Smith K.S., Ferry J.G. A plant-type ( $\beta$ -class) carbonic anhydrase in the thermophilic methanoarchaeon *Methanobacterium thermoautotrophicum*. J Bacteriol 1999; 181: 6247-53.
- Smith K.S., Ferry J.G. Prokaryotic carbonic anhydrases. FEMS Microbiol Rev 2000; 24: 335-66.

- Smith K.S., Jakubzick C., Whittam T.S., Ferry J.G. Carbonic anhydrase is an ancient enzyme widespread in prokaryotes. *Proc Natl Acad Sci U S A*. 1999; 96(26):15184-9.
- Soto W., Punke E.B., Nishiguchi M.K. Evolutionary perspectives in a mutualism of sepiolid squid and bioluminescent bacteria: combined usage of microbial experimental evolution and temporal population genetics. *Evolution* 2012; 66:1308-1321.
- Stams T., Christianson D.W. X-ray crystallographic studies of mammalian carbonic anhydrase isozymes. In *The Carbonic Anhydrases—New Horizons*; Chegwidde, W. R., Edwards, Y., Carter, N., Eds.; Birkhäuser Verlag, Basel, 2000; 159–174.
- Strop P., Smith K.S., Iverson T.M., Ferry J.G., Rees D.C. Crystal structure of the "cab"-type beta class carbonic anhydrase from the archaeon *Methanobacterium thermoautotrophicum*. *J Biol Chem* 2001; 276: 10299-305.
- Sun M.K. and Alkon D.L. Carbonic anhydrase gating of attention: memory therapy and enhancement. *Trends Pharmacol. Sci.* 2002; 23, 83–89.
- Sun M.K. and Alkon D.L. Pharmacological enhancement of synaptic efficacy, spatial learning, and memory through carbonic anhydrase activation in rats. *J. Pharmacol. Exp. Ther.* 2001; 297, 961–967.
- Supuran C.T. and Winum J.Y. In *Drug Design of Zinc-Enzyme Inhibitors: Functional, Structural, and Disease Applications*. Ophthalmologic Drugs. 2009; 139–154.
- Supuran C.T. Bacterial carbonic anhydrases as drug targets: toward novel antibiotics? *Front Pharmacol.* 2011; 2:34
- Supuran C.T. Carbonic anhydrase inhibition/activation: trip of a scientist around the world in the search of novel chemotypes and drug targets. *Curr Pharm Des* 2010; 16 : 3233 – 45.
- Supuran C.T. Carbonic anhydrase inhibitors and activators for novel therapeutic applications. *Future Med Chem.* 2011; 3(9):1165-80. Review.
- Supuran C.T. *Carbonic Anhydrases – An Overview Current Pharmaceutical Design*. Bentham Science Publishers Ltd, 2008; 14,603-614.

- Supuran C.T. Carbonic anhydrases: novel therapeutic applications for inhibitors and activators. *Nat Rev Drug Discovery* 2008; 7:168 – 81.
- Supuran C.T. Inhibition of bacterial carbonic anhydrases and zinc proteases: from orphan targets to innovative new antibiotic drugs. *Curr Med Chem* 2012; 19:831-44.
- Supuran C.T., Capasso C. The eta-class carbonic anhydrases as drug targets for antimalarial agents. *Expert Opin Ther Targets* 2014; 1-13.
- Supuran C.T., De Simone G. Carbonic Anhydrase: An Overview. *The Carbonic Anhydrases as Biocatalyst* 2015; 3-11.
- Supuran C.T., Di Fiore A., Alterio V., Monti S.M., De Simone G. Recent advances in structural studies of the carbonic anhydrase family: the crystal structure of human CA IX and CA XIII. *Curr Pharm Des.* 2010; 16(29):3246-54.
- Supuran C.T., Diuretics: from classical carbonic anhydrase inhibitors to novel applications of the sulfonamides. *Current Pharmaceutical Design* 2008; 14, 641-648.
- Supuran C.T., Scozzafava A., Conway J. (Eds.): Carbonic anhydrase- Its inhibitors and activators, CRC Press, Boca Raton (FL), USA, 2004; 1-363.
- Supuran C.T., Scozzafava A., Ilies M.A. and Briganti F. Carbonic anhydrase inhibitors. Synthesis of sulfonamides incorporating 2,4,6-trisubstituted-pyridinium-ethylcarboxamido moieties possessing membrane-impermeability and *in vivo* selectivity for the membrane-bound (CA IV) versus the cytosolic (CA I and CA II) isozymes. *Journal of Enzyme Inhibition and Medicinal Chemistry.*2000; 15, 381–401.
- Supuran CT. 2008. Carbonic anhydrases: novel therapeutic applications for inhibitors and activators. *Nat Rev Drug Discov* 7: 168-181.
- Supuran, C.T, Ilies M.A. and Scozzafava A. Carbonic anhydrase inhibitors. Part 29. Interaction of isozymes I, II and IV with benzolamide-like derivatives. *European Journal of Medicinal Chemistry.* 1998; 33, 739–752.
- Supuran, C.T., Di Fiore A., De Simone G. Carbonic anhydrase inhibitors as emerging drugs for the treatment of obesity. *Expert Opinion on Emerging Drugs* 2008; 13, 383-392.

- Supuran, C.T., Scozzafava A., Conway J., Eds.; Carbonic Anhydrase. Its Inhibitors and Activators; CRC Press: Boca Raton (FL), USA, 2004; 1–363.
- Tanc M., Carta F., Scozzafava A., Supuran C.T.  $\alpha$ -Carbonic Anhydrases Possess Thioesterase Activity. *ACS Med Chem Lett.* 2015; 6(3):292-5.
- Temperini C., Innocenti A., Scozzafava A., Mastrolorenzo A., Supuran C.T. Carbonic anhydrase activators: LAdrenaline plugs the active site entrance of isozyme II, activating better isoforms I, IV, VA, VII, and XIV. *Bioorg. Med. Chem. Lett.*, 2007; 17, 628-635.
- Temperini C., Innocenti A., Scozzafava A., Supuran C.T., Carbonic anhydrase activators: kinetic and X-ray crystallographic study for the interaction of D- and L-tryptophan with the mammalian isoforms I-XIV. *Bioorg. Med. Chem.*, 2008; 16, 8373-8378.
- Temperini C., Scozzafava A., Puccetti L., Supuran C.T., Carbonic anhydrase activators: X-ray crystal structure of the adduct of human isozyme II with L-histidine as a platform for the design of stronger activators. *Bioorg. Med. Chem. Lett.*, 2005; 15, 5136-5141.
- Temperini C., Scozzafava A., Supuran C.T. Carbonic anhydrase activators: the first X-ray crystallographic study of an adduct of isoform I. *Bioorg. Med. Chem. Lett.* 2006; 16, 5152–5156.
- Temperini C., Scozzafava A., Vullo D., Supuran C.T. Carbonic anhydrase activators. Activation of isozymes I, II, IV, VA, VII, and XIV with l- and d-histidine and crystallographic analysis of their adducts with isoform II: engineering proton-transfer processes within the active site of an enzyme. *Chemistry*, 2006; 12, 7057-7066.
- Tibayrenc M., Ayala F.J. Reproductive clonality of pathogens: A perspective on pathogenic viruses, bacteria, fungi, and parasitic protozoa. *Proc Natl Acad Sci USA* 2012. 109: E3305-3313.
- Treva M. Techniques of Immobilization. In: *Immobilized Enzymes. An Introduction and Applications in Biotechnology* (Treva, M., ed.), 1980 Wiley, Chichester-New York, pp. 1–9.
- Tripp B.C., Bell C.B. 3rd, Cruz F., Krebs C., Ferry J.G. A role for iron in an ancient carbonic anhydrase. *J Biol Chem.* 2004; 279(8):6683-7.

- Tripp B.C., Smith K., Ferry J.G. Carbonic anhydrase: new insights for an ancient enzyme. *J Biol Chem.* 2001; 276(52):48615-8.
- Ueda K., Nishida H., Beppu T. Dispensabilities of carbonic anhydrase in proteobacteria. *Int J Evol Biol* 2012; 2012:324549 (1–5).
- Viparelli F., Monti S.M., De Simone G., Innocenti A., Scozzafava A., Xu Y., Morel F.M., Supuran C.T. Inhibition of the R1 fragment of the cadmium-containing zeta-class carbonic anhydrase from the diatom *Thalassiosira weissflogii* with anions. *Bioorg Med Chem Lett.* 2010; 20(16):4745-8.
- Vullo D., Del Prete S., Fisher G.M., Andrews K.T., Poulsen S.A., Capasso C., Supuran C.T. Sulfonamide inhibition studies of the  $\eta$ -class carbonic anhydrase from the malaria pathogen *Plasmodium falciparum*. *Bioorg Med Chem.* 2015; 23(3):526-31.
- Vullo D., Del Prete S., Osman S.M., Scozzafava A., Alothman Z., Supuran C.T., Capasso C. Anion inhibition study of the  $\beta$ -class carbonic anhydrase (PgiCAb) from the oral pathogen *Porphyromonas gingivalis*. *Bioorg Med Chem Lett.* 2014; 24(18):4402-6.
- Vullo D., Isik S., Del Prete S., De Luca V., Carginale V., Scozzafava A., Supuran C.T., Capasso C. Anion inhibition studies of the  $\alpha$ -carbonic anhydrase from the pathogenic bacterium *Vibrio cholera*. *Bioorg Med Chem Lett.* 2013; 23(6):1636-8..
- Wang M., Lawal A., Stephenson P., Sidders J. and Ramshaw C. Post-combustion CO<sub>2</sub> capture with chemical absorption: a state-of-the-art review. *Chemical Engineering Research and Design*, 2011; 89(9), 1609-1624.
- Wassmer S.C., Taylor T.E., Rathod P.K., Mishra S.K., Mohanty S., Arevalo-Herrera M., Duraisingh M.T., Smith J.D. Investigating the Pathogenesis of Severe Malaria: A Multidisciplinary and Cross-Geographical Approach. *Am J Trop Med Hyg.* 2015 Aug 10. pii: 14-0841.
- Webb S.A.R. and Kahler C.M. Bench-to-bedside review: Bacterial virulence and subversion of host defences. *BioMed Central Ltd* 2008; 12:234.
- Winum J.Y., Ram, M., Scozzafava A., Montero J.L., Supuran C.T. Carbonic anhydrase IX: a new druggable target for the design of antitumor agents. *Med. Res. Rev.*, 2008; 28, 445-463.

- Winum J.Y., Temperini C., El Cheikh K., Innocenti A., Vullo D., Ciattini S., Montero J.L., Scozzafava A., Supuran C.T. Carbonic anhydrase inhibitors: clash with Ala65 as a means for designing inhibitors with low affinity for the ubiquitous isozyme II, exemplified by the crystal structure of the topiramate sulfamide analogue. *J. Med. Chem.* 2006; 49, 7024–7031.
- Xu Y., Feng L., Jeffrey P.D., Shi Y., Morel F.M. Structure and metal exchange in the cadmium carbonic anhydrase of marine diatoms. *Nature.* 2008; 452(7183):56-61.
- Yang H., Xu Z., Fan M., Gupta R., Slimane R.B., Bland A.E. and Wright I. Progress in carbon dioxide separation and capture: A review. *Journal of Environmental Sciences*, 2008; 20(1), 14-27.
- Yu C.H., Huang C.H., Tan C.S. A review of CO<sub>2</sub> capture by absorption and adsorption. *Aerosol and Air Quality Research*, 2012; 12.5: 745-769.
- Zimmerman S., Innocenti A., Casini A., Ferry J.G., Scozzafava A., Supuran C.T. Carbonic anhydrase inhibitors. Inhibition of the prokaryotic beta and gamma-class enzymes from Archaea with sulfonamides. *Bioorg Med Chem Lett.* 2004; 14(24):6001-6.